DEVELOPMENT OF GEOPOLYMER FOR DYE INDUSTRIAL AND HEAVY METAL REMOVAL

WARANGKANA KITTIWONGWISAN

A THESIS SUBMITTED IN PARTIAL FULFILLMENT OF THE
REQUIREMENTS FOR THE DEGREE OF MASTER OF SCIENCE
MAJOR IN CHEMISTRY
FACULTY OF SCIENCE
UBON RATCHATHANI UNIVERSITY
ACADEMIC YEAR 2020

UBON RATCHATHANI UNIVERSITY

UBON RATCHATHANI UNIVERSITY
THESIS APPROVAL
MASTER OF SCIENCE
MAJOR IN CHEMISTRY FACULTY OF SCIENCE

TITLE DEVELOPMENT OF GEOPOLYMER FOR DYE INDUSTRIAL AND HEAVY METAL REMOVAL

AUTHOR MISS WARANGKANA KITTIWONGWISAN

EXAMINATION COMMITTEE

PROF. DR. BUNJERD JONGSOMJIT	CHAIRPERSON
ASST. PROF. DR. SAISAMORN LUMLONG	MEMBER
ASSOC. PROF. DR. PORNPAN PUNGPO	MEMBER
ASST. PROF. DR. CHAN INNTAM	MEMBER

ADVISORS

Saisamorn Lumlong
.... ADVISOR
(ASST. PROF. DR. SAISAMORN LUMLONG)

Pornpan Pungpo
.... CO-ADVISOR
(ASSOC. PROF. DR. PORNPAN PUNGPO)

Charida Pukahuta
....
(ASST. PROF. DR. CHARIDA PUKAHUTA)
DEAN, FACULTY OF SCIENCE

A. Pongrat
....
(ASSOC. PROF. DR. ARIYAPORN PONGRAT)
VICE PRESIDENT FOR ACADEMIC AFFAIRS

ACADEMIC YEAR 2020

ACKNOWLEDGEMENT

This thesis would have never started if I had not been given invaluable opportunity, guidance, support and help from the following person, First of all, I would like to express my deepest gratitude and appreciation to my advisor, Assistant Professor Dr. Saisamorn Lumlong and co-advisor, Associate Professor Dr. Pornpan Pungpo for her valuable suggestion, guidance, friendly discussions, continuous support and encouragement throughout my study. I'm deeply appreciated Dr. Parjaree Thavornniti and Mr. Khemmakorn Gomonsirisuk who always provides me for constructive comments and continuous supports in various ways.

Furthermore, I would like to thank my thesis committees, Professor. Bunjerd Jongsomjit and Assistant Professor Dr. Chan Inntam for their helpful guidance.
My grateful acknowledgement is expressed to all the staff of Department of Chemistry, Ubonratchathani University and National Metal and Materials Technology Center (MTEC) at NASDA, Thailand for their helpful during the experiment.

Most of all, I always feel indebted to my family, relatives and friend both inside and outside campus during the very long journey of this study. Any mistakes all I had made in this study must be my own responsibility. If there were any benefit due to the results of my thesis in the future, I would like to contribute to my forgone father and mother.

Warangkana Kittiwongwisan

Researcher

บทคัดย่อ

เรื่อง : การพัฒนาจีโอพอลิเมอร์สำหรับการกำจัดสีย้อมในอุตสาหกรรมและโลหะหนัก
ผู้วิจัย : วรางคณา กิตติวงศ์วิศาล
ชื่อปริญญา : วิทยาศาสตรมหาบัณฑิต
สาขาวิชา : เคมี
อาจารย์ที่ปรึกษา : ผู้ช่วยศาสตราจารย์ ดร.สายสมร ลำลอง
อาจารย์ที่ปรึกษาร่วม : รองศาสตราจารย์ ดร.พรพรรณ พึ่งโพธิ์
คำสำคัญ : การดูดซับ, จีโอพอลิเมอร์, สีย้อม, แกลบข้าว, เถ้าลอย

งานวิจัยนี้ได้ทำการศึกษาการกำจัดสารละลายสีย้อมและโลหะหนัก โดยใช้จีโอโพลิเมอร์ที่สังเคราะห์จากดินขาว ซิลิกาทางการค้า สกัดจากแกลบและเถ้าลอยจากโรงงานไฟฟ้าแม่เมาะเพื่อเตรียมเป็นโซเดียมซิลิเกต (Na_2SiO_3) สำหรับใช้แทน และเถ้าลอยที่ไม่ผ่านการปรับปรุงพื้นผิวเป็นตัวดูดซับ ทำการพิสูจน์เอกลักษณ์ตัวดูดซับด้วยเทคนิค X-ray diffraction (XRD), X-ray fluorescence (XRF) Scanning Electron Microscope (SEM), Brunauer-Emmett-Teller or (BET) และ Fourier Transform infrared spectroscopy (FT-IR) จากการศึกษาประสิทธิภาพในการดูดซับพบว่าจีโอพอลิเมอร์ที่เตรียมจาก Na_2SiO_3 ทางการค้า (GEO8M5D) มีประสิทธิภาพในการดูดซับสีย้อมเมทิลลีน บลู และบริลเลียน กรีนสูงมากกว่า 90 เปอร์เซ็นต์ ศึกษาปริมาณและเวลาในการดูดซับที่เหมาะสม ศึกษาไอโซเทอร์ม, จลนศาสตร์, อุณหพลศาสตร์ และการนำตัวดูดซับกลับมาใช้ใหม่ ในการดูดซับสีย้อมเมทิลลีน บลู ความเข้มข้นเริ่มต้นของสีย้อม 300 ppm น้ำหนักที่เหมาะสม 20 g/L เวลาที่เหมาะสมคือ 60 นาที มีประสิทธิภาพการดูดซับสีเมททิลลีน บลู 95 เปอร์เซ็นต์ เมื่อนำกลับมาดูดซับใหม่โดยวิธีการเผา สามารถนำกลับมาดูดซับได้ 9 ครั้ง (ความจุการดูดซับสะสม 296.92 มิลลิกรัมต่อกรัม) สำหรับจีโอพอลิเมอร์ที่ใช้ Na_2SiO_3 โดยซิลิกาที่สกัดจากแกลบ (GSiRH) และเถ้าลอย (GFA) มากำจัดสีย้อมเมทิลลีน บลู ดังนั้นจึงเลือก GSiRH มาศึกษาประสิทธิภาพการกำจัดสีย้อมเมทิลีน บลู ที่เหมาะสม โดยน้ำหนักที่เหมาะสมคือ 40 g/L เวลาที่เหมาะสมคือ 60 นาที มีประสิทธิภาพการดูดซับสีเมททิลลีน บลู 91 เปอร์เซ็นต์ เมื่อนำกลับมาดูดซับใหม่โดยวิธีการเผา สามารถนำกลับมาดูดซับได้ 4 ครั้ง (ความสามารถในการดูดซับสะสม 71.92 มิลลิกรัมต่อกรัม)

สำหรับการนำเถ้าลอย ดูดซับสีย้อมบริลเลียน กรีน พบว่า น้ำหนักที่เหมาะสมคือ 4 g/L เวลาที่เหมาะสมคือ 30 นาที มีประสิทธิภาพการดูดซับ 93 เปอร์เซนต์การนำกลับมาดูดซับใหม่ได้ 3 ครั้ง (ความจุในการดูดซับสะสม 227.10 มิลลิกรัมต่อกรัม) ตัวดูดซับ GEO8M5D, GSiRH และ fly ash

ให้ผลไอโซเทอร์มในการดูดซับที่สอดคล้องกันคือแลงเมียร์ไอโซเทอร์มเป็นการดูดซับแบบชั้นเดียว จลนศาสตร์สอดคล้องกับปฏิกิริยาอันดับสองเสมือน และเปลี่ยนแปลงเอนโทรปี (ΔS°) เป็นบวกแสดงให้เห็นว่ากระบวนการดูดซับมีผลทำให้โมเลกุลของตัวดูดซับและตัวถูกดูดซับที่บริเวณรอยต่อของพื้นผิวตัวดูดซับกับตัวถูกดูดซับมีความไม่เป็นระเบียบเพิ่มสูงขึ้นเอนทาลปี (ΔH°) เป็นบวกแสดงว่ากระบวนการดูดซับเป็นปฏิกิริยาดูดความร้อน และ พลังงานอิสระกิบส์ (ΔG°) ของการดูดซับมีค่าเป็นลบแสดงว่ากระบวนการดูดซับเกิดขึ้นได้เอง

นอกจากนี้ได้นำ GEO8M5D มากำจัดโลหะหนักจากสารละลาย คือ Cr(III), Zn(II) และ Cd(II) มีประสิทธิภาพการดูดซับที่ 90.68, 92.86 และ93.48 เปอร์เซนต์ สามารถลดปริมาณโลหะหนักจากสารละลายได้ ดังนั้นผลจากการศึกษาแสดงว่าจีโอพอลิเมอร์และเถ้าลอยสามารถเป็นตัวดูดซับที่มีประสิทธิภาพเพื่อประยุกต์ใช้บำบัดน้ำเสียในอุตสาหกรรม

ABSTRACT

TITLE : DEVELOPMENT OF GEOPOLYMER FOR DYE INDUSTRIAL AND HEAVY METAL REMOVAL
AUTHOR : WARANGKANA KITTIWONGWISAN
DEGREE : MASTER OF SCIENCE
MAJOR : CHEMISTRY
ADVISOR : ASST. PROF. SAISAMORN LUMLONG, Ph.D.
CO- ADVISOR : ASSOC. PROF. PORNPAN PUNGPO, Ph.D.
KEYWORDS : ADSORPTION, GEOPOLYMER, DYE, RICE HUSK, FLY ASH

The aim of this work is to study removal of dyes and heavy metal ions from aqueous solutions by using geopolymers synthesized from metakaolin and commercial silica extracted from rice husks and fly ash from the Mae Moh power plant of preparing sodium silicate (Na_2SiO_3). Non-treated fly ash was used as an adsorbent. Geopolymer was synthesized from metakaolin. The adsorbent materials were characterized by x-ray diffraction (XRD), x-ray fluorescence (XRF) scanning electron microscope (SEM), brunauer-emmett-teller or (BET) and Fourier transform infrared spectroscopy (FT-IR). Based on the adsorption efficiency of the geopolymers from commercial Na_2SiO_3 (GEO8M5D) for methylene blue and brilliant green dyes, it was found that the adsorption efficiency for both dyes are higher than 90 %. The optimum parameters for adsorption including adsorbent dosage and adsorption time, adsorption isotherm, kinetic, thermodynamic and regeneration test parameters were studied at the initial dye concentration of 300 ppm. The optimum dosage is 20 g/L. The contact time is 60 minutes. The adsorption efficiency is 95%. The regeneration of GEO8M5D can be obtained for 9 cycles (q_e = 296.92 mg/g). The geopolymer prepared from rice husks (RH) and fly ash (GSiRH and GFA) for MB removal were also investigated. The results showed that the adsorption efficiency of GSiRH is higher than GFA. Therefore, GSiRH was selected for optimal conditions for the study. The results showed that the optimum dosage is 40 g/L, the contact time is 60 minutes and the adsorption efficiency is 91%. The regeneration of GSiRH can be obtained for 4 cycles (q_e = 71.92 mg/g). Fly ash's adsorption efficiency for removing brilliant green was investigated. It was found that the optimum dosage is 4 g/L, the contact time is 30 minutes and the adsorption efficiency is 93%. The regeneration of fly ash can be obtained for 3 cycles (q_e = 227.10 mg/g).

The adsorption isotherm onto GEO8M5D, GSiRH and fly ash corresponded well to the Langmuir isotherm which described the monolayer adsorption. Kinetic study showed that the adsorption was followed the pseudo-second–order model. The thermodynamic properties of the adsorption, the positive value of ΔS^o indicated the increment of revealing the samples, affinity for the dyes showed increasing instability and randomness in the dyes interaction interface which resulted from the excess endothermic heat. Negative ΔH^o and ΔG^o indicated that dyes adsorption are an endothermic and spontaneous physisorption, respectively.

In addition, application of GEO8M5D was used for heavy metal removal from solution. The adsorption efficiency of Cr(III), Zn(II) and Cd(II) onto GEO8M5D are 90.68, 92.86 and 93.48%, respectively. The result indicated that GEO8M5D can be used to reduce heavy metals from the solutions. Therefore, these results indicated that the synthetic geopolymer and the fly ash can be used as potential adsorbents for dyes and heavy metal removal from industrial wastewater.

CONTENTS

CONTENTS (CONTINUED)

PAGE

CHAPTER 4 RESULTS AND DISCUSSIONS

CONTENTS (CONTINUED)

PAGE

CHAPTER 5 DISCUSSION AND CONCLUSION

APPENDICES

LIST OF TABLES

LIST OF TABLES (CONTINUED)

LIST OF TABLES (CONTINUED)

LIST OF FIGURES

FIGURE **PAGE**

LIST OF FIGURES (CONTINUED)

FIGURE **PAGE**

LIST OF FIGURES (CONTINUED)

FIGURE **PAGE**

LIST OF FIGURES (CONTINUED)

CHAPTER 1
INTRODUCTION

1.1 Background

Water pollution concerned with the dye concentration is a major serious problem in Thailand. It is known that elevated concentrations of them are detrimental for aquatic living things organism. Through the food chain are toxic for all organisms especially human who related with water.[1]

Cationic dyes are important compound commonly used in various industries such as paper, leather and plastic manufacture. The textile dyes most used in industry are methylene blue, brilliant green, safranin red and malachite green. Methylene blue (MB) was one of the very famous cationic dyes. It has wide applications that include coloring papers, dyeing cottons, wools, silk, leather, and coating for paper stock. Although MB isn’t strongly hazardous, it can cause some harmful effects, such as heartbeat increase, shock, cyanosis, jaundice, quadriplegia, and tissue necrosis in humans.[2]

However, brilliant green (BG) dye is a common dye used in textile, paper, leather, cosmetic and other industries for making a coloured compound. It may be allergic reaction on the human body, eye irritation and even leads to blindness. If BG dye is pocket then it is toxic in nature which directly effects in liver and kidney failure, cancer-causing agent and even mutations in human beings.[3]

The American dye manufacturers institute reported that the standard value of dyes in industrial in wastewater lower 300 ADM. [4] Therefore, intense scientific research is being directed towards the implementation of novel approaches dealing with the efficient removal of toxic dyes from solution.

Many researches have used different method to treat the dye wastewater. Typical the treatment method such as ultra-filtration, adsorption, chemical precipitation, etc. are used for removal of dyes, heavy metal and other pollutant from wastewater with own advantages and disadvantages. Compared with other treatment method, the adsorption method is discussed as prevailing over other dye waste water treatment technology due to its advantage include low cost, simple operation and high efficiency.

Adsorption is the most extensively used technique for the removal dyestuff and other pollutants from wastewater due to effectiveness, simple procedure and economical. A large number of adsorbent materials have been studied for their capacity to remove of cationic dyes, heavy metal and other pollutant including zeolite, activated carbon, clay minerals, fly ash.

Fly ash a type of solid waste, which is produced in the process of power plant. It is estimated that the annual production of fly ash waste is about 40,000 tons for power plant per day, which accounts for a quarter of the power plant waste of Thailand [5].

Fly ash is known as one of the waste materials causing environmental pollution in the form of air and water. It is a particle of pozzolanic properties and the mineral constituents such as quartz, mullite and hematite etc. Fly ash is composed silicon dioxide (SiO_2) rich. Adriano et al [6] reported that the SiO_2 of fly ash at 34.10 wt% using by XRF technique for prepared geopolymer concrete block. The results showed that the compressive strength of geopolymer concrete block increase with the increase in NaOH concentration and curing temperature. Ngamcharussrivichai et al [7] reported that the elemental analysis by technique of XRF indicated that mae moh coal fly ash consisted of SiO_2 at 31.30% wt% for prepare zeolite precursor. Fly ash is recycled about 43 % often used as a pozzolan to concrete [8], brick production [9] and adsorbent.

Many researcher have focused on use of fly ash in removal dye and heavy metal using by adsorption method i.e. Saakshy et al reported that the adsorption capacity at 76.33 mg/g for direct black dye removal. El et al [10] reported that the chemical treatment of fly ash using HCl and microwave for MB, crystal violet (CV) and rhodamine B removal. It is found the acid treatment will improve the adsorption capacity of 92.00 mg/g depending on heating method for MB dye removal. On the other hand, CV and rhodamine B molecules are much bigger than methylene blue, which will prevent the molecules entering the smaller pores of adsorbents, resulting in lower adsorption.

Mishra et al [11] investigated effect of Pb (II) , Cu (II) and Zn (II) removal using fly ash treatment by HCl. The adsorption capacity are 20.00 ,21.28 and 22.14 mg/g. It can be seen that the selectivity of fly ash treatment toward metal ions is found to be in the order Zn (II) > Cu (II) > Pb (II) ions. Since Zn (II) ions have smaller ionic radius than Pb (II) and Cu (II) ions, Zn (II) ions tend to move faster to the potential adsorption sites on absorbents.

Fly ash are sources of aluminosilicates which could have potential as geopolymer precursors for treatment dye and heavy metal. El et al [12] reported that the MB dye removal using by fly ash based geopolymer. This shows the adsorption capacity of 37.04 mg/g of 120 minutes of contact time and the initial concentration at 60 ppm. Novais et al [13] reported that the MB dye removal using by fly ash based geopolymer sphere. The adsorption capacity was 30.10 mg/g of 1440 minutes of contact time and the initial concentration at 250 ppm which lower the initial concentration than [12]. Mužek et al [14] studied effect of Cu(II) removal using by fly ash based geopolymer , the maximum adsorption capacity of 90.00 mg/g.

As mentioned previously, it is interesting to apply fly ash two ways. The first way is applied as an adsorbent without modification for the removal of BG an industrial dye from aqueous solutions using a batch adsorption experiment. The second way, apply to extract silica for prepared as sodium silicate (Na_2SiO_3) for geopolymer precursor. The extraction of silica from fly ash was studied by Patthra et al [15]. This study aims to investigate the optimal condition to extract and precipitate silica from biomass fly ash. Results showed that the best condition to extract silica from fly ash in this study was by treating with 1M H_2SO_4 for 2 hr and refluxing with 3M NaOH solution at 90^o C for 3 hr precipitating silica using citric acid solution at initial pH of 4. The yield of silica is 98.50. XRF showed that the examined product was mainly composed of silica at 95.6%. Gao et al [16] reported that the extraction of silica from fly ash. Fly ash was stirred with 1M HCl and dissolving with NaOH solution (1:4.5), then filtered of silica. The resulting Na_2SiO_3 solution was transferred to silica hydrosol by adjusting pH to 6–7 with silica solution with ultrasonication-assisted. After gelation dehydrogenation, dried and obtained white powder SiO_2. The results showed that the yield and purity of SiO_2 were 51.00 and 98.65%. After that, its adsorption capacities in MB and malachite green (MG) removal from wastewater were studied. The result showed good adsorption capacity to the cationic dyes at 97.00 and 99 % of MG and MB. The contact time is 3 hr and 100 s of MG and MB.

Rice husk (RH) is cultivated in every region of Thailand, the total annual rice production being measured as 20 million tons. RH is the outer cover of rice that accounts for about 20% by weight of the rice. In previous, RH was mostly dumped as waste that may be due to waste disposal problem for the mills. Many countries, including in Thailand use RH to produce electricity. Only 50 to 70% of the RH in Thailand is utilized [17]. RH can be used for power generation through either the steam or gasification route. However, the mainly composition of RH are SiO_2 and quartz crystalline form of silica, which is mainly used in industry. Utilizing silica from RH to synthesize useful materials such as ZSM-5, silica nanoparticles, catalysts are green and eco-friendly methods. The purity of silica used as prepared base precursor including silica precursor for prepare zeolite NaY . This paper is to explore the synthesis of zeolite NaY from rice husk ash as a source of silica after extraction in the amorphous form by acid leaching of husks. The overall weight of SiO_2 in the rice husk ash was 89.00 wt%. The particle size distribution showed homogeneity of zeolite NaY. Therefore, it is interesting apply to extract silica for prepared as Na_2SiO_3 for geopolymer precursor. The several researchers are investigating economical, eco-friendly, easy ways of extracting high-purity silica from rice husk by [18]. This paper is to identify the synthesis of zeolite NaY from RH and RHA as a source if silica after extraction in silica form by 3M HCl and calcined at 823 K for 6 h to finally produce the rice husk silica (RHS). After calcination of acid-treated RH, white RHS was produced with an average yield of 18.07% by weight based on the onset weight of rice husk. The RHAS was produced at an average yield of 59.11% by weight. RH is the better source than RHA for zeolite NaY synthesis taking into account the efficiency in product recovery and simplicity of extraction. Silica from RH was amorphous whereas that from RHA contained crystalline tridymite and cristobalite. Silica extracted from RH was found to contain exclusively SiO_2 while silica from RHA has 97.56% of SiO_2.

In this study, RH was refluxed using HCl acid for 2 hr and muffle furnace at 600˚C for 2 hr. The diagram of extract silica from RH was shown in Figure 1.1.

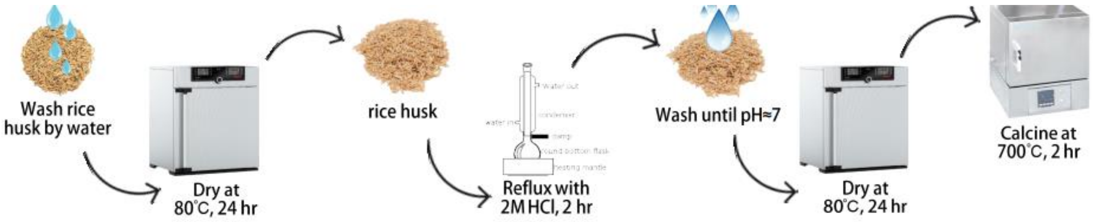

Figure 1.1 The diagram of extract silica from rice husk

New aluminosilicate materials are continuously discovered such as metakaolin, fly ash, bottom ash, rice husk and clays which could have potential as geopolymer precursors.The formation process is termed as geopolymerization reaction. Commonly used alkali activators include NaOH / KOH with sodium and potassium silicate in solution are sometimes added in the synthesis of geopolymers. In Figure 1.2, the terminology of geopolymers can be categorized into three forms which are poly(sialate), poly (sialate-siloxo) and poly (sialate-disiloxo). The action of strong alkali solution dissolves the aluminosilicate materials to form free aluminate and silicate tetrahedral units [19-20]. This leaves a negative charge in the IV-fold coordinated Al that is charge-balanced by cations (Na$^+$, K$^+$, and Li$^+$). The charge-balancing by cation is important in determining the structural integrity and fragility of geopolymer [21]. Therefore, many researchers have investigated various aspects of dyes removal from synthetic aqueous solution and wastewater by using geopolymer as adsorbent.

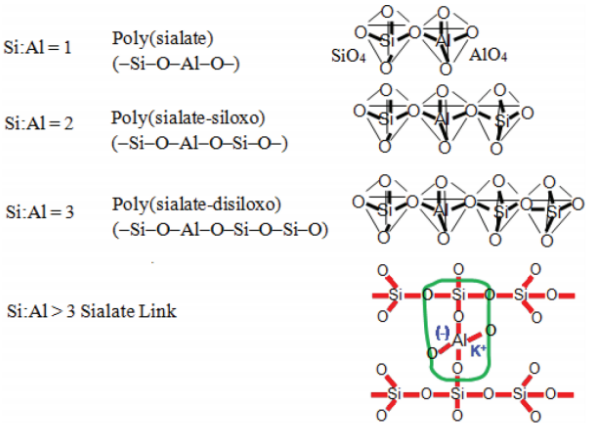

Figure 1.2 Geopolymer systems based number of Si-O unit [22]

Geopolymers are used in a variety of applications such as a green construction material [23], ceramics, coatings, adhesives [22], fire and chemical resistance applications [23] and others. Recently, geopolymer are widely applied for the treatment of wastewater owing to porous structure and low cost.

Geopolymers also can be used as material for removing dye and heavy metal from wastewater via adsorption. They could become a new method for industries, consequently affecting both the environment and societies positively. El Alouani et al reported that the MB dye removal using by metakaolin based geopolymer with 12 M of NaoH. The adsorption capacity was 43.48 mg/g of 120 minutes of contact time and the initial concentration at 40 ppm. Barbosa et al [24] reported methyl violet 10B dye adsorption behavior of metakaolin based geopolymer and its porous counterpart. The adsorption capacity of the geopolymer increased by porosity with the maximum adsorption capacity of mesoporous geopolymer was 276.9 mg/g within 120 minutes. Tang et al investigated a fabricated porous metakaolin based geopolymer spheres with 54 m^2/g surface area, 15 nm pore size and 60% porosity to remove Cu(II), Pb(II), Ca(II) and other ions from waste water.The adsorption capacity of 35.50, 45.60 and 24.00 mg/g. The aim of the present study was contacted to explore the feasibility of using metakaolin based geosorbent for removal MB dye and heavy metal from solution. Adsorption process were examined in batch method.

As seen from the background, a relatively new type of materials called geopolymer are porous aluminosilicates materials which have been discovered to possess adsorbent. But the other researches using geopolymer and fly ash for treatment of dye solution are few high initial concentration and regeneration of adsorbent. So, in this research carried out on geopolymer and silica extracted for prepared Na_2SiO_3 of geopolymer precursor. The synthesized geopolymer adsorbent used removal MB dye from solution. Fly ash without modified was utilized for removal of BG dye solution. The discussion focuses on the characteristics of adsorbent and adsorption, isotherm, kinetic, thermodynamic as well as the mechanism of the system.

Finally, the challenge is regeneration of adsorbent for cationic removal at high initial concentration.

1.2 Objectives

1.2.1 To prepare Na_2SiO_3 using by silica extracted from rice husk and fly ash for geopolymer precursor.

1.2.1 To determine effectiveness of removing MB and BG dye using geopolymer and fly ash study effects of various experimental parameters on adsorption.

1.2.3 To carry out adsorption isotherm, kinetic, thermodynamic and regeneration studies of MB and BG removal.

1.3 Scope of study

The aim of this work used geopolymer from metakaolin and fly ash without modified as inexpensive materials for MB and BG removal from solution.

1.3.1 Extraction of silica from rice husk

RH was extracted by refluxing with 0.1 M HCI for 2 h. Then, it was washed with DI water and dried for 48 h. After that, it was calcined at 600˚C for 2 h.

1.3.2 Extraction of silica from fly ash

Fly ash was treated with 1M H_2SO_4 for 2 h and washed with DI water. Then, fly ash was refluxed by 3M NaOH solution at 90^o C for 3 h and filtered. After that, it was precipitated silica using HCl acid solution at pH of 4.

1.3.3 Preparation of Na_2SiO_3 as a source of silica

Na_2SiO_3 was prepared by using silica and NaOH (raito 1 : 2.2).
Silica 3.4520 g is mixed with 3.60 g of water. Then, 2.9480 g of NaOH is slowly added to dissolve the silica and the mixture was stirred and heated at 60˚C until the suspension became homogeneous solution.

1.3.4 Geopolymer synthesis

The mixtures of metakaolin with activator solution are prepared by stirring until obtained a homogenous slurry. Then, the slurry mixture was transferred to mound, air bubble removal and seal with a plastic film. All samples are left at room temperature.

1.3.5 Characterization of sample

1.3.5.1 The powder sample was characterized by XRD for crystal structure determination.

1.3.5.2 The determination of molecular vibration of the geopolymer was shown by FTIR.

1.3.5.3 The evaluation morphology and component were analyzed by SEM and SEM-EDX.

1.3.5.4 BET surface area was measured by adsorption-desorption before and after adsorption.

1.3.5.5 Zeta potential is defined as the potential difference between the dispersion medium and the stationary layer of fluid attached to the particle and it is measured by a zeta potential analyzer.

1.3.5.6 The point of zero charge is the pH at which the surface of adsorbent.

1.3.6 Adsorption parameters tests

1.3.6.4 Adsorption of geopolymer

1) Effect of optimal dosage are 0.25, 0.50, 1.00 and 2.00 g.

2) Effect of contact time are 30, 60, 120 and 240 minutes.

3) Effect of initial solution pH are 2, 4, 6, 8 and 10.

4) Effect of initial dye concentration are 300, 350, 400, 450 and 550 ppm.

5) Effect of temperature are 20, 30, 40 and 60˚C.

6) The solution pH was adjusted to optimum value using 0.1 M HCl or 0.1 M NaOH. Afterwards, the sample was centrifuged for 10 minutes.

The initial solution of MB were measured using UV- visible spectrophotometer at a wavelength of 664 nm. The removal efficiency of the metakaolin based geopolymer, adsorption capacity at equilibrium q_e (mg/g) and adsorption capacity at any time q_t (mg/g) were obtained.

1.3.6.5 Adsorption of fly ash without modified

1) Effect of optimal dosage are 0.05, 0.10, 0.15 and 0.20 g.

2) Effect of contact time are 5, 10, 15, 30 and 120 minutes.

3) Effect of initial dye concentration are 300, 350, 400, 450 and 550 ppm.

4) Effect of temperature are 20, 30, 40 and 60˚C. The initial solution of BG were measured using UV- visible spectrophotometer at a wavelength of 625 nm.

1.3.7 Isotherm study

With the aim of getting insights into the adsorption mechanism, the data were fitted using both the Lamgmuir and Freundlich model.

1.3.8 Kinetic study

These are several mathematical models used to describe the adsorption kinetics onto the adsorbent materials. In this study, two kinetic models pseudo first order and pseudo second order were applied for the adsorption of dye by geopolymer and fly ash to explain the adsorption process.

1.3.9 Thermodynamic study

Thermodynamic parameters have an important role to evaluate the phenomenon of the adsorption process. The thermodynamic parameter namely, free energy, enthalpy and entropy for adsorption process were used.

1.3.10 Regeneration of adsorbent

Regeneration was achieved by heating the samples at 400 ˚C for 2 hr to promote dye thermal decomposition. Afterwards the sample were reused and the adsorption of dye (C_0 = 300 ppm) was evaluated. Characterization of adsorbents was FTIR and BET surface area.

1.4 Significance of the research

1.4.1 The successfully synthesis of metakaolin based geopolymer from RH and fly ash as a source of silica after extraction in the amorphous form for prepared as a Na_2 SiO_3.

1.4.2 The successfully of high removal dye from solution used geopolymer comparing between Na_2SiO_3 commercial and Na_2SiO_3 from silica sources.

14.3 The removal efficiency increased with high initial concentration of MB and BG showed high adsorption in water solution.

1.4.4 The suitability of application of the geopolymer for removal heavy metal and dye treatment.

1.4.5 Fly ash without modified could be used as a potential and low-cost adsorbent for removal of brilliant green dye from aqueous solutions.

CHAPTER 2

LITERATURE REVIEWS

2.1 Adsorption

Water is a very basic source for existence on the earth. The increase of industrialization has patronized negatively to clean water resources. A large number of substances such as dyes, heavy metal, pharmaceuticals, food and drink in household. Many people care products have contaminated the water resources. These pollutants are environmentally hazardous to human beings and animals. Heavy metals and dyes in excess are harmful to human beings and aquatic life due to their toxicity and bio-accumulation [27].

The excess quantity of heavy metals in water causes irritation of central nerve system and damage to kidney and liver [28]. Dyes and their breakdown products are toxic and mutagenic [29]. As a cationic dye, methylene blue ($C_{16}H_{18}ClN_3S$, MB) is widely used in chemical indicators, dyes and biological dyes.

A large amount of organic dye wastewater is produced in the processes of the industries. The dye wastewater has characteristics such as large discharge, high chromaticity, high organic matter concentration, and poor biodegradability, and greatly affects the water body health and the photosynthesis of microorganisms in the water environment [30]. The revelation to dyes results in effect of respiratory system, skin, eyes and allergic contract dermatitis [31].

Many techniques such as ion exchange, adsorption [32], filtration, electrochemical process [33] and membrane bioreactors, chemical precipitation, floatation, and reverse osmosis were used for the removal of heavy metals, dyes and other pollutants from wastewater.

Adsorption is the most worldwide used technique for the removal of heavy metals, dyes and other pollutants from wastewater due to effectiveness, simple procedure and economical. This process was not widely used till the 40’s and 50’s.

An activated carbon was used for water treatment [34]. These processes efficiency are eco-friendly and low cost treatment method [35]. Many adsorbent for adsorption such as activated carbon, zeolites, chitosan and others were used for the removal pollutants from wastewater. Due to its effectiveness and versatility, activated carbon is widely employed in water treatment.

In recent years, there is an increasing interest in utilize such as clay and rice husk [36]. Synthesis of geopolymer prepared by using different SiO_2/Al2O_3 (GP-1, GP-2 and P-3) ratios and then equilibrium and kinetic behavior of adsorption of MB dye. Geopolymer GP-1, GP-2 and GP-3 had adsorption capacities of 15.95, 17.89 and 20.22 mg/g, respectively Increase in Si/Al ratio in geopolymer caused by use of difference clays increased the ability to remove MB dyes from synthetic wastewater. The isotherm and kinetic adsorption were corresponded Langmuir and pseudo second order.

Boukhemkhem et al [37] study three adsorbents were prepared with the raw kaolin issued from Tamazert kaolin (KT), for removal of MB dye from aqueous solution.

The first adsorbent, KT-1 was shown by thermal treatment; KT-2 was obtained by thermal and acid treatment; and the last, KT-3 was obtained by thermal, acid and alkaline treatment. The adsorption of MB onto KT-3 is highly dependent on various operating parameters such as adsorbent dosage, contact time, pH initial dye concentration and temperature. The maximal adsorption capacity at 111 mg/g was shown with KT-3.The kinetic adsorption is pseudo second order. The thermodynamic study revealed that the adsorption process was spontaneous, endothermic and positive value of ΔS° corresponded the affinity of MB molecule to the adsorbent surface. The adsorption process is generally classified as physisorption characterization of the adsorbed molecules and solid surface. Its attractive force are Van der Waals. The consequence of adsorption is reversible in nature. However, if the attractive force between adsorbate and solid surface occur is chemical bonding, the adsorption process is called chemisorption; the binding is strong and difficult to remove adsorbate from solid surface. The difference force was shown in Table 2.1.

Table 2.1 Properties of physisorption and chemisorption [38]

Physisorption	Chemisorption
The adsorbate is attached to the surface of the adsorbent that weakly forces of Van der Waal's attraction.	The strong chemical bonds are formed between the adsorbate and the surface of the adsorbent.
No new compound is formed in the process.	At the surface of the adsorbent are new compounds.
Reversible in nature	Irreversible in nature
Enthalpy of adsorption is low as weak Van der Waal's forces of attraction are involved. The values lie in the range of 20-40 kJ/mol.	Enthalpy of adsorption is low as weak Van der Waal's forces of attraction are involved. The values lie in the range of 40-400 kJ/mol.
It is favored by low temperature conditions.	It is favored by high temperature conditions.
Multilayer adsorption	Monolayer adsorption

Therefore, the search for a highly efficient, environmentally friendly and cost effectively adsorbents is ever increasing.

A new type of materials called geopolymers are porous aluminosilicate materials which have been discovered to obtain good adsorbent characteristics.

The research carried out on geopolymers for the treatment of wastewater. Many materials such as rice husk, fly ash and water sludge were used to synthesis. The discussion focuses on the characteristics of geopolymers and the optimal parameters, isotherms, kinetics, thermodynamics and the mechanism of the system. Finally, the future challenges of adsorbent were obtained. The most important factors affecting adsorption are;

(1) Surface of adsorbent, large size imply a better adsorption capacity.

(2) Smaller particle size reduce internal diffusional and mass transfer limitation to the penetration of the adsorbate inside the adsorbent such as equilibrium is more simply achieved and closely full adsorption capability can be attained.

However, wastewater drop across columns packed with powered by their removal.

(3) The longer the time the more complete the adsorption will be. However, the equipment will be larger.

(4) Substances slightly soluble in water will be more easily removed from water (i.e., adsorbed) than substance with high solubility. Also, non-polar will be more simply removed than polar- substances will be because the letter have a better affinity for water [39].

2.2 Geopolymer

Geopolymer are inorganic polymer materials come from alkali activation of aluminosilicate materials such as metakaolin, fly ash, water sludge and normally used alkali activators consists sodium or potassium hydroxide with sodium or potassium silicate are perhaps added in the synthesis of geopolymer.

The new aluminosilicate materials are always detected such as fly ash, biomass fly ash, bottom ash, waste glass, clays which could have ability as geopolymer. Geopolymerization related to dissolution, gelation and condensation reactions occurring concurrently to form a geopolymer material. The mechanism was illustrated

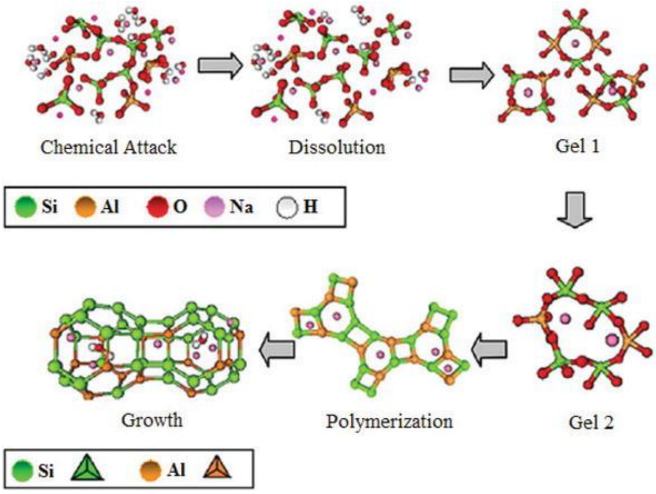

Figure 2.1 Image model of alkali activation of geopolymer [25]

The reaction of stronger alkali solution dissolves the aluminosilicate materials to form free AlO_4 and SiO_4 tetrahedral units. Then water splits out and silicate and aluminate tetrahedral groups link alternatively to produce polymorphic precursors ($-SiO_4-$ AlO_4-,SiO_4-AlO_4-, or $-SiO_4-AlO_4-SiO_4-SiO_4-$) by sharing all oxygen atoms between two tetrahedral units forming an amorphous to semi crystalline geopolymer in which the negative charge on Al is balanced by alkali metal cations [40] Geopolymers contained of three-dimensional porous and the structure of pores are produced during synthesis of geopolymers below 100 °C that is useful for processes of adsorption [19]. They are frequently considered as environmental friendly and low cost green materials. The characteristics of geopolymer depends upon raw materials, mix proportions, and curing conditions [41] and include quick setting with a high resultant strength [42], chemical resistance [43] and low permeability [44].

Geopolymer are used in a variety of applications such as a green construction material [23], ceramics, coatings, adhesives [24], fire and chemical resistance applications [25] and others. Recently, geopolymer are widely applied for the treatment of wastewater owing to porous structure and low cost. Therefore, geopolymer have successfully been used for the adsorption of heavy metals such as Cd, Ni, Pb^{2+}, Cu^{2+}, and Ni^{2+} [40], [45],[46] and dyes such as methylene blue (MB) [47], congo red (CR) [48], methyl violet (MV) (Zhang et al., 2016)[49] and methyl orange (MO) [28] from wastewater. The porous structure, tunable nature, and negative charge on aluminum play vital roles in the removal of heavy metals and dyes from wastewater. The presence of negative charge from charge imbalance at its Al enables geopolymer to attract cations [50], [51]. The tunable nature enables tailoring the properties of geopolymer according for specific applications such as modifying the pore size ranges the molecular sizes of adsorbates.

Pristine aluminosilicate materials processes some adsorption capacity but geopolymerization enhances this ability due to overall pores and charges generated [52].

2.3 Dye

Substances that add color to textiles. They are incorporated into the fiber by chemical reaction, absorption, or dispersion.

Dyes differ in their resistance to sunlight, perspiration, washing, gas, alkalies, and other agents; their affinity for different fibers; their reaction to cleaning agents and methods; and their solubility and method of application.

2.3.1 Dyeing process

A process of coloring fibers, yarns, or fabrics with either natural or synthetic dyes. Dyeing is an ancient art which predates written records. It was practiced during the Bronze age in Europe. Primitive dyeing techniques included sticking plants to fabric or rubbing crushed pigments into cloth. The methods became more sophisticated with time and techniques using natural dyes from crushed fruits, berries and other plants, which were boiled into the fabric and gave light and water fastness (resistance), were developed. Dyeing can be done at any stage of the manufacturing of textile- fiber, yarn, fabric or a finished textile product including garments and apparels. The property of color fastness depends upon two factors- selection of proper dye according to the textile material to be dyed and selection of the method for dyeing the fiber, yarn or fabric.

2.3.2 Type of dyes

2.3.2.1 Acid dyes

Acid dyes are highly water soluble, and have better light fastness than basic dyes.The textile acid dyes are effective for protein fibers such as silk, wool, nylon and modified acrylics. They contain sulphonic acid groups, which are usually present as sodium sulphonate salts. These increase solubility in water, and give the dye molecules a negative charge. In an acidic solution, the $-NH^{2}$ functionalities of the fibres are protonated to give a positive charge: $-NH^{3+}$.This charge interacts with the negative dye charge, allowing the formation of ionic interactions. As well as this, Van-der-Waals bonds, dipolar bonds and hydrogen bonds are formed between dye and fibres. As a group, acid dyes can be divided into two sub-groups: acid-leveling or acid-milling. The structure of acid dyes were showed in Figure 2.2

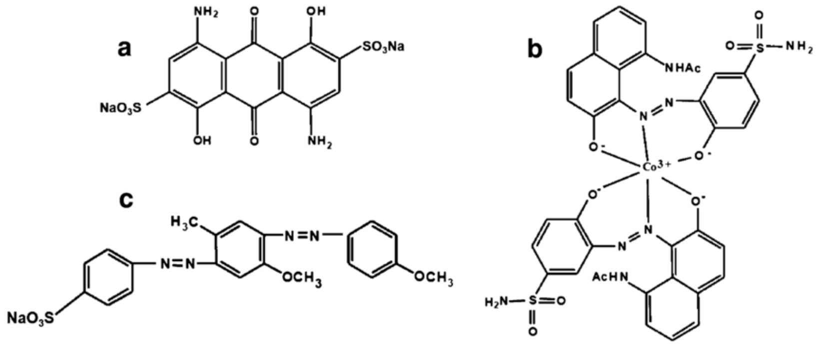

Figure 2.2 Chemical structures of acid dyes: (a) C.I. Acid Blue 45, (b) C.I. Acid Blue 171, (c) C.I. azo Orange 156

1) Hazards

1.1) In general, the long-term hazards of many of these dyes are unknown. Many acid dyes used to be food dyes, which have been shown to cause liver cancer in animal studies.

1.2) Glacial acetic acid and concentrated sulfuric acid are highly corrosive by skin contact, inhalation, or ingestion. Vinegar and dilute sulfuric acid are only slightly irritating by skin contact; repeat and long-term inhalation of the acetic acid and sulfuric acid vapors may cause chronic bronchitis. Splashing hot or boiling dye bath containing acid into the eyes could be extremely hazardous.

1.3) Glauber's salt (sodium sulfate) is only slightly toxic by ingestion, causing diarrhea.

2) Precautions

2.1) Use vinegar as a dyeing assistant rather than diluting glacial acetic acid or using sulfuric acid.

2.2) If dilute of concentrated acids, always add the acid to the water. Wear gloves, goggles, and a protective apron. An eyewash fountain and emergency shower should be available.

2.3) Wear goggles when dyeing at high temperatures to avoid splashing hot liquid in your eyes.

2.4) Boiling dye baths should be exhausted with a canopy hood, since the steam can carry dye with it into the air. [53]

2.3.2.2 Basic dyes

Basic dyes, these dyes are also known as cationic dyes. This a class of synthetic dyes, that act as bases and when made soluble in water, they form a colored cationic salt, which can react with the anionic sites on the surface of the substrate.

The basic dyes produce bright shades with high tinctorial values, on textile materials. Basic dyes are cationic soluble salts of colored bases. Basic dyes are applied to substrate with anionic character where electrostatic attractions are formed. Basic dyes are not used on cotton as the structures are neither planar nor large enough for sufficient substantively or affinity. Basic dyes are called cationic dyes because the chromophore in basic dye molecules contains a positive charge. The basic dyes react on the basic side of the isoelectric points. Basic dyes are salts, usually chlorides, in which the dyestuff is the basic or positive radical. Basic dyes are powerful coloring agents. It’s applied to wool, silk, cotton and modified acrylic fibres. Usually acetic acid is added to the dye bath to help the take up of the dye onto the fibre. Basic dyes are also used in the coloration of paper. The chemical structure of basic dyes were showed in Figure 2.3

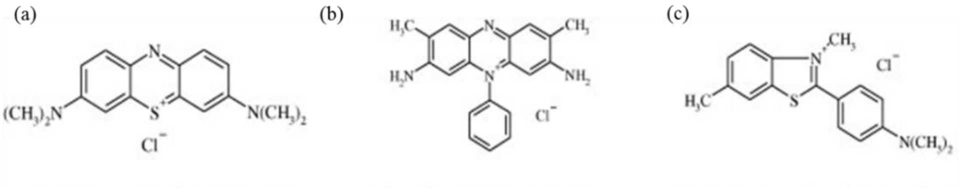

Methylene Blue (C.I. Basic Blue 9) Safranine O (C.I. Basic Red 2) Thioflavin T (C.I. Basic Yellow 1)

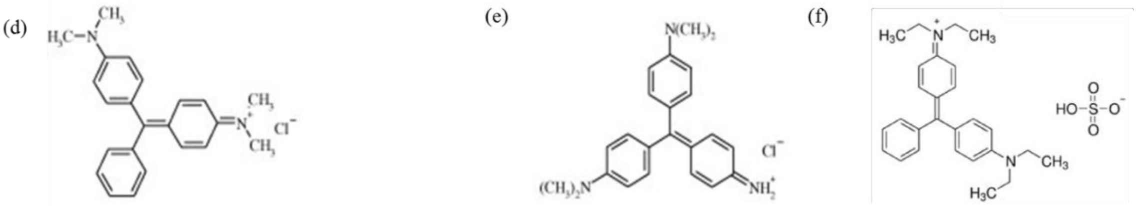

Malachite Green (C.I. Basic Green 4) Crystal Violet (C.I. Basic Violet 3) Brilliant green

Figure 2.3 Chemical structures of basic dyes

The most common anionic group attached to acrylic polymers is the sulphonate group, $-SO^{3-}$, closely followed by the carboxylate group, $-CO^{2-}$. These are either introduced as a result of co-polymerisation, or as the residues of anionic polymerization inhibitors. It is this anionic property which makes acrylics suitable for dyeing with cationic dyes, since there will be a strong ionic interaction between dye and polymer (in effect, the opposite of the acid dye-protein fibre interaction).

1) Hazards

1.1) Some basic dyes are known to cause skin allergies. Whether they cause respiratory allergies if inhaled is not known.

Precautions

1.2. See General Precautions.

2.3.2.3 Azo dyes

Dyes characterized by the presence of an azo group (-N=N-) as the chromophore. Azo dyes are found in many of the synthetic dye classes. The structure of azo dye were obtained in Figure 2.4 [54].

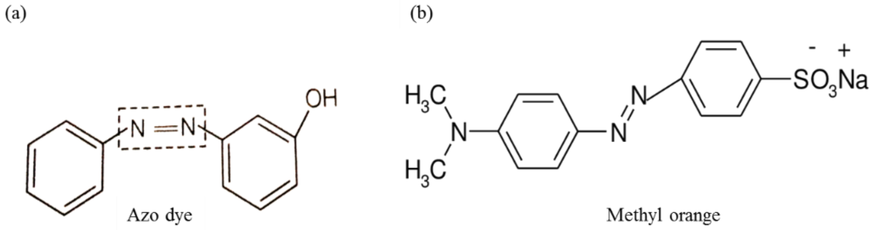

Figure 2.4 Chemical structure of azo dye: (a) Basic structure of azo dye, (b) Methyl orange

1) Hazards

1.1) Azoic dyes are very reactive, and may cause severe skin irritation (dermatitis, hyperpigmentation). Long-term effects of these dyes have not been well studied.

1.2) Lye (sodium hydroxide) is highly corrosive by skin and eye contact and ingestion.

1.3) Sulfonated castor oil is moderately toxic by ingestion.

2.4 Heavy matal

2.4.1 Cromium [55]

Chromium is a chemical element which has the symbol Cr and aromatic number 24. It is a steel-gray, lustrous, hard metal takes a high polish and has a high melting point. It is also odorless, tasteless and malleable.

Chromium is a naturally occurring element found in rocks and soil. It is present in the environment in general different form; the most common is trivalent chromium [Cr (III) or Cr^{3+}] and hexavalent [Cr (VI) or Cr^{6+}].Chromium is steels-grey, lustrous and hard. It is used on large scale in the metallurgical and chemical industries. Metallurgical industry commonly uses chromium for the production of stainless steels, alloy cast iron and nonferrous alloys as well as for plating steel. In the chemical industry, Cr^{3+} and Cr^{6+} are used primarily in pigments, metal finishing and electroplating as well as wood preservatives and leather tanning. In the past, chromium was also used in cooling towers as a rust and corrosion inhibitor and as a fungicide.

2.4.1.1 Applications of chromium

The following are the application areas of chromium:

1) In metal ceramics
2) In chrome plating
3) As dyes and paints
4) To produce synthetic rubies
5) In alloys, e.g., stainless steel
6) To manufacture molds for the firing of bricks
7) As a catalyst in dyeing and tanning of leather
8) In metallurgy to provide corrosion resistance and a shiny finish

2.4.1.2 Toxicity

People can be exposed to chromium through breathing, eating or drinking and through skin contact with chromium or chromium compounds. The level of chromium in air and water is generally low. In drinking water the level of chromium is usually low as well, but contaminated well water may contain the dangerous chromium(IV); hexavalent chromium. For most people eating food that contains chromium (III) is the main route of chromium uptake, as chromium(III) occurs naturally in many vegetables, fruits, meats, yeasts and grains. Various ways of food preparation and storage may alter the chromium contents of food. When food in stores in steel tanks or cans chromium concentrations may rise.

1) Chromium (III) is an essential nutrient for humans and shortages may cause heart conditions, disruptions of metabolisms and diabetes. But the uptake of too much chromium (III) can cause health effects as well, for instance skin rashes.

2) Chromium (VI) is a danger to human health, mainly for people who work in the steel and textile industry. People who smoke tobacco also have a higher chance of exposure to chromium.

3) Chromium(VI) is known to cause various health effects. When it is a compound in leather products, it can cause allergic reactions, such as skin rash. After breathing it in chromium (VI) can cause nose irritations and nosebleeds.

Other health problems that are caused by chromium (VI) are:

3.1) Skin rashes
3.2) Upset stomachs and ulcers
3.3) Respiratory problems
3.4) Weakened immune systems
3.5) Kidney and liver damage
3.6) Alteration of genetic material
3.7) Lung cancer
3.8) Death

2.4.2 Cadmium [56]

Cadmium is a chemical element with the symbol Cd and atomic number 48. This soft, silvery-white metal is chemically similar to the two other stable metals in group 12, zinc and mercury. Like zinc, it demonstrates oxidation state +2 in most of its compounds, and like mercury, it has a lower melting point than the transition metals in groups 3 through 11. Cadmium and its congeners in group 12 are often not considered transition metals, in that they do not have partly filled d or f electron shells in the elemental or common oxidation states.

The average concentration of cadmium in Earth's crust is between 0.1 and 0.5 parts per million (ppm). It was discovered in 1817 simultaneously by Stromeyer and Hermann, both in Germany, as an impurity in zinc carbonate. Cadmium occurs as a minor component in most zinc ores and is a byproduct of zinc production. Cadmium was used for a long time as a corrosion-resistant plating on steel, and cadmium compounds are used as red, orange and yellow pigments, to color glass, and to stabilize plastic.

Cadmium use is generally decreasing because it is toxic (it is specifically listed in the European Restriction of Hazardous Substances) and nickel-cadmium batteries have been replaced with nickel-metal hydride and lithium-ion batteries. One of its few new uses is in cadmium telluride solar panels.

Although cadmium has no known biological function in higher organisms, a cadmium-dependent carbonic anhydrase has been found in marine diatoms.

2.4.2.1 Application

Cadmium is a common component of electric batteries, pigments, coatings and electroplating.

1) Batteries Ni-Cd batteries

In 2009, 86% of cadmium was used in batteries, predominantly in rechargeable nickel-cadmium batteries. Nickel-cadmium cells have a nominal cell potential of 1.2 V. The cell consists of a positive nickel hydroxide electrode and a negative cadmium electrode plate separated by an alkaline electrolyte (potassium hydroxide). The European Union put a limit on cadmium in electronics in 2004 of 0.01%, with some exceptions, and reduced the limit on cadmium content to 0.002%. Another type of battery based on cadmium is the silver-cadmium battery.

2) Electroplating A photograph and representative spectrum of photoluminescence from colloidal CdSe quantum dots

3) Cadmium electroplating, consuming 6% of the global production, is used in the aircraft industry to reduce corrosion of steel components. This coating is passivated by chromate salts. A limitation of cadmium plating is hydrogen embrittlement of high-strength steels from the electroplating process. Therefore, steel parts heat-treated to tensile strength above 1300 MPa (200 ksi) should be coated by an alternative method (such as special low-embrittlement cadmium electroplating processes or physical vapor deposition).

4) Titanium embrittlement from cadmium-plated tool residues resulted in banishment of those tools (and the implementation of routine tool testing to

detect cadmium contamination) in the A-12/SR-71, U-2, and subsequent aircraft programs that use titanium.

5) Nuclear fission

Cadmium is used in the control rods of nuclear reactors, acting as a very effective "neutron poison" to control neutron flux in nuclear fission. When cadmium rods are inserted in the core of a nuclear reactor, cadmium absorbs neutrons, preventing them from creating additional fission events, thus controlling the amount of reactivity. The pressurized water reactor designed by Westinghouse Electric Company uses an alloy consisting of 80% silver, 15% indium, and 5% cadmium.

6) Televisions

QLED TVs have been starting to include cadmium in construction. Some companies have been looking to reduce the environmental impact of human exposure and pollution of the material in televisions during production.

7) Anticancer drugs Complexes based on heavy metals have great potential for the treatment of a wide variety of cancers but their use is often limited due to toxic side effects. However, scientist are advancing on the field and new promising cadmium complex compounds with reduced toxicity have been discovered.

2.4.2.2 Toxicity

Chromium is used in metal alloys and pigments for paints, cement, paper, rubber, and other materials. Low-level exposure can irritate the skin and cause ulceration. Long-term exposure can cause kidney and liver damage, and damage too circulatory and nerve tissue. Chromium often accumulates in aquatic life, adding to the danger of eating fish that may have been exposed to high levels of chromium.

2.4.3 Zinc [57]

Zinc is a transition metal with the following characteristics: period 4, group IIB, atomic number 30, atomic mass 65.4, density 7.14 g cm^{-3}, melting point 419.5°C, and boiling point 906 °C. Zinc occurs naturally in soil (about 70 mg kg^{-1} in crustal rocks), but Zn concentrations are rising unnaturally, due to anthropogenic additions. Most Zn is added during industrial activities, such as mining, coal, and waste combustion and steel processing. Many foodstuffs contain certain concentrations of Zn. Drinking water also contains certain amounts of Zn, which may be higher when it is stored in metal tanks. Industrial sources or toxic waste sites may cause the concentrations of Zn in drinking water to reach levels that can cause health problems. Zinc is a trace element that is essential for human health. Zinc shortages can cause birth defects. The world’s Zn production is still on the rise which means that more and more Zn ends up in the environment. Water is polluted with Zn, due to the presence of large quantities present in the wastewater of industrial plants. A consequence is that Zn-polluted sludge is continually being deposited by rivers on their banks. Zinc may also increase the acidity of waters. Some fish can accumulate Zn in their bodies, when they live in Zn-contaminated waterways. When Zn enters the bodies of these fish, it is able to bio magnify up the food chain. Water-soluble zinc that is located in soils can contaminate groundwater. Plants often have a Zn uptake that their systems cannot handle, due to the accumulation of Zn in soils. Finally, Zn can interrupt the activity in soils, as it negatively influences the activity of microorganisms and earthworms, thus retarding the breakdown of organic matter.

2.4.3.1 Applications

1) Zinc has good electromagnetic field resistance properties. In the case of radio frequency interference, zinc plate is a very effective shielding material.

And as zinc is non-magnetic, it is suitable for making components and covers of instruments and meters. Since zinc produces no sparks, either alone or in collision with other metals, it is suitable for making explosion-proof equipment.

2) Zinc fertilizer (e.g. zinc sulfate and zinc chloride) can promote plant cell respiration and carbohydrate metabolism.

3) Zinc powder, lithopone and zinc chrome can be made into pigments.

4) Zinc oxide can also be used in the pharmaceutical, rubber, paint and other industries.

2.4.3.2 Toxicity

1) Signs and symptoms

Following an oral intake of extremely high doses of zinc (where 300 mg Zn/d – 20 times the US RDA – is a "low intake" overdose), nausea, vomiting, pain, cramps and diarrhea may occur. There is evidence of induced copper deficiency, alterations of blood lipoprotein levels, increased levels of LDL, and decreased levels of HDL at long-term intakes of 100 mg Zn/d. The USDA RDA is 15 mg Zn/d. There is also a condition called the "zinc shakes" or "zinc chills" or metal fume fever that can be induced by the inhalation of freshly formed zinc oxide formed during the welding of galvanized materials.

2) Zinc has been used therapeutically at a dose of 150 mg/day for months and in some cases for years, and in one case at a dose of up to 2000 mg/day zinc for months. A decrease in copper levels and hematological changes have been reported; however, those changes were completely reversed with the cessation of zinc intake.

However, zinc has been used as zinc gluconate and zinc acetate lozenges for treating the common cold and therefore the safety of usage at about 100 mg/day level is a relevant question. Thus, given that doses of over 150 mg/day for months to years have caused no permanent harm in many cases, a one-week usage of about 100 mg/day of zinc in the form of lozenges would not be expected to cause serious or irreversible adverse health issues in most persons. Unlike iron, the elimination of zinc is concentration-dependent.

2.5 Kailin/Metakaolin

Kaolinite is the most common clay mineral used in geopolymer synthesis. It has 1:1 uncharged dioctahedral layer structure (Figure2.5a) where by the layers are $(Si_2O_5)_n^{2-}$ sheet and the $Al(OH)_3$ (gibbsite) sheet linked by sharing oxygen atoms. The layers are held together by weak Van Der Waals and hydrogen bonds leading to the layered structure (Figure 2.5b).

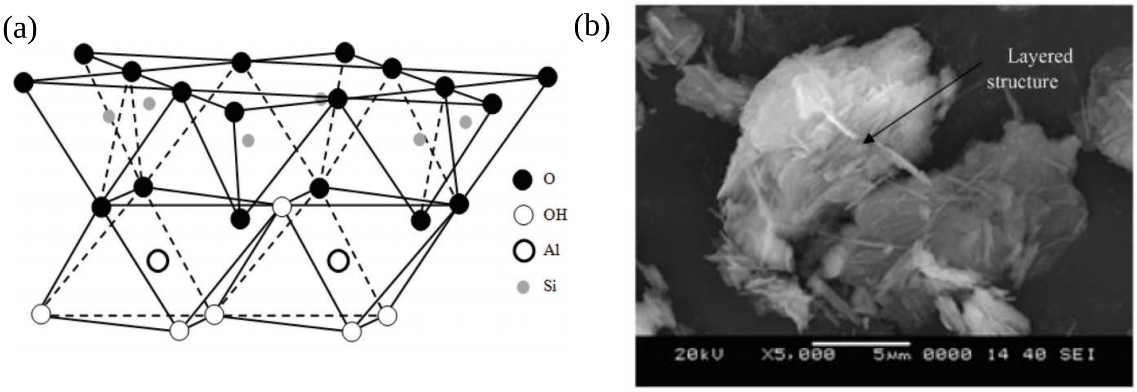

Figure 2.5 Structure of kaolin (a); SEM image of metakaolin (b) [58]

Thermal treatment of kaolinite leads to the transformation of crystalline phases into reactive amorphous phases [59], which is the active constituent that determines the final strength of geopolymer.

The thermal treatment is usually carried out at temperature in the range of 550–800°C which accompanied by dehydroxylation of strongly bounded hydroxyl ions on the Al-constitutive layer. Thus, kaolinite is transformed into metakaolin. Metakaolin also has layered structure as kaolinite even after the thermal treatment process.

However, the layer structure appeared more open than kaolinite [60]. Also, the thermal treatment damages the hexagonal layer of kaolinite and cause atomic preparation that transformed the hexa coordinated Al ion of kaolinite are transformed into penta and tetra-coordinated Al ions [61]. The amount of penta and tetra-coodinated ions reflects the reactivity of metakaolin [62].

2.6 Process of power plant

A power plant's a bit like an energy production line. Fuel feeds in at one end, and electricity zaps out at the other. A whole series of different steps, roughly along these lines:

Artwork showing the steps involved in how a power plant makes electricity

(1) Fuel: The energy that finds its way into your TV, computer, or toaster starts off as fuel loaded into a power plant. Some power plants run on coal, while others use oil, natural gas, or methane gas from decomposing rubbish.

(2) Furnace: The fuel is burned in a giant furnace to release heat energy.

(3) Boiler: In the boiler, heat from the furnace flows around pipes full of cold water. The heat boils the water and turns it into steam.

(4) Turbine: The steam flows at high-pressure around a wheel that's a bit like a windmill made of tightly packed metal blades. The blades start turning as the steam flows past. Known as a steam turbine, this device is designed to convert the steam's energy into kinetic energy (the energy of something moving). For the turbine to work efficiently, heat must enter it at a really high temperature and pressure and leave at as low a temperature and pressure as possible.

(5) Cooling tower: The giant, jug-shaped cooling towers you see at old power plants make the turbine more efficient. Boiling hot water from the steam turbine is

cooled in a heat exchanger called a condenser. Then it's sprayed into the giant cooling towers and pumped back for reuse. Most of the water condenses on the walls of the towers and drips back down again. Only a small amount of the water used escapes as steam from the towers themselves, but huge amounts of heat and energy are lost.

(6) Generator: The turbine is linked by an axle to a generator, so the generator spins around with the turbine blades. As it spins, the generator uses the kinetic energy from the turbine to make electricity.

(7) Electricity cables: The electricity travels out of the generator to a transformer nearby.

(8) Step-up transformer: Electricity loses some of its energy as it travels down wire cables, but high-voltage electricity loses less energy than low-voltage electricity. So the electricity generated in the plant is stepped-up (boosted) to a very high voltage as it leaves the power plant.

(9) Pylons: Hugh metal towers carry electricity at extremely high voltages, along overhead cables, to wherever it is needed.

(10) Step-down transformer: Once the electricity reaches its destination, another transformer converts the electricity back to a lower voltage safe for homes to use.

(11) Homes: Electricity flows into homes through underground cables.

(12) Appliances: Electricity flows all round your home to outlets on the wall. When you plug in a television or other appliance, it could be making a very indirect connection to a piece of coal hundreds of miles away. The process of power plant was showed in Figure 2.3.

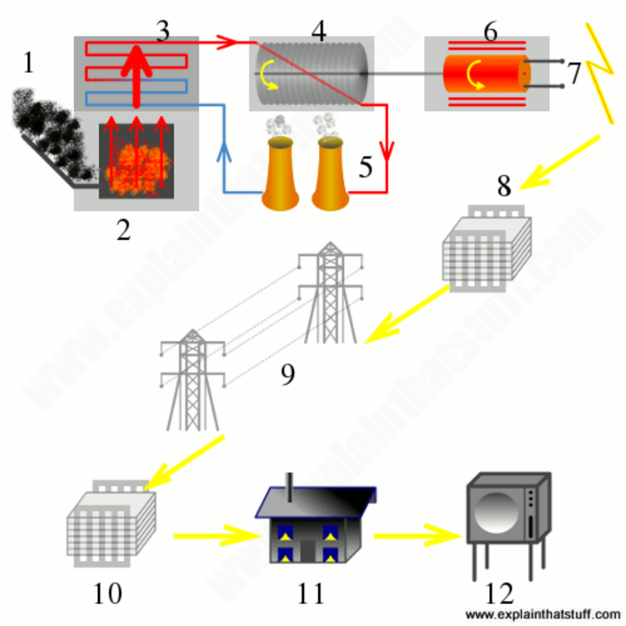

Figure 2.6 Process of power plant [63]

2.6.1 Mae Moh fly ash

Electricity Generating Authority of Thailand or EGAT produces and sells three types of lignite products from the lignite-fired power generation of Mae Moh Power Plant in Lampang province, such as:

2.6.1.1 Lignite Fly Ash

2.6.1.2. Lignite bottom ash

2.6.1.3. Synthetic gypsum

2.6.2 Lignite Fly Ash

2.6.2.1 Quality

EGAT's lignite fly ash is classified as C (ASTM C 618) type, with specific gravity of 2.00-2.60 and containing free lime of less than 3% and sulfur trioxide (SO_3) of less than 5%.

2.6.2.2 Uses and benefits

EGAT's lignite fly ash products have good pozzolan or binding properties and are therefore an excellent choice for construction material to substitute Portland Cement Type 1 at a much cheaper cost. Fly ash products can also be used as filler for the ready-mixed concrete production, enhancing strength and durability of concrete. Lignite fly ash products also help save energy used during the concrete mixing process as the spherical and fine shape of the fly ash grains contributes to low friction between particles.

2.6.3 Lignite Bottom Ash

2.6.3.1 Quality

EGAT's lignite bottom ash is black color with its particle size of 0.1-10 mm. and specific gravity of 3-5.

3.6.3.2 Uses and benefits

EGAT's researches and studies on the application of lignite bottom ash from Mae Moh Power Plants have indicated the Mae Moh lignite bottom ash offers excellent potential for use as an aggregate in road construction or concrete as well in the production of concrete blocks for various construction works. Bottom ash can also be used for agricultural purposes. [5]

2.7 Rice husk [65]

Rice husk are the coatings of seeds, or grains, of rice. The husk protects the seed during the growing season and is formed from hard materials, including opaline silica and lignin. The hull is hard to eat or swallow and mostly indigestible to humans because of its enriched fiber components. However, some poor people in ancient China made a type of pastry which mixes rice husks, wild vegetables, and soybean powder as the portion of daily food for satisfying the hunger, especially during periods of drought and crop-failure. One idiom, cereals hulls and vegetables as the chow of a half year, is to describe people suffering with economic hardships and food shortage. Winnow used to separate the rice from hulls, is to put the whole rice into a pan and throw it into the air while the wind blows. The light hulls are blown away while the heavy rice fall back into the pan. Later pestles and a simple machine called a rice pounder were developed to remove hulls. In 1885 the modern rice hulling machine was invented in Brazil. During the milling processes, the hulls are removed from the raw grain to reveal whole brown rice, which may then sometimes be milled further to remove the bran layer, resulting in white rice.

2.7.1 Uses and benefits

2.7.1 Ash
2.7.2 Toothpaste
2.3.3 Brewing
2.7.4 Fertilizer and substrate
2.7.5 Fireworks

2.8 Adsorption isotherm

Adsorption is usually explained through isotherm, which are functions that connect the amount of adsorbate on the adsorbent, with its pressure or concentration (if gas or liquid).

The equilibrium of the adsorption and the kinetics are two important physiochemical aspects for the assessment of the adsorption process as a unit operation. Equilibrium studies give the capacity of the adsorbent. The relationship of equilibrium between adsorbate and adsorbent are explained by adsorption isotherm, normally the ratio between the quantity adsorbed and remaining in solution as a fixed temperature at the equilibrium. There are two types of adsorption isotherms that are popular and easily to operate: Freundlich and Langmuir isotherm

2.8.1 Freundlich isotherm

In 1906, Herbert Max Finley Freundlich, a German physical chemist, showed an empirical adsorption isotherm for non-ideal system. The Freundlich adsorption isotherm is an adsorption isotherm that is a curve relating the concentration of a solute on the surface of an adsorbent and the concentration of the solute in the liquid with which it is in contact.

Freundlich adsorption isotherm is the earliest known relationship explaining the adsorption equation and is frequently expressed as equation 2.1:

$$\log q_e = \log K_F + \frac{1}{n} \log C_e, \tag{2.1}$$

Where;	C_{ads}	is	the concentration of dyes solution adsorbed onto adsorbent
	C_e	is	the equilibrium concentration of dyes in solution

n	is	a characteristic constant for the adsorption system under study
K	is	a parameter related to the temperature

A plot of log C_{ads} as y- axis against log C_e as x-axis yielding a straight line indicates the conformation of the Freundlich isotherm. The constant can be defined from the slope and the intercept.

K and 1/n are constants for a given adsorbent and adsorbate at a particular temperature. The value of n between 2to 10 presents the best adsorption. The value of $0<1/n<1$ indicates that adsorption capacity is only slightly suppressed at lower equilibrium concentrations. This isotherm doesn’t predict any saturation of the adsorbent by adsorbates; therefore infinite surface coverage is predicted mathematically, indicating multilayer adsorption on the surface.[65]

2.8.2 Langmuir isotherm

Langmuir Isotherm model was originally developed to explain and quantify sorption on a set of evident localized adsorption sites and has been used to describe both physical and chemical adsorption and monolayer adsorption. This model can be suppositions are following [66] :

2.8.2.1 Molecule of adsorbate on define localized site and the fullness corresponds to full occupancy of these sites.

2.8.2.2 The adsorption site are all forcefully homogeneous, and there isn’t interaction between adsorbed molecules.

2.8.2.3 Each active site interactions with only one adsorbate.

This model is expressed by the following equation 2.2;

$$\frac{C_e}{q_e} = \frac{1}{q_m K_e} + \frac{C_e}{q_m}, \qquad (2.2)$$

When;	q_e	is	the amount of dye at equilibrium (mg g^{-1})
	C_e	is	the equilibrium concentration of dye (mg L^{-1})
	K_L	is	the Langmuir constant (L mg^{-1})

q_m	is	amount of monolayer adsorption capacity (mg g^{-1})

The linear form can be used for linearization of experimental data by plotting C_e/C_{ads} as y-axis against C_e as x-axis over the entire concentration range of investigated adsorbate. The value of K_L represents monolayer coverage of adsorbate with adsorbent and K_e represents enthalpy of adsorption and should vary with temperature. Minimum value of K_e represents chemical bonding between adsorbate and adsorbent are stable and strong.

2.9 Adsorption kinetic [67]

Adsorption kinetics explain the reaction pathways, as well as the time to reach the equilibrium. It also showed large dependence on the physical and chemical characteristics of the adsorbent material, which also influence the adsorption mechanism that can be either film or pore diffusion or due the combination of both depending on the system hydrodynamics.

2.9.1 Pseudo-First Order Model

The Lagergren pseudo-first order model is most usually used to explains the adsorption of solute from a liquid solution. The pseudo-first order equation is expressed by the following equation 2.3;

$$\frac{dq_t}{dt} = k_1(q_e - q_t) \qquad (2.3)$$

Where;	q_t and q_e	are	the amounts of adsorbed at time t and equilibrium (mg/g)
	k_1	is	the pseudo-first order rate constant for the adsorption (min).

After integration and applying boundary conditions t = 0 to t = t and $q_t = 0$ to $q_t = q_t$, the integrated form of Equation 2.3 becomes equation 2.4;

$$\text{Log}\,(q_e - q_t) = \text{Log}\, q_e - k_1 t \tag{2.4}$$

When the value of log (q_e-q_t) were linearly correlated with t, the plot of log (q_e-q_t) versus t will give a linear relationship from which k_1 and q_e can be determined from the slope and intercept of the graph respectively.

2.9.2 Pseudo-Second Order Model

In this model, the rate limiting step is the surface adsorption that involves chemisorption, where the adsorbate removal from a solution is due to physicochemical interactions between the two phases; the kinetics rate equation is expressed as equation 2.5;

$$\frac{dq_t}{dt} = k_2 (q_e - q_t)^2 \tag{2.5}$$

Where; k_2 is the equilibrium rate constant of pseudo-second order equation (g/mg min). For the boundary conditions t=0 and t=t and $q_t=0$ and $q_t = q_t$, the integrated form of Equation 2.5 becomes;

$$\frac{1}{q_e - q_t} = \frac{1}{q_e} + k_2 t \tag{2.6}$$

Which is the integrated rate law for a pseudo-second order reaction. Equation 2.6 can be rearranged to obtain;

$$q_t = \frac{1}{\left(\frac{1}{k_2 q_e^2}\right) + \frac{t}{q_e}} \tag{2.7}$$

Which has a linear form :

$$\frac{1}{q_t} = \frac{1}{h} + \frac{t}{q_e} \quad (2.8)$$

Where h (mg/g. min) can be regarded as the initial sorption rate ($h = k_2q_e$)

2.10 Thermodynamic

In order to applying the principles of thermodynamics in adsorption system, it is important to consider that the substance adsorbed onto the solid surface constitutes a separate phase. The combination of the adsorbed substance and the sorbent may be considered as a subsystem and the equilibrium sorption can be regarded as phase equilibrium between this subsystem and the free substance. In other words, adsorption maybe considered as the distribution of a chemical species between a phase and an inter face which is generated at the boundaries, when a phase is separated from another. Thermodynamic parameters (ΔH°, ΔG°, ΔS°) are useful for the elucidation of the mechanism of adsorption. These parameters provide quantitative data on the phenomenon and information about the changes of the adsorbent during the progress of adsorption [68].

2.10.1 Change in enthalpy

The energy of adsorption can be characterized by the standard enthalpy of sorption ΔH° (kJ mol^{-1}), which is the amount of heat absorbed or released during adsorption and is directly related to the interaction energy between the molecules of the adsorbed substance and the points of the solid adsorbent. Reactions that absorb heat is the positive ΔH° molecules endothermic reaction. Negative ΔH° is molecules exothermic reaction. Under standard conditions, the Van't Hoff equation is [69];

$$\frac{\partial \ln K_d}{\partial T} = \frac{\Delta H^0}{RT^2} \quad (2.9)$$

Where;	R (8.314 J mol-1 K-1)	is	the gas constant
	K_d	is	the coefficient of the substance between the phases of solid and liquid.

$$\ln K_c = \frac{-\Delta H^\circ}{RT} + c \qquad (2.10)$$

ΔH^o is calculated from the slope obtained by plotting the $\ln K_c$ versus 1/T and is independent of the units of K_c .

2.10.2 The change in Gibbs free energies

The change in Gibbs free energies is calculated with equation 2.11;

$$\Delta G^\circ = -RT\ln K_c \qquad (2.11)$$

Entropy is a statistical measurement of the number of states or accessible conformations. A positive ΔS^o is an indication that the disorder or number of accessible of the system is increasing and vice versa.

2.11 Literature reviews

Wang et al. (2005) [35] studied fly ash and red mud as adsorbents for the removal of a typical basic dye, methylene blue, from aqueous solution. Heat treatment and chemical treatment have also been applied to the as-received fly ash and red mud samples. It is found that fly ash generally shows higher adsorption capacity than red mud. The raw fly ash and red mud show adsorption capacity at 1.4×10^{-5} and 7.8×10^{-6} mol/g, respectively. Heat treatment reduces the adsorption capacity for both fly ash and red mud but acid treatment by HNO_3 induces a different effect on fly ash and red mud. Nitric acid treatment results in an increase in adsorption capacity of fly ash (2.40×10^{-5} mol/g) while it decreases the adsorption capacity for red mud (3.20×10^{-6} mol/g). The adsorption data have been analysed using Langmuir, Freundlich and Redlich–Peterson isotherms. The results indicate that the Redlich–Peterson model provides the best correlation of the experimental data. Isotherms have also been used to obtain the thermodynamic parameters such as free energy, enthalpy and entropy of adsorption. For fly ash and red mud, adsorption of methylene blue is endothermic reaction with at 76.10 and 10.80 kJ/mol, respectively.

Sindhunata et al. (2006) [70] studied the development of the pore structure of geopolymers synthesized from class F fly ash using electron microscopy and porosimetry. Fly-ash-based geopolymer can be classified as a mesoporous aluminosilicate material, with a Si/Al composition varying from 1.51 to 2.24.

The Si/Al composition and pore structure of fly-ash-based geopolymer vary depending on the curing temperature and the silicate ratio of the activating solutions (SiO_2/M_2O, M = Na or K). A higher Si/Al ratio and pores are obtained in geopolymers synthesized at higher temperature and silicate ratios. Elevating the curing temperature increases the extent and rate of reaction, shown through an increase in mesopore volume, surface area, and an accelerated setting time. The kinetics appears to be temperature-controlled only before the material is hardened. Very high silicate ratios ($SiO_2/M_2O \geq 2.0$) are also believed to slow the reactions. The pore structure of K-based geopolymer is more susceptible to change in temperature than that of Na-based geopolymer.

Wongyai et al. (2006) [71] studied the fly ash from Mae Moh power plants for the removal of trace metals in wastewater. The purpose of this study was to investigate the possibility of the utilization of lignite fly ash as a low cost adsorbent. Additionally, the distribution of the fly ash composition was also tested. The study region is the Mae Moh power plants area with the large accumulation of byproducts (~3,000 million tonnes/ year). Batch adsorption method were conducted under various conditions of metal concentration, pH and a dosage of fly ash. The heavy metals used in this study were arsenic, lead, copper and selenium. Adsorption studies were done at various pH values (3 to12) at 25 ˚ C and at heavy metal concentrations of 50 to 400 ppm using fly ash concentrations of 10 and 20 g/L. The fly ash contained of silica, aluminum, iron, calcium, manganese sodium and potassium was analyzed and the composition of Mae Moh fly ash is similar to clay with large amounts of silica, aluminum and some unburned carbon. The leachates water from fly ash not found to be enriched in heavy metals to exceed significantly the standard concentrations. The feasibility of using fly-ash to remove arsenic and other metals from wastewater was estimated. These results showed that the arsenic concentration in wastewater decreased up to 75.30 %. Other metals mobility shows a similar pattern to that of arsenic, with similar reduction of concentrations.

The pH of the experiment solution batch is the key factor affecting the mobility of these trace elements in this wastewater. The positive relationship was shown between amount of arsenic and other metals adsorbed per unit weight of adsorbent and increasing fly ash concentrations. The adsorption of all the metal ions increased with increasing temperature indicating endothermic nature of the adsorption process.

Mane et al. (2007) [72] was studied the adsorption of brilliant green (BG) on rice husk ash (RHA). RHA is a solid waste obtained from the particulate collection equipment attached to the flue gas lines of rice husk fired boilers. Batch adsorption studies were performed to evaluate the influences of various experimental parameters like initial pH, contact time, adsorbent dose and initial concentration on the removal of BG. Optimum conditions for BG removal were pH = 3.0, adsorbent dose = 6 g/L of solution and equilibrium time = 5 hr for the range of 50–300 ppm. Adsorption of BG followed pseudo-second-order kinetics. Equilibrium isotherms for the adsorption of BG on RHA were analyzed by Freundlich, Langmuir, Redlich–Peterson (R–P), Dubnin–Radushkevich (D–R), and Temkin isotherm models using a non-linear regression technique.

Langmuir and R–P isotherms were best represent the data for BG adsorption onto RHA. Adsorption of BG on RHA is favourably influenced by an increase in the temperature of the operation. Values of the change in entropy (ΔS^0) and heat of adsorption (ΔH^0) for BG adsorption on RHA were positive. The high negative value of change in Gibbs free energy (ΔG^0) indicates the feasible and spontaneous adsorption of BG on RHA.

Mane et al. (2007) [73] studied the adsorption of brilliant green (BG) on carbon rich bagasse fly ash (BFA). BFA is a solid waste obtained from the particulate collection equipment attached to the flue gas line of the bagasse-fired boilers of cane sugar mills. Batch adsorption studies were performed to evaluate the influences of various experimental parameters like initial pH, contact time, adsorbent dose and initial concentration on the removal of BG. Optimum conditions for BG removal were pH_0 = 3, adsorbent dose = 3 g/L of solution and equilibrium time = 5 hr. Adsorption of BG followed pseudo-second-order kinetics. Intra-particle diffusion does not seem to control the BG removal process. Equilibrium isotherms for the adsorption of BG on BFA were analyzed by Freundlich, Langmuir, Redlich–Peterson, Dubnin–Radushkevich, and Temkin isotherm models using non-linear regression technique. Redlich–Peterson and Langmuir isotherms were found to best represent the data for BG adsorption onto BFA.

Adsorption of BG on BFA is favourably influenced by an increase in the temperature of the operation. Values of the change in entropy (ΔS^0) and heat of adsorption (ΔH^0) for BG adsorption on BFA were positive. The high negative value of change in Gibbs free energy (ΔG^0) indicates the spontaneous adsorption of BG on BFA.

Yao et al. (2009) [74] studied the geopolymerization process of metakaolinite activated by alkali and alkali silicate solutions. The effects of alkali concentration, modulus of alkali silicate solution and reaction temperature on geopolymerization were studied systematically by isothermal calorimetry, as well as XRD and 27Al/29Si MAS NMR. Results shows that the geopolymerization process of metakaolinite under alkali activation condition can be reasonably supposed into three stages: (I) destruction, (II) polymerization and (III) stabilization. The rate of geopolymerization in KOH solution is higher than in NaOH solution and reaches the maximum in 15 mol/L KOH solution during stage II. The extent of geopolymerization increases with increasing of alkali content regardless of the existence of silicate anions in activator.

Rovnanik et al. (2010) [75] studied the properties of metakaolin-based geopolymer directly impacted not only by the specific surface and composition of initial metakaolin and the type, composition and relative amount of alkali activator usedbut they also depend on the conditions during the initial period of geopolymerization reaction. This study aimed to analyze the effect of curing temperature (10, 20, 40, 60 and 80˚C) and time on the compressive and flexural strengths, pore distribution and microstructure of alkali activated metakaolin material. The results have shown that the treatment of fresh mixture at elevated temperatures accelerates the strengths development but the 28 days mechanical properties are deteriorated in comparison with results obtained for mixtures that were treated at an ambient or slightly decreased temperature. The influence of curing temperature on microstructure of geopolymer matrix was verified in terms of pore distribution studied by means of mercury intrusion porosimetry.

The study revealed a tendency to increase pore size and cumulative pore volume with rising temperature, which is reflected in mechanical properties. It has been also shown the possibility of monitoring the geopolymerization reaction by means of infrared spectroscopy.

White et al. (2010) [76] investigated Neutron pair distribution function (PDF) analysis utilized to advance the understanding of the local atomic structural characteristics of geopolymer binders derived from metakaolin, specifically the nature and amount of the water associated with these materials. Samples were heated in air to temperatures up to 1200˚C, then analyzed ex situ by high momentum transfer neutron total scattering and PDF analysis. Water contained in large pores, along with water associated with hydration of potassium cations in the geopolymer framework structure, comprise the majority of water in this material.

The remaining water is situated in small pores and as terminal hydroxyl groups attached to the Si–Al framework. The Si–Al framework structure undergoes only subtle rearrangement upon heating, but maintains a tetrahedral aluminosilicate framework environment. After crystallization with heating beyond 1000˚C, the geopolymer gel is predominantly converted to leucite, with small amounts of amorphous mullite and glassy silica, which have never before been observed in heated geopolymers. This demonstrates the value of neutron PDF analysis to probe the local structure of these important geopolymeric materials.

Zhang et al. (2012) [77] investigated isothermal conduction calorimetry (ICC) to measure the kinetics of geopolymerisation of metakaolin by reaction with NaOH solution under a variety of conditions. Three exothermic peaks are observed in the calorimetric curve, and are assigned to the dissolution of metakaolin, the formation of geopolymer with disordered or locally ordered structure, and finally the reorganization and partial crystallization of this inorganic polymer gels. For the purpose of further quantifying the ICC data, the geopolymeric reaction products are assumed to have an analcime-like local structure, and their standard formation enthalpies are estimated from the available data for this structure. This assumption enables ICC to be used for the first time in a quantitative manner to determine the real reaction kinetics of geopolymerization. Increasing the NaOH concentration up to a molar overall Na/Al ratio of 1.1 seen to enhance the reaction extent observed at 3 days, up to a maximum of around 40% in the high liquid/solid ratio systems studied and accelerates the crystallization process. However, further addition of NaOH does not give any additional reaction within this period, or any further acceleration. Raising the reaction temperature from 25 °C to 40 °C increases the initial reaction rate but has little effect on the final reaction extent, particularly when Na/Al > 1.

Zhang et al. (2013) [48] investigated the outcomes of a study using isothermal conduction calorimetry (ICC) to characterize the geopolymerization kinetics of metakaolin activated with sodium silicate. Two exothermic peaks are observed in the calorimetric curves for all systems reacting within the temperature range 20–40˚C. The peaks are assigned to the dissolution of metakaolin and the formation of geopolymeric gels with disordered structure, respectively. Compared with the use of NaOH solution to activate metakaolin, the presence of soluble silicate in the activator hinders the reorganization of the local structure of geopolymeric gels and also suppresses the formation of zeolites or zeolite precursors.

Decreasing the modulus from 1.6 to 1.0 increases the fractional reaction extent from 0.12 to 0.26 after 72 hr at 25 ˚C. When the modulus is 1.2, increasing the reaction temperature from 20 ˚C to 35 ˚C results in an improved reaction extent from 0.24 to 0.35. The rapid polymerization that occurs at 40 ˚C appears to hinder the further reaction of MK and consequently results in a lower reaction extent than at 35 ˚C. Combined with the findings from previous analysis of systems where NaOH used to activate MK, the concentration of available Na^+ appears to have a more pronounced influence on the extent of geopolymerization than temperature and the concentration of soluble Si. The higher reaction extent of the solid precursor particles with the soluble Si from the activator results in binders with more compact microstructure and higher mechanical strength.

Ferrero et al. (2015) [78] coal fly ash was characterized in batch adsorption with acid and basic dyes.Good results of removal were obtained, although strongly dependent on initial dye concentration, ash dosage and above all on pH of the solution. The maximum adsorption capacities per g of fly ash were 410 mg/g of acid blue 25 and 142 mg/g of basic blue 9, both with an ash dosage of 2 g/L at pH 11 after a contact time of 1 hr. However, increasing the ash dosage to 20 g/L and contact time to 24 hr, the maximum adsorption capacity of basic blue 9 raised 187 mg/g fly ash at pH 11, but this value was lowered to 8.4 mg/g at pH 7. Afterwards, flow experiments were carried out in semi-batch mode with a fixed amount of ash and continuous flow of dye solution in continuous stirred tank reactor, to determine the exhaustion curves of fly ash. In this last equipment, the optimum conditions were investigated to obtain the highest yields of dye removal from solutions at low concentrations (5 to 20 ppm) such as those occur in rinsing waters arising from dyeing processes.

Khan et al. (2015) [79] investigated the synthesized geopolymers for the adsorption of methylene blue (MB) by investigating the effect of the amount of adsorbent, pH of the solution and shaking period. The batch kinetics study fitted best into the pseudo second order (PSO) reaction kinetic model. In isotherm modelling studies, the Langmuir isotherm model was best fitted and was used to describe the mechanism of the adsorption. Experimental adsorption capacities (q_e) of 2.84 and 3.01 mg/g were recorded for both GP-1M and GP-2M, respectively. Used adsorbents were successfully regenerated by furnace treatment at 400 °C for two hours, and the regenerated adsorbents presented enhanced adsorption capacities in the range of 4.9 to 5.07 mg/g for five repeat cycles, elucidating that the material is suitable at multiple time use.

Malkawi et al. (2016) [80] investigated geopolymer binders as green building materials that have increasing potential to replace the ordinary portland cement in the concrete industry. This study shown the alkali solution effects on the physical and mechanical properties of the high calcium fly ash based geopolymers.

The parameters involved in this study were the NaOH solution molarity and the Na_2SiO_3/NaOH ratio. Three NaOH concentrations (8, 10, and 12 molars) were investigated. The Na_2SiO_3/NaOH ratio was varied between 1 and 2.5. The results showed that the studied parameters significantly affected the properties of the produced geopolymer mortars. The workability and setting time were decreased by increasing the NaOH concentration or by increasing the Na_2SiO_3/NaOH ratio. The influence of the NaOH concentration was higher on the workability and setting time while the Na_2SiO_3/NaOH ratio highly affected the compressive strength.The initial setting time was shown in the range of 45 to105 minutes while the final setting occurred quickly after that within 70 to 115 minutes. Oven curing method resulted in high strength at early ages where all of the mixes were able to achieve more than 75% of the 28 days strength within the first 3 days. The 28 days compressive strength ranged between 60-85 MPa, which promotes the use of the high calcium fly ash for the production of early high strength geopolymer concrete.

Boukhemkhem et al. (2017) [37] investigated three adsorbents with the raw kaolin issued from Tamazert kaolin (KT) for the removal of basic dye MB from aqueous solutions. KT-1 was obtained by thermal treatment. The second, KT-2 was obtained by thermal followed by acid treatment. The third KT-3 was obtained by thermal followed by acid and alkaline treatments. Characterization were used XRD, FTIR, BET and SEM. The maximal adsorption capacity (111 mg/g) was shown with modified kaolin (KT-3). The removal of MB by adsorbent increased with an increase in adsorbent dose and initial concentration. The results shown that the adsorption of MB by KT-3 was well described by the pseudo-second-order kinetic model. The thermodynamic study revealed that the adsorption process was spontaneous, endothermic, and the positive value of ΔS° indicated the affinity of MB molecules to the adsorbent surface.

Jackson et al. (2017) [81] the toughness of geopolymer matrix composites (GMC) has been identified as a limiting factor to their use in structural applications. Advanced ceramic matrix composites (CMC), which also are limited by brittle behavior, have shown gains in toughness through careful tailoring of the interface between fiber and matrix. This can create various crack dissipating mechanisms and prevent premature composite failure. Such interface modification has already been applied to a fiber reinforced geopolymer and while the resulting composite showed a reduction in brittle behavior, the modified interface produced an unacceptable loss in modulus without any other well-defined quantitative gains. Information gathered from other studies suggests the large decrease in modulus observed in the GMCs with the weakened interface may have been the result of poor matrix properties stemming from an inadequate cure. Therefore, this current study explores the effects of initial cure time on composite performance by measuring the mechanical properties GMCs with a modified interface. GMCs containing unidirectional Nextel 610 fiber were cured under two different sets of process conditions to better understand the influence of matrix properties. Additionally, specimens consisted of cleaned and carbon coated fiber surfaces, in an attempt to evaluate extremes of interfacial strength. Mechanical properties were then evaluated for comparison to determine if improved geopolymer matrix properties would allow a weakened interface to yield performance gains more in keeping with expectations based on CMC's. The results of the study indicate that specimens with carbon coating benefited from the longer initial cure time. The average increase in flexural modulus and strength over samples with one hour initial cure time was 65 and 170%. Stress-strain behavior of the carbon-coated specimens with an extended cure time also indicated a greater degree of damage tolerance as compared to those without interphase.

Kara et al. (2017) [82] studied Metakaolin based geopolymer (MKG) as an adsorbent to remove Zn(II) and Ni(II) ions from aqueous solution. The parameters of initial pH, adsorbent amount, time of contact and initial metal ion concentration on metal removal performance of MKG were studied using a batch method at 25 °C. The amount of Zn(II) and Ni(II) ions adsorbed onto MKG increased with increasing contact time with an adsorption equilibrium being reached within 40 and 50 minutes for Zn(II) and Ni(II). The Langmuir isotherm described the adsorption data very well and the maximum monolayer adsorption capacities determined from the Langmuir adsorption isotherm were 1.14×10^{-3} and 7.26×10^{-4} mol/g for Zn(II) and Ni(II), respectively. The kinetic studies showed that adsorption followed the pseudo-second-order . The breakthrough points were observed at 150 and 280 min for Zn(II) and Ni(II), respectively. It is concluded that Zn(II) and Ni(II) ions in aqueous solutions are efficiently removed by MKG which could be employed as a low-cost and excellent alternative for wastewater treatment.

Livi et al. (2017) [83] studied the effect of alkali concentration and curing temperature regime on fly ash-based geopolymer pastes by using NaOH solutions. Prismatic specimens were molded, cured at 65 and 85 °C to flexural and compressive strength tests. Unreacted fly ash and geopolymers were characterized by X-ray diffraction and thermogravimetric analysis. In general, the mechanical strength was enhanced by increasing the molar concentration and the curing temperature. This trend was confirmed by thermogravimetric data. However, for a lower amount of NaOH there were no significant differences between the strength results. The mixture with the highest strength was shown with the 16 M at NaOH solution and curing temperature of 85 °C, which resulted in flexural strength of 4.20 MPa, compressive strength of 21.35 MPa and also the highest weight loss of 9.89%.

Barbosa et al. (2018) [84] mesoporous geopolymer was synthesized using a novel and easy synthesis route employing metakaolin and rice husk ash as sources of silica and alumina, and soybean oil as a mesostructure directing agent. Geopolymer sample was produced without the use of oil. The samples were characterized by FT–IR, XRD and BET. The materials were tested to remove methyl violet 10B dye from aqueous solutions. The results showed that the mesoporous geopolymer presented adsorptive superior behavior compared to the geopolymer prepared without the use of oil, being attributed to its superior pore properties. The adsorption equilibrium was attained within 120 minutes, and the maximum adsorption capacity of mesoporous geopolymer was 276.9 mg/g. Thus, the mesoporous geopolymer prepared in this work comprises a potential adsorbent, presenting pore intrinsic properties that result in a high adsorption capacity.

Ge et al. (2018) [85] new geopolymer/alginate hybrid spheres (GAS) was fabricated from the green geopolymer and sodium alginate by a feasible one-pot method. The effect of mass ratio of geopolymer and sodium alginate (Geo/SA) on the properties of GAS was investigated.The results demonstrated that the GAS-4 (Geo/SA = 1: 0.16) had a good sphericity with an inner honeycomb structure. The GAS-4 was used as an adsorbent for the removal of Cu(II) in water. Batch adsorption method indicated GAS-4 possessed an excellent Cu(II) removal efficiency (99 ± 3.4%) from a 50 mg/L solution with a dosage of 0.15 g/100 mL. The adsorption kinetic was fitted well by the pseudo-second-order model, indicating the chemical interaction of GAS-4 and Cu(II). The adsorption isotherm followed the Langmuir model indicating a monolayer adsorption of Cu(II) on GAS-4.

Zhao et al. (2020) [86] freeze-thaw (F-T) durability of geopolymers synthesized from the mixture of red mud slurry-class F fly ash (RMSFFA) was investigated, with an emphasis on the influence of curing conditions (i.e., curing time and curing temperature). F-T durability was evaluated on the basis of the sustained mechanical strength of RMSFFA geopolymer specimens after subjected to 50F-T conditioning cycles. The change in their chemical bonding, mineralogy, and pore characteristics at various F-T conditioning cycles was examined with FT-IR , XRD, and BET testing, respectively, to reveal the underlying processes during F-T conditioning. 14-day cured RMSFFA samples at 50 °C, they experienced further geopolymerization at the early stage of F-T conditioning but the partial dissolution of geopolymer gel at the later stage of F-T conditioning. For 28-day cured samples at 50 °C, only the partial dissolution of geopolymer gel was likely to occur during the F-T conditioning because the strength development was likely to complete prior to the conditioning.

Arslan et al. (2019) [87] mechanical and durability properties of geopolymer composites using metakaolin and colemanite binding materials with basalt and polyvinyl alcohol fibers were investigated under the influence of curing systems. For the 7 series prepared, two different curing conditions have been applied: wetting-drying and heat curing. The mechanical properties of geopolymer samples were 7 and 28 days strength and ultrasonic pulse velocity results, water absorption, unit weight and porosity. After the abrasion test, weight loss and length change were examined and after the high temperature tests of 200, 400 and 600 °C, the results of strength, ultrasonic pulse velocity and weight loss found.

The result showed that a higher rate of geopolymerization and increased strength values. The main reason for this situation is the formation of a resistant layer with the effect of basalt and polyvinyl alcohol fibers. The compact structure of the geopolymeric matrix brings along a good degree of adhesion. This allows geopolymer samples to resist freezing-thawing. In geopolymer samples, despite the 90 cycles, the residual strength were high and the decrease in the ultrasonic pulse velocity rate results were limited.

Novais et al. (2019) [13] fly ash (FA)-based geopolymer ($d = 2.6$ mm) spheres used to extract methylene blue from synthetic wastewaters. The influence of contact time, dye initial concentration and adsorbent amount on the dye removal efficiency and uptake by the porous spheres was evaluated. The adsorbents recyclability and their dye fixation efficiency were also considered. The initial dye concentration strongly affected the uptake and removal efficiency by the porous bodies, the former rising from 1.1 to 30.10 mg/g when the dye initial concentration jumped from 10 to 250 ppm, and the latter increasing from 82.30 to 94.30% when the dye initial concentration varied from 10 to 125 ppm. Results showed that a much faster (24 hr.) and higher (30.1 mg/g) MB uptake in comparison with the other bulk-type geopolymers reported to date (30 hr.,15.4 mg/g). The cumulative methylene blue uptake shown by these innovative spheres (79.70 mg/g) surpasses all other powdered geopolymer adsorbents, being among the highest values ever reported for geopolymers. The adsorbent was successfully regenerated and reused eight times. Regeneration was found to negatively affect the MB uptake, but nevertheless, even after eight regeneration cycles a very high MB removal efficiency (83%) was maintained.

Maleki et al. (2019) [88] bentonite clay was employed to synthesize geopolymer for removal heavy metals such as Cu(II), Pb(II), Ni(II), Cd(II), and Hg(II) from industrial wastewaters, respectively. The Fe_3O_4 nanoparticles were applied to modify the geopolymer and the use of a geopolymer/Fe_3O_4 nanocomposite as an efficient and magnetic adsorbent for heavy metals removal from aqueous solution. The influence of different contact time and initial concentrations of metal ions was examined and the best result was achieved in 2 minutes in the presence of 0.05 g nanocomposite.

Geopolymer and nanocomposite samples were characterized by FT-IR, SEM, thermogravimetric analysis, energy dispersive X-ray analysis, XRD pattern and BET analysis. The magnetic geopolymer based on bentonite clay showed 99, 99, 92, 96 and 92% removal efficiency for the sorption of copper, lead, nickel, cadmium, and mercury ions from industrial wastewaters, respectively.

Cai et al. (2020) [89] studied the heat evolution and compressive behavior of KOH activated geopolymer materials based on low-calcium fly ash, metakaolin, and fly ash with slag. An isothermal calorimeter was adopted to study the heat evolution. Study variables include alkali activator concentration, curing temperature, and slag replacement ratio. The results showed that the cumulative released heat for both fly ash and metakaolin based geopolymer increased with the increasing in alkali concentration and slag replacement ratio.

The increase in curing temperature significantly increased both the heat flow and the cumulative heat of the heat evolution during geopolymerization, especially the fly ash-based geopolymers. The compressive behavior of geopolymers with different initial curing temperatures was also investigated. Results showed that the 28 day compressive strength for all geopolymers increased with the increasing of alkali concentration and slag replacement ratio cured under ambient temperature.

The initial curing temperature has a significant influence on the compressive strength of the fly ash-based geopolymer, but a negligible influence on the compressive strength of the metakaolin-based geopolymer.

Cai et al. (2020) [90] the electrical resistivity behavior of fly ash and metakaolin based geopolymer was investigated with the two-probe measurement method. The effects of alkali activator concentration, curing temperature and slag substitution rate on the electrical resistivity and pore size distribution were discussed.

The results showed that the electrical resistivity for fly ash based geopolymer is much higher than that of metakaolin based geopolymers. Increasing alkali concentration, the electrical resistivity of both fly ash and metakaolin based geopolymers decreased significantly. The curing temperature has a significant influence on the electrical resistivity of fly ash based geopolymers, while the influence of curing temperature of metakaolin based geopolymer is negligible with a prolonged curing period.

The increase of slag replacement ratio would increase the electrical resistivity for fly ash based geopolymer.

Hua et al. (2020) [91] a magnetic geopolymer (MG) used as an effective adsorbent for water decolorization, in particular, for the removal of acid green (AG) and procion red (PR) from aqueous solutions.

AG and PR dyes adsorption mechanism for this adsorbent was experimentally and theoretically characterized via the analysis and description of eight adsorption isotherms obtained at 298 to 328 K.

The temperature effect on parameters was analyzed concluding that this operating parameter had a minor effect on the number of accepted amount of AG and PR dyes per receptor site of MG adsorbent (n) and the density of receptor sites (Dm). The trends of parameters n and Dm led to a slightly variation of the adsorption capacity at saturation ($Q_{sat} = 2.n.Dm$) as a function of temperature.

Particularly, it was also concluded that AG and PR dyes retained their adsorption orientations on the magnetic geopolymer surface.

Calculated adsorption energies varied from 18.55 to 29.14 kJ/mol and from 8.55 to 14.77 kJ/mol for the AG-GP and PR-GP systems, respectively. These adsorption energies indicated that physical interactions were involved during the adsorption mechanism of these water pollutants.

Maleki et al. (2020) [3] geopolymer paste synthesized from industrial and agricultural waste materials was employed as an adsorbent to remove methylene blue from aqueous solutions. The geopolymer sample was characterized by XRF , SEM, BET, and particle size The isotherms of dye adsorption by the geopolymer sample was corresponded by the Langmuir adsorption models. The removal efficiency increased with increasing geopolymer dosage, contact time and temperature. The Freundlich isotherm exhibited the best fit to the adsorption data.

CHAPTER 3
EXPERIMENTAL

In the present work the geopolymer after lead adsorption was used as an adsorbent for removal of MB and BG from aqueous solutions. The optimal parameter was investigated. Figure 3.1 describes the work in a stepwise manner. The adsorbents GEO8M5D (geopolymer commercial) and GSiRH (geopolymer extracted silica from rice husk) were characterized by XRD, SEM, BET and FTIR to reveal the properties of adsorbents before and after dye adsorption.

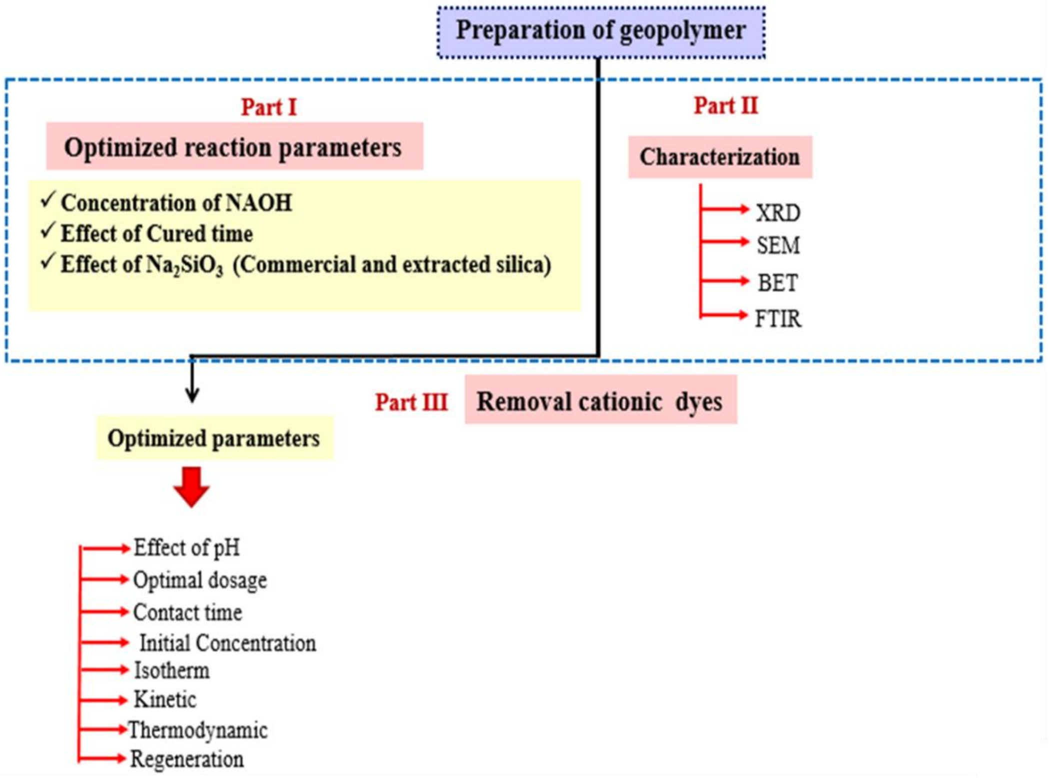

Figure 3.1 Flowchart showing the steps for the adsorbent preparation and its further application for dyes removal

3.1 Materials

Materials were presented in Table 3.1

Table 3.1 Sources of materials

Materials	Sources
RH	Ban Kwang, Kèuang Kam sub-district, Muang Yasothon district, Yasothon province, Thailand
FA	Mae Moh power plant is located in Mae Moh sub-district, Mae Moh district, Lampang province, Thailand.
Kaolin (K)	Ranong province, the southern part of Thailand

3.2 Chemical reagent

3.2.1 Solvent

DI- water from nano pure ultrapure water system (Dubuque, Iowa, USA) was used throughout this work.

3.2.2 Chemicals

Industrial grade Na_2SiO_3, HCl and NaOH was purchased from Italmar (Thailand) Co., Ltd.

3.3 Preparation of silica powder from RH

RH was washed with 1000 mL of DI water and dried at 50°C for 24 hr. Then, RH was extracted by refluxing with 0.1 M HCI for 2 hr. Then, it was washed repeatedly with DI water and dried at 50°C for 48 hr. in the oven. After that, it was calcite at 600˚C for 2 hr. The obtained product was shown in Figure 3.2. Silica content is calculated as the following equation:

$$\%\,\text{Yield} = \frac{\text{Pure of materials (g)}}{\text{Impure of materials (g)}} \times 100$$

Figure 3.2 Photographs of (a) RH and (b) Si-RH

3.4 Preparation of Na_2SiO_3

Na_2SiO_3 was prepared by using silica and NaOH (raito 1 : 2.2). Silica 3.4520 g is mixed with 3.60 g of water. Then, 2.9480 g of NaOH is slowly added to dissolve the silica and the mixture was stirred and heated at 60˚C until the suspension became homogeneous solution.

3.5 Preparation of adsorbent

3.5.1 Geopolymer

MK was prepared by calcined kaolin at 600˚C for 2 hr. The activator solution was prepared by mixing NaOH concentrations were varied 6, 8, 10 and 12 M (GEO6M, GEO8M, GEO10M and GEO12M) and Na_2SiO_3 until the mixtures become homogeneous. Initially, the mixtures of metakaolin with activator solution (ratio of NaOH : Na_2SiO_3 = 2:3) are prepared by stirring until obtained a homogenous slurry. Then, the slurry mixture was transferred to mound, air bubble removal and seal with a plastic film. All samples are left for 3, 5 and 7 days (GEO3D, GEO5D and GEO7D) at room temperature.

3.6 Preparation of standard solution

3.6.1 Standard MB Solution and Calibration Curve

3.6.1.1 0.5000 g of MB was solved by DI water, then put in the 500 mL volumetric flask. Volume adjustment was performed by DI water. The obtained MB standard solution was 300.00 ppm.

3.6.1.2 33.30 mL of 300.00 ppm MB solution was pipetted and put in the 100 mL volumetric flask. Volume adjustment was performed by DI water. The obtained MB standard solution was 100.00 ppm.

3.6.1.3 The 100.00 ppm MB standard solution was pipetted in the volume of 0.25, 0.50, 1.00, 2.50 and 5.00 mL into the 50 mL volumetric flask. Volume adjustment was performed by DI water. The obtained MB standard solution was 0.50, 1.00, 2.00, 5.00 and 10.00 ppm, respectively.

3.6.1.4 Absorbance of all standard MB solution was measured by using UV-visible spectrophotometer at λ_{max} of 665 nm. DI water was used as blank.

3.6.1.5 Calibration curve of MB standard solution was investigated by plotting entire standard MB concentration as X-axis with their absorbance value as Y-axis. Preparation of MB calibration curve was shown in Figure 3.3

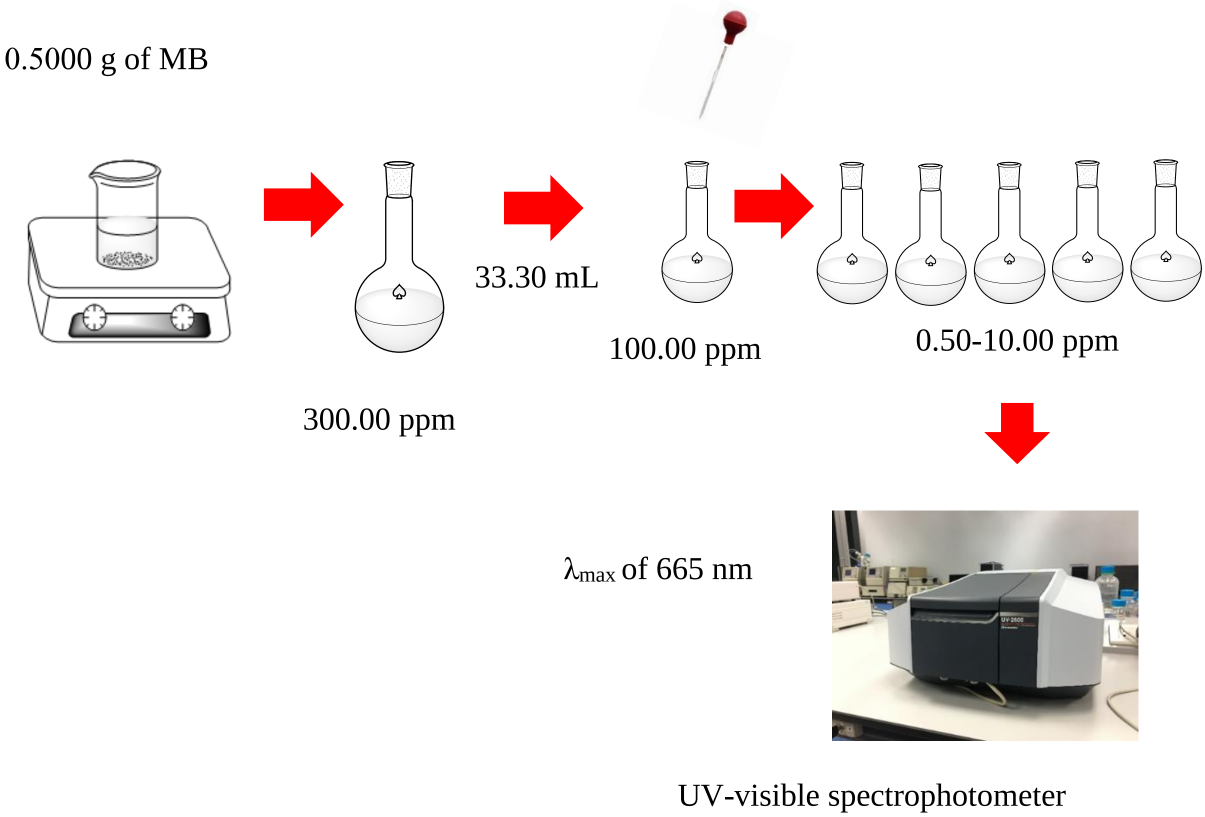

Figure 3.3 Preparation of calibration curve MB using UV-visible spectrophotometer

3.6.2 Standard BG Solution and Calibration Curve

3.6.2.1 0.5000 g of BG was solved by DI water, then put in the 500 mL volumetric flask. Volume adjustment was performed by DI water. The obtained BG standard solution was 300.00 ppm.

3.6.2.2 33.30 mL of 300.00 ppm BG solution was pipetted and put in the 100 mL volumetric flask. Volume adjustment was performed by DI water. The obtained BG standard solution was 100.00 ppm.

3.6.5.3 The 100.00 ppm BG standard solution was pipetted in the volume of 0.25, 0.50, 1.00, 2.50 and 5.00 mL into the 50 mL volumetric flask. Volume adjustment was performed by DI water. The obtained BG standard solution was 0.50, 1.00, 2.00, 5.00 and 10.00 ppm, respectively.

3.6.3.4 Absorbance of all standard BG solution was measured by using UV-visible spectrophotometer at λ_{max} of 625 nm. DI water was used as blank.

3.6.2.5 Calibration curve of standard BG solution was investigated by plotting entire standard BG concentration as X-axis with their absorbance value as Y-axis.

3.6.3 Standard CR Solution and Calibration Curve

3.6.3.1 0.5000 g of CR was solved by DI water, then put in the 500 mL volumetric flask. Volume adjustment was performed by DI water. The obtained CR standard solution was 300.00 ppm.

3.6.3.2 33.30 mL of 300.00 ppm CR solution was pipetted and put in the 100 mL volumetric flask. Volume adjustment was performed by DI water. The obtained CR standard solution was 100.00 ppm.

3.6.3.3 The 100.00 ppm CR standard solution was pipetted in the volume of 0.25, 0.50, 1.00, 2.50 and 5.00 mL into the 50 mL volumetric flask. Volume adjustment was performed by DI water. The obtained CR standard solution was 0.50, 1.00, 2.00, 5.00 and 10.00 ppm, respectively.

3.6.3.4 Absorbance of all standard CR solution was measured by using UV-visible spectrophotometer at λ_{max} of 498 nm. DI water was used as blank.

3.6.3.5 Calibration curve of standard CR solution was investigated by plotting entire standard CR concentration as X-axis with their absorbance value as Y-axis.

3.6.4 Standard MO Solution and Calibration Curve

3.6.4.1 0.5000 g of MO was solved by DI water, then put in the 500 mL volumetric flask. Volume adjustment was performed by DI water. The obtained MO standard solution was 300.00 ppm.

3.6.4.2 33.30 mL of 300.00 ppm MO solution was pipetted and put in the 100 mL volumetric flask. Volume adjustment was performed by DI water. The obtained MO standard solution was 100 ppm.

3.6.4.3 The 100.00 ppm MO standard solution was pipetted in the volume of 0.25, 0.50, 1.00, 2.50 and 5.00 mL into the 50 mL volumetric flask. Volume adjustment was performed by DI water. The obtained MO standard solution was 0.50, 1.00, 2.00, 5.00 and 10.00 ppm, respectively.

3.6.4.4 Absorbance of all standard MO solution was measured by using UV-visible spectrophotometer at λ_{max} of 465 nm. DI water was used as blank.

3.6.4.5 Calibration curve of MO standard solution was investigated by plotting entire standard MO concentration as X-axis with their absorbance value as Y-axis.

3.7 Adsorption study by using adsorbent

3.7.1 Determination of MB concentration before adsorption

3.7.1.1 1.00 mL of 300 ppm MB solution was pipetted, then put in the 50 mL volumetric flask. Volume adjustment was performed by DI water.

3.7.1.2 Absorbance of MB solution was measured by using UV-visible spectrophotometer at λ_{max} of 665 nm. DI water was used as blank.

3.7.1.3 Concentration of MB solution was calculated by using linear equation from MB calibration curve.

3.7.2 Determination of MB concentration after adsorption

3.7.2.1 0.5000 g of geopolymer was put into the 100 mL beaker, then 25 mL of 300 ppm MB solution was added into all above beaker (Replication 3 flasks).

3.7.2.2 The mixture was stirred by using magnetic stirrer for 30 seconds every 30 minutes, 60 minutes of contact time.

3.7.2.3 The mixture was centrifuged.

3.7.2.4 The clear solution was pipetted and put in the 50 mL volumetric flask. Volume adjustment was performed by DI water. Systematic perturbation was performed by using UV-visible spectrophotometer at λ_{max} of 665 nm

3.7.3 Determination of BG concentration before adsorption

3.7.3.1 1.00 mL of 300 ppm BG solution was pipetted, then put in the 50 mL volumetric flask. Volume adjustment was performed by DI water.

3.7.3.2 Absorbance of BG solution was measured by using UV-visible spectrophotometer at λ_{max} of 625 nm. DI water was used as blank.

3.7.3.3 Concentration of BG solution was calculated by using linear equation from BG calibration curve.

3.7.4 Determination of BG concentration after adsorption

3.7.4.1 0.5000 g of geopolymer was put into the 100 mL beaker, then 25 mL of 300 ppm BG solution was added into all above beaker. (Replication 3 flask).

3.7.4.2 Systematic was investigated by using magnetic stirrer at the time of 30 minutes for a 30 second, 60 minutes of contact time.

3.7.4.3 The mixture was centrifuged.

3.7.4.4 The clear solution was pipetted and put in the 50 mL volumetric flask. Volume adjustment was performed by DI water. Systematic perturbation was performed by using UV-visible spectrophotometer at λ_{max} of 625 nm.

3.7.5 Determination of CR concentration before adsorption

3.7.5.1 1.00 mL of 300 ppm CR solution was pipetted, then put in the 50 mL volumetric flask. Volume adjustment was performed by DI water.

3.7.5.2 Absorbance of CR solution was measured by using UV-visible spectrophotometer at λ_{max} of 498 nm. DI water was used as blank.

3.7.5.3 Concentration of CR solution was calculated by using linear equation from CR calibration curve.

3.7.6 Determination of CR after adsorption

3.7.6.1 0.5000 g of geopolymer was put into the 100 mL beaker, then 25 mL of 300 ppm CR solution was added into all above beaker. (Replication 3 flask).

3.7.6.2 Systematic was investigated by using magnetic stirrer at the time of 30 minutes for a 30 second, 60 minutes of contact time.

3.7.6.3 The mixture was centrifuged.

3.7.6.4 The clear solution was pipetted and put in the 50 mL volumetric flask. Volume adjustment was performed by DI water. Systematic perturbation was performed by using UV-visible spectrophotometer at λ_{max} of 498 nm.

3.8 Investigation of optimum parameters for adsorption of dye by geopolymer

3.8.1 Effect of initial pH solution

3.8.1.1 Determination of MB solution concentration before adsorption

1) The initial pH of MB solution of 300.00 ppm was measured by using pH meter and adjusted by using 1.0 M HCl or 1.0 M NaOH for uptake the initial pH solution of 2.0, 4.0, 6.0, 8.0 and 10.0.

2) 1.00 mL of 300.00 ppm MB solution was pipetted, then put in the 50 mL volumetric flask. Volume adjustment was performed by DI water.

3) Absorbance of MB solution was measured by using UV-visible spectrophotometer at λ_{max} of 665 nm. DI water was used as blank.

4) Concentration of MB solution was calculated by using linear equation from MB calibration curve. Preparation of pH was shown in Figure 3.4

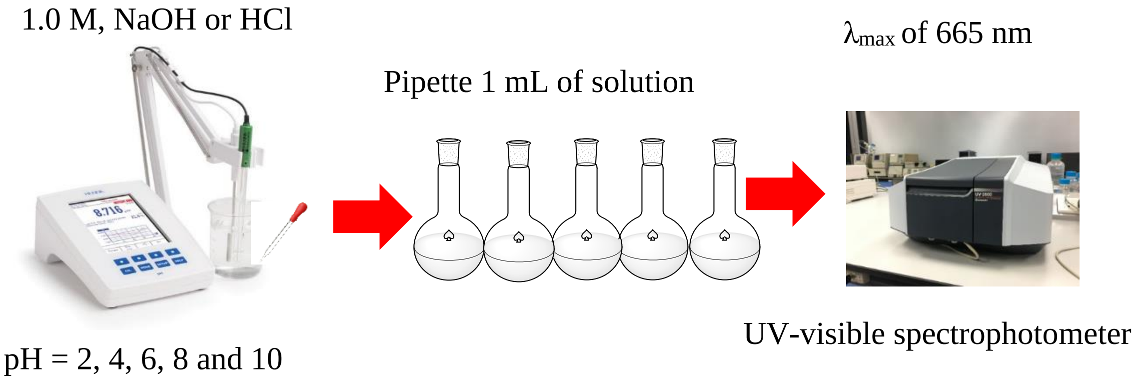

Figure 3.4 Preparation of pH MB solution

3.8.1.2 Determination of MB solution concentration after adsorption

1) 0.5000 g of geopolymer was put into the 100 mL beaker, then 25 mL of 300.00 ppm MB solution was added into the above beaker. Effect of initial solution pH was performed 2, 4, 6, 8 and 10 by 1.0 M NaOH or HCl (replication 3 flasks) .

2) The mixture was stirred by using magnetic stirrer for 30 seconds every half an hour, 60 minutes of contact time.

3) The mixture was centrifuged.

4) The clear solution was pipetted and put in the 50 mL volumetric flask. Volume adjustment was performed by DI water. Systematic perturbation was performed by using UV-visible spectrophotometer at λ_{max} of 665 nm. The flow chart of experiment was showed in Figure 3.5.

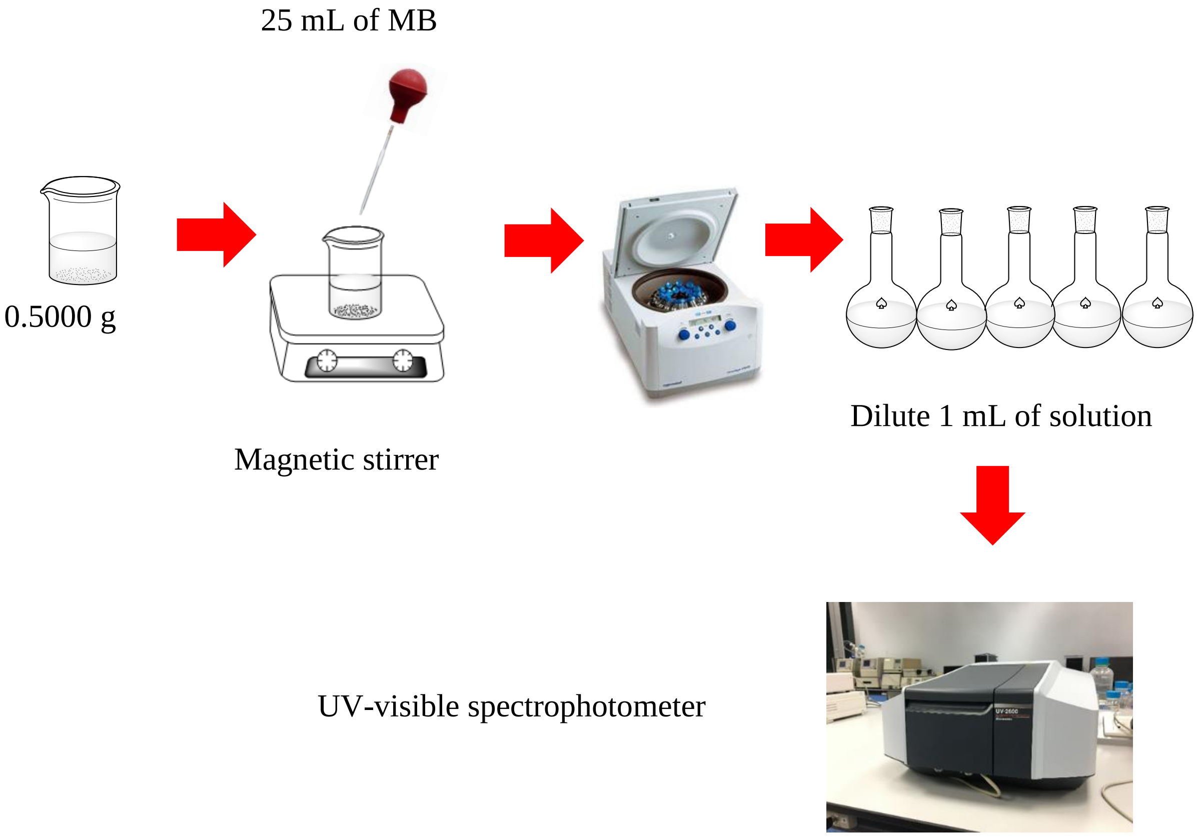

Figure 3.5 Flow chart of effect of initial pH MB solution

3.8.2 Effect of geopolymer dosage

3.8.2.1 Determination of MB solution concentration before adsorption

1) 1.00 mL of 300.00 ppm MB solution was pipetted, then put in the 50 mL volumetric flask. Volume adjustment was performed by DI water.

2) Absorbance of MB solution was measured by using UV-visible spectrophotometer at λ_{max} of 665 nm. DI water was used as blank.

3) Concentration of MB solution was calculated by using linear equation from MB calibration curve.

3.8.2.2 Determination of MB solution concentration after adsorption

1) Geopolymer was put into the 100 mL beaker, then 25 mL of 300.00 ppm MB solution was added into above beaker (replication 3 flasks). The amount of geopolymer dosage was varied 0.2500, 0.5000, 1.0000 and 2.0000 g.

2) The mixture was stirred by using magnetic stirrer for 30 seconds every 30 minutes, 60 minutes of contact time.

3) The mixture was centrifuged.

4) The clear solution was pipetted and put in the 50 mL volumetric flask. Volume adjustment was performed by DI water. Systematic perturbation was performed by using UV-visible spectrophotometer at λ_{max} of 665 nm.

3.8.3 Effect of FA dosage

3.8.3.1 Determination of BG solution concentration before adsorption

1) 1.00 mL of 300.00 ppm BG solution was pipetted, then put in the 50 mL volumetric flask. Volume adjustment was performed by DI water.

2) Absorbance of BG solution was measured by using UV-visible spectrophotometer at λ_{max} of 625 nm. DI water was used as blank.

3) Concentration of BG solution was calculated by using linear equation from BG calibration curve.

3.8.3.2 Determination of BG solution concentration after adsorption

1) FA was put into the 100 mL beaker, then 25 mL of 300.00 ppm BG solution was added into above beaker (replication 3 flasks).

2) The mixture was stirred by using magnetic stirrer for 30 seconds every 30 minutes, 60 minutes of contact time.

3) The mixture was centrifuged.

4) The clear solution was pipetted and put in the 50 mL volumetric flask. Volume adjustment was performed by DI water. Systematic perturbation was performed by using UV-visible spectrophotometer at λ_{max} of 625 nm.

3.8.4 Effect of adsorption time

3.8.4.1 Determination of MB solution concentration before adsorption

1) 1.00 mL of 300.00 ppm MB solution was pipetted, then put in the 50 mL volumetric flask. Volume adjustment was performed by DI water.

2) Absorbance of MB solution was measured by using UV-visible spectrophotometer at λ_{max} of 665 nm. DI water was used as blank.

3) Concentration of MB solution was calculated by using linear equation from MB calibration curve.

3.8.4.2 Determination of MB solution concentration after adsorption

1) 0.5000 g geopolymer was put into the 100 mL beaker, then 25 mL of 300.00 ppm MB solution was added into above beaker (replication 3 flasks).

2) The mixture was stirred by using magnetic stirrer for 30 seconds every 30 minutes. The contact time were varied 30, 60, 120 and 240 minutes

3) The mixture was centrifuged.

4) The clear solution was pipetted and put in the 50 mL volumetric flask. Volume adjustment was performed by DI water. Systematic perturbation was performed by using UV-visible spectrophotometer at λ_{max} of 665 nm.

3.8.4.3 Determination of BG solution concentration before adsorption

1) 1.00 mL of 300.00 ppm BG solution was pipetted, then put in the 50 mL volumetric flask. Volume adjustment was performed by DI water.

2) Absorbance of BG solution was measured by using UV-visible spectrophotometer at λ_{max} of 625 nm. DI water was used as blank.

3) Concentration of BG solution was calculated by using linear equation from BG calibration curve.

3.8.4.4 Determination of BG solution concentration after adsorption

1) 0.1000 g of fly ash was put into the 100 mL beaker, then 25 mL of 300.00 ppm BG solution was added into above beaker (replication 3 flasks).

2) The mixture was stirred by using magnetic stirrer for 30 seconds every 30 minutes. The contact time were varied 30, 60, 120 and 240 minutes.

3) The mixture was centrifuged.

4) The clear solution was pipetted and put in the 50 mL volumetric flask. Volume adjustment was performed by DI water. Systematic perturbation was performed by using UV-visible spectrophotometer at λ_{max} of 625 nm.

3.8.5 Effect of initial dyes concentration

3.8.5.1 Determination of MB solution concentration before adsorption

1) 50.00, 58.33, 66.67, 75.00, 83.33 and 91.67 mL of 600 ppm MB solution was pipetted, then put in the 100 mL volumetric flask. Volume adjustment was performed by DI water. The obtained initial MB concentration was 300.00, 350.00, 400.00, 450.00, 500.00 and 550.00 ppm, respectively.

2) 1.00 mL of MB solution concentration was pipetted, then put in the 50 mL volumetric flask. Volume adjustment was performed by DI water.

3) Absorbance of all MB solution was measured by using UV-visible spectrophotometer at λ_{max} of 665 nm. DI water was used as blank.

4) Concentration of MB solution was calculated by using linear equation from MB calibration curve.

3.8.5.2 Determination of MB solution concentration of after adsorption

1) 0.5000 g of geopolymer was put into the 100 mL beaker, then 25 mL of 300.00 ppm MB solution was added into above beaker (replication 3 flasks). The initial MB solution was varied 300.00, 350.00, 400.00, 450.00, 500.00 and 550.00 ppm.

2) The mixture was stirred by using magnetic stirrer for 30 seconds every 30 minutes, 60 minutes of contact time.

3) The mixture was centrifuged.

4) The clear solution was pipetted and put in the 50 mL volumetric flask. Volume adjustment was performed by DI water. Systematic perturbation was performed by using UV-visible spectrophotometer at λ_{max} of 665 nm.

3.8.5.3 Determination of BG solution concentration before adsorption

1) 50.00, 58.33, 66.67, 75.00, 83.33 and 91.67 mL of 600 ppm BG solution was pipetted, then put in the 100 mL volumetric flask. Volume adjustment was performed by DI water. The obtained initial BG concentration was 300.00, 350.00, 400.00, 450.00, 500.00 and 550.00 ppm, respectively.

2) 1.00 mL of all BG solution concentration was pipetted, then put in the 50 mL volumetric flask. Volume adjustment was performed by DI water.

3) Absorbance of all BG solution was measured by using UV-visible spectrophotometer at λ_{max} of 625 nm. DI water was used as blank.

4) Concentration of BG solution was calculated by using linear equation from BG calibration curve.

3.8.5.4 Determination of BG solution concentration of after adsorption

1) 0.1000 g of fly ash was put into the 100 mL beaker, then 25 mL of 300.00 ppm BG solution was added into above beaker (replication 3 flasks). The initial BG solution was varied 300.00, 350.00, 400.00, 450.00, 500.00 and 550.00 ppm.

2) The mixture was stirred by using magnetic stirrer for 30 seconds every half an hour, 60 minutes of contact time.

3) The mixture was centrifuged.

4) The clear solution was pipetted and put in the 50 mL volumetric flask. Volume adjustment was performed by DI water. Systematic perturbation was performed by using UV-visible spectrophotometer at λ_{max} of 625 nm.

3.8.6 Effect of temperature on adsorption of dyes solution

3.8.6.1 Determination of MB solution concentration of before adsorption

1) 1.00 mL of 300 ppm MB solution was pipetted, then put in the 50 mL volumetric flask. Volume adjustment was performed by DI water.

2) Absorbance of MB solution was measured by using UV-visible spectrophotometer at λ_{max} of 665 nm. DI water was used as blank.

3) Concentration of MB solution was calculated by using linear equation from MB calibration curve.

3.8.6.2 Determination of MB solution concentration of after adsorption

1) 0.5000 g of geopolymer was put into the 100 mL beaker, then 25 mL of 300.00 ppm MB solution was added into above beaker (replication 3 flasks). The effect of temperature on adsorption was studied by using temperature range 20, 30, 40, and 60°C.

2) The mixture was stirred by using magnetic stirrer for 30 seconds every 30 minutes, 60 minutes of contact time.

3) The mixture was centrifuged.

4) The clear solution was pipetted and put in the 50 mL volumetric flask. Volume adjustment was performed by DI water. Systematic perturbation was performed by using UV-visible spectrophotometer at λ_{max} of 665 nm.

3.8.6.3 Determination of BG solution concentration of before adsorption

1) 1.00 mL of 300.00 ppm BG solution was pipetted, then put in the 50 mL volumetric flask. Volume adjustment was performed by DI water.

2) Absorbance of BG solution was measured by using UV-visible spectrophotometer at λ_{max} of 625 nm. DI water was used as blank.

3) Concentration of BG solution was calculated by using linear equation from BG calibration curve.

3.8.6.4 Determination of BG solution concentration of after adsorption

1) 0.1000 g of fly ash was put into the 100 mL beaker, then 25 mL of 300.00 ppm BG solution was added into above beaker (replication 3 flasks). The effect of temperature on adsorption was studied by using temperature range 20, 30, 40, and 60°C.

2) The mixture was stirred by using magnetic stirrer for 30 seconds every 30 minutes, 60 minutes of contact time.

3) The mixture was centrifuged.

4) The clear solution was pipetted and put in the 50 mL volumetric flask. Volume adjustment was performed by DI water. Systematic perturbation was performed by using UV-visible spectrophotometer at λ_{max} of 625 nm.

3.9 Investigation of adsorption isotherms

3.9.1 Freundlich isotherm

Freundlich isotherm for dye adsorption was investigated by plotting the value of log C_e as X-axis against log C_{ads} as Y-axis over total concentration range of methylene blue solution. The Freundlich isotherm equation is as following:

$$\log C_{ads} = 1/n \log C_e + \log K$$

Where;	C_{ads}	is	the concentration of dyes solution adsorbed onto adsorbent
	C_e	is	the equilibrium concentration of dyes in solution
	n	is	a characteristic constant for the adsorption system under study
	K	is	a parameter related to the temperature

The Freundlich constants (n and K) were calculated from slope and intercept from linear equation. The investigated Freundlich constant (K and n) were compared with experimental results from preliminary adsorption for checking of the accuracy and consistency between them. R^2 of all linear equation were discussed the appropriate of isotherm model.

3.9.2 Langmuir isotherm

Langmuir isotherm for methylene blue adsorption was obtained by plotting the value of C_e as X-against C_e/C_{ads} as Y-axis over total concentration range of methylene blue . The Langmuir isotherm equation is as following ;

$$C_e/C_{ads} = C_e/Q + 1/Qb$$

Where;	C_e	is	the equilibrium concentration of methylene blue in solution
	C_{ads}	is	the concentration of methylene blue adsorb onto adsorbent
	Q	is	Langmuir constants related to sorption capacity

b is Langmuir constants related to sorption energy

3.10 Investigation of kinetic adsorption

3.10.1 Pseudo first order

Pseudo first order for dye adsorption was investigated by plotting the value of time as X-axis against $\ln(q_e-q_t)$ as Y-axis over entire time range of dye. Pseudo first order equation is as following;

$$\ln(q_e-q_t) = \ln q_e - k_1 t$$

Where; q_e and q_t are the amount of dye (mg/g) at equilibrium and time

K_1 is the rate constant of the pseudo first order

3.10.2 Pseudo second order

Pseudo second order for adsorption was investigated by plotting the value of time as X-axis against t/q_t) as Y-axis over entire time range of dye. Pseudo first order equation is as following;

$$t/q_t = (1/k_2q_e^2) + t/q_e$$

Where; q_e and q_t are the amount of dye at equilibrium (mg/g) and t (minutes)

K_2 is the rate constant of the Pseudo first order (g/mg min)

3.11 Investigation of thermodynamic adsorption

Thermodynamic parameters (ΔH^o, ΔG^o and ΔS^o) are useful for the elucidation of the mechanism of adsorption. These parameters provide quantitative data on the phenomenon and information about the changes of the adsorbent during the progress of adsorption. Thermodynamic equation is as following;

$$\ln K_c = -\Delta H^\circ RT + \Delta S^\circ R$$

Where;	R (8.314 $J/mol^{-1} K^{-1}$)	is	the gas constant
	K_c	is	the coefficient of the substance between the phases of solid and liquid

$$\ln K_c = \frac{-\Delta H^\circ}{RT} + c$$

ΔHº is calculated from the slope obtained by plotting the $\ln K_c$ versus 1/T and is independent of the units of. K_c .

The change in Gibbs free energies (ΔGº) is as calculated with equation;

$$\Delta G^\circ = -RT\ln K_c$$

Entropy is a statistical measured of the number of states or accessible conformations. A positive ΔSº is an indication that the disorder or number of accessible of the system is increasing and vice versa.

3.12 Regeneration test

The adsorbent was performed using thermal regeneration methods. The geopolymer was calcined at 400 °C for 2 h. The concentration of MB at 300 ppm in solution was measured using a UV-visible spectrophotometer. The adsorption capacity was obtained as following;

$$q_e=[(C_i-C_f)*V] / W$$

Where;	C_i	is	the initial concentration (mg/L)
	C_f	is	the final concentrations (mg/L)
	V	is	the solution volume (mL)

W is the mass of adsorbent (g)

3.13 Characterization

The structural characterization data of adsorbent was investigated from department of physics, faculty of science, Ubonratchathani university. The results derived from XRD patterns of adsorbent were analyzed by PANalytical X Pert PRO using Cu Kα radiation (λ = 1.5406 Å) at 40 kV and 30 mA.

3.13.1 Metakaolin were characterized by WD-XRF (Rigaku, ZSX PrimusII). The morphology of the microspheres was visualized by scanning electron microscope (SEM, SSX-550, Shimadzu, Japan). The bands of sample was analyzed using by Fourier Transform infrared spectroscopy or (FTIR), Thermo Scientific, ANTRRIS II FT-NIR Analyzer at a 4 cm^{-1} resolution . Samples in powder form were scanned and recorded between 4000 – 400 cm^{-1} in KBr mode.

3.13.2 The surface properties of sample was investigated using by Brunauer-Emmett-Teller or (BET), (Quantachrome Instruments, Quadrasorb evo), previously outgassed at 200˚C for 6 hr. under 0.1 Torr vacuum was determined by N_2 adsorption-desorption test.

3.13.3 The zeta potential was measured on a potentiometer (Malvern Zetasizer, nano ZS) of DI water, the instrument was calibrated using NaCl solution at pH of 5.

3.13.4 The pH_{pzc} were prepared by a series of 0.01 M NaCl solution (V=25 mL) and the initial pH of NaCl was adjusted to a given from pH 2 to 13 by the addition of HCl 0.1 M or NaOH 0.1 M. To each solution, 0.50 g of geopolymer was added and shaken for 24 h at room temperature. The differences between pH value of the initial solution and the final pH were plotted as a function of initial pH.

CHAPTER 4

RESULTS AND DISCUSSIONS

In this work, a geopolymerization method was applied to synthesize the metakaolin-based geopolymer. The extraction of silica from rice husk used in alkaline activator. The structural and morphological properties of adsorbent were obtained by XRF, XRD, FTIR, SEM, BET, zeta potential analyses and point of zero charge. The adsorption properties of the samples were studied in different experimental conditions, including cured time, pH, amount of dosage, contact time, the initial concentration and regeneration. The adsorption kinetics, isotherms, thermodynamic data of the adsorption were investigated to study the batch adsorption process of the cationic dye using the synthesized metakaolin-based geopolymer and fly ash without modified.

4.1 Geopolymer from metakaolin

4.1.1 Characterization

The XRD pattern of K, MK and GEO8M5D was shown in Figure 4.1 . The results of XRD analysis for K show the material is crystallized in illite at 9˚. The peak at 20˚ to 25 ˚ and 26.5 to 35˚ are kaolinite and quartz, respectively.

After calcination, they still show quartz and kaolinite. The disappearance of peaks corresponding to kaolinite is observed at 25 ˚ and 26.5 ˚, which didn’t participate in the geopolymerization process; their intensities are moderately lower according to a dilution effect.

After the activation process, GEO8M5D indicate that amorphous product was formed. The only sharp reflection peaks are those from quartz and calcite then existing in the raw MK. Because the crystalline phases were dissolved in the alkaline solution. The aluminosilicates phase was formed in the structure of MK by polymerization reaction. They’re formed by dissolution and precipitation of hydrolysed silica species only on the surface of particles. The data confirm that the geopolymer structure is completely amorphous and consist of randomly arranged Si-O-Al. These only sharp reflection peaks observe the sharp of K, MK and GEO8M5D have been reported [82] synthesis geopolymer from metakaolin plus different weight percent of phosphorus slag (10-100 wt.%). Lecomte et al [93] investigated alkali activation of dehydroxylate kaolin or clay yielded high-strength polymeric materials, so-called geopolymer. They were synthesized by mixing the aluminosilicate with solutions of sodium metasilicate and KOH followed by adding 45 wt.% of ground-granulated blast furnace slag.

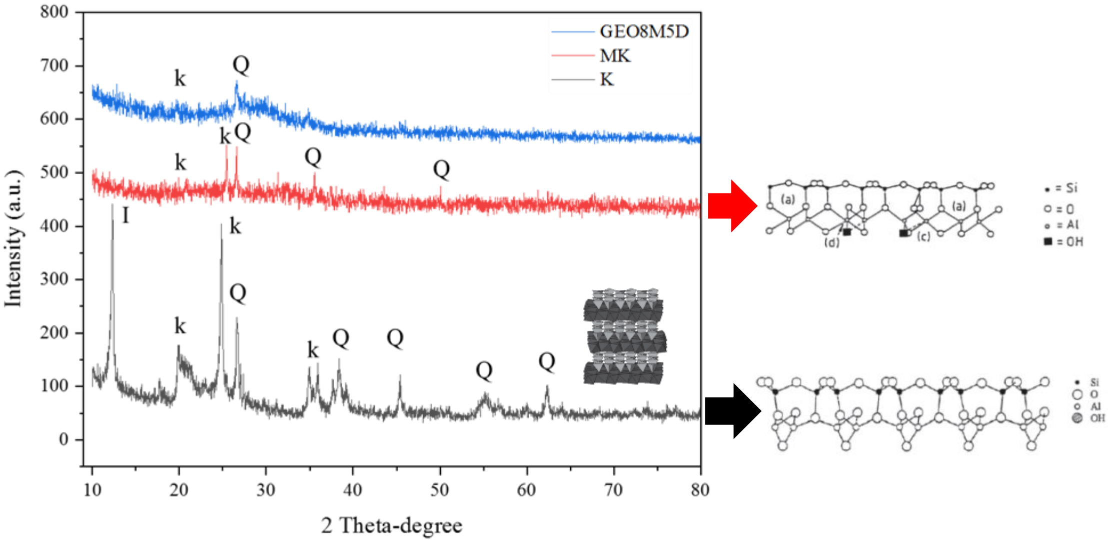

Figure 4.1 XRD patterns of (a) Kaolin (K); (b) Metakaolin (MK) and (c) geopolymer (GEO8M5D)

The weight percent of the chemical ingredients of the metakaolin showed in Table 4.1. It is a rich source of silicon and aluminium. Percentage of SiO_2 was 60.99, 55.40% and that of Al_2O_3 was 35.98, 26.50% for MK amd GEO8M5D, respectively. Therefore, after activationof matakaolin by alkaline solution, it found that a new inorganic material with an Si/Al ratio of approximately 2.08 was fomed, indicating the –Si-O-Al-O-Si-O poly (sailalate-silico)*n* nature of the foemed material.The ratio of SiO_2/Al_2O_3 calculated from the results gives an approximation about the charge density of the aluminosilicate framework structure: the lower value is related to a more negativecharge as the Al tetrahedron, [AlO_4], are negatively charged. Nevertheless, also kaolinite and quartzdiscovered by XRD affect the SiO_2/Al_2O_3 ratio in addition to the actual geopolymer framework structure and consequently the SiO_2/Al_2O_3 ratio in this case gives only a rough estimation about the charge density. All the elements were below 2% in all MK and GEO8M5D with the exception of K_2O and Fe_2O_3 at 1.53, 1.74, 12.8 and 0.88%. According to the literature, the formation of a new product with a structure different from that metakaolin [94].

Table 4.1 The compositions of MK and GEO8M5D

Composition (%)	MK	GEO8M5D	MK (El et al., 2019)	Geopolymer (El et al., 2019)
SiO_2	60.99	55.40	37.60	31.00
Al_2O_3	35.98	26.50	19.60	13.40
K_2O	1.53	1.74	1.50	1.13
Fe_2O_3	1.28	0.88	2.75	1.85

The chemical mechanism can be proposed in the following way, with NaOH (steps 1 to 6-7):

Step 1: Alkalination and formation of tetravalent Al in the side group sialate -Si-O-Al-$(OH)^{3-}Na^{+}$

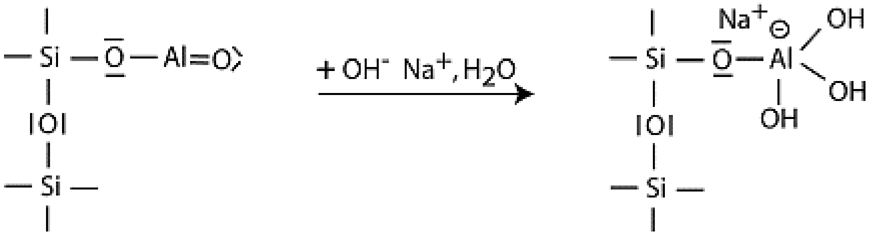

(1)

Step 2: Alkaline dissolution starts with the attachment of the base OH- to the silicon atom, which is thus able to extend its valence sphere to the penta- covalent state,

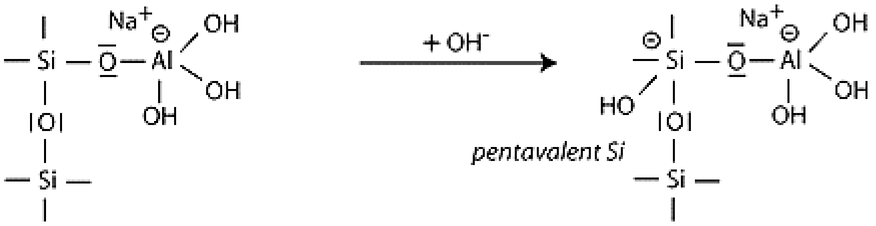

(2)

Step 3: The subsequent course of the reaction can be explained by the cleavage of the siloxane oxygen in Si-O-Si through transfer of the electron from Si to O, formation of intermediate silanol Si-OH on the one hand, and basic siloxo Si-O- on the other hand.

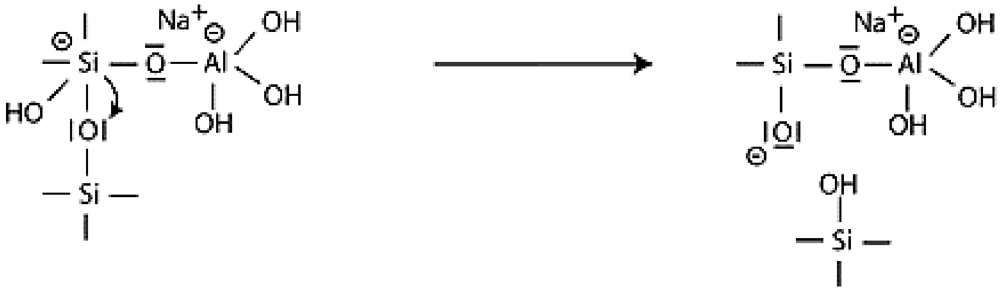

(3)

Step 4: Further formation of silanol Si-OH groups and isolation of the ortho-sialate molecule, the primary unit in geopolymerization.

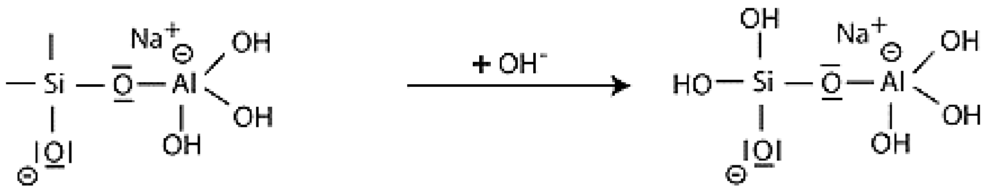

(4)

Step 5: Reaction of the basic siloxo Si-O- with the sodium cation Na^+ and formation of Si-O-Na terminal bond.

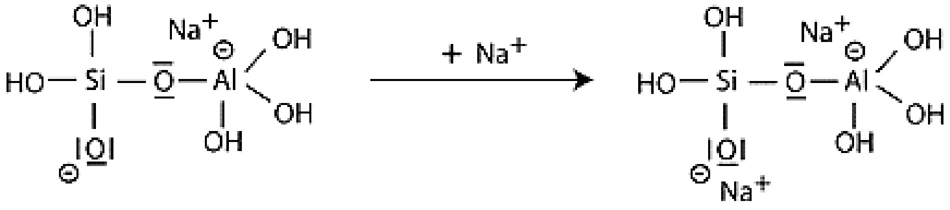

(5)

Step 6a: Condensation between ortho-sialate molecules, reactive groups Si-ONa and aluminum hydroxyl OH-Al, with production of NaOH, creation of cyclo-tri-sialate structure, whereby the alkali NaOH is liberated and reacts again and further polycondensation into Na-poly(sialate) nepheline framework.

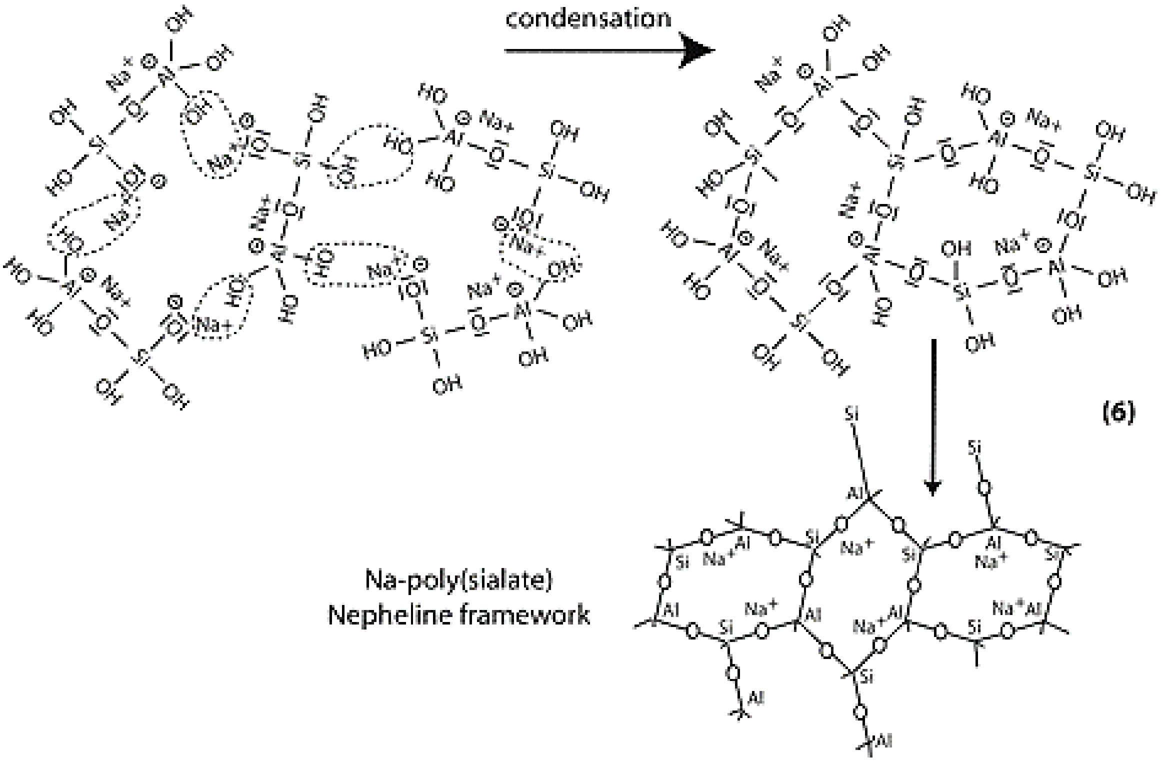

Step 6b: Na_2SiO_3 (Soluble Na-polysiloxonate) one get condensation between si-siloxonale and ortho-sialate molecules, reactive groups Si-O-Na, Si-OH and OH-Al, creation of ortho-dissilixo cyclic structure, whereby the alkali NaOH is released and reacts again.

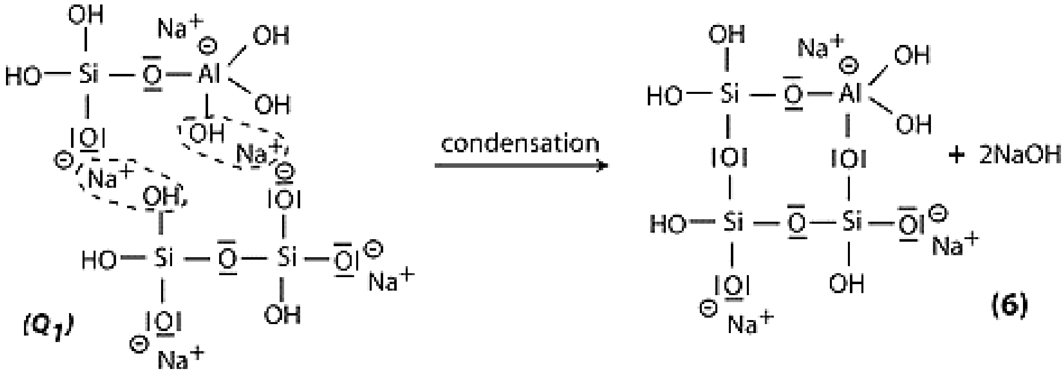

Step 7: Further polycondensation into Na-poly(sialate) albite framework with its typical feldspar crankshaft chain structure.

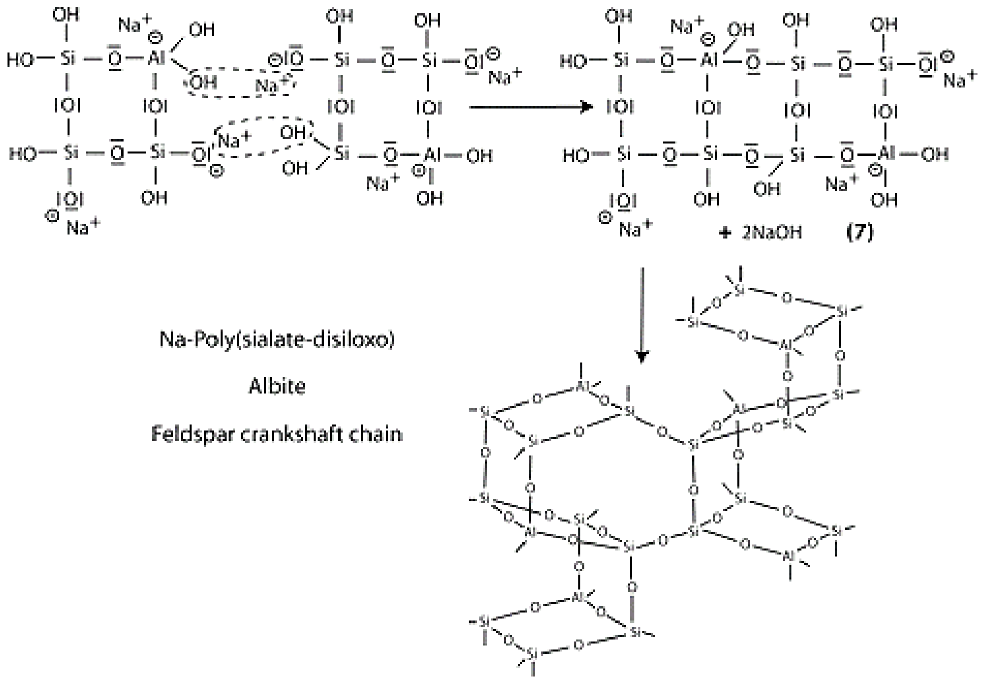

This finding is in agreement with the results reported by [47]. Researchers investigated metakaolin- based geopolymer with addition of polymer admixtures. The surface analysis, fourier transform infrared spectroscopy (FTIR) of geopolymer adsorbents are described in Figure 4.2. Metakaolin based geopolymer are exhibits main FTIR band at 1017 and 1383 cm^{-1} the asymmetrical stretching of Si-O bond Another band at 692 cm^{-1} (Si-O-Al/Si-O/Si stretching), 539 cm^{-1} (Tetrahedral aluminum stretching bands) are also show in metakaolin geopolymer high silica content in geopolymer structure strong geopolymer as the Si-O-Si are strong more than Si-O-Al bond .

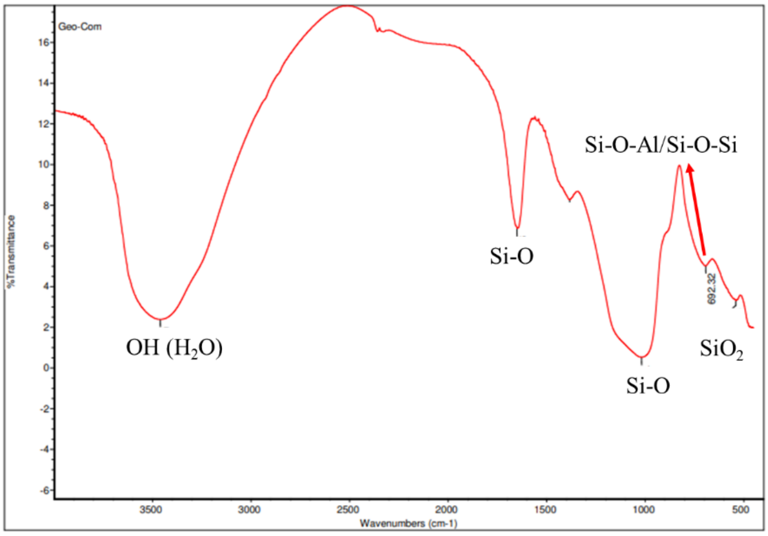

Figure 4.2 FTIR of GEO8M5D

The morphological characteristic of geopolymer shows in Figure 4.3 indicates that the microstructure of geopolymer was obtained. Figure 4.3 (a) was shown metakaolin sheets and sodium hydroxide onto surface of geopolymer. The reaction of MK sheets have been filled with formed sodium aluminosilicate particles more sponge- like amorphous gel. This finding is in agreement with the results reported by [94], who produced partially amorphous sodium aluminosilicates after activation of MK with sodium silicate formed, indicating that the structure experiences "enlargement". This reported that geopolymerization reaction has taken place. This may be probably because of the excess of Na^+ ion as stated above. Figure b, the morphology was obtained porous structure GEO8M5D. The reaction between species was proceed by polycondensation to the formation of amorphous to semi-crystalline aluminosilicate polymers.

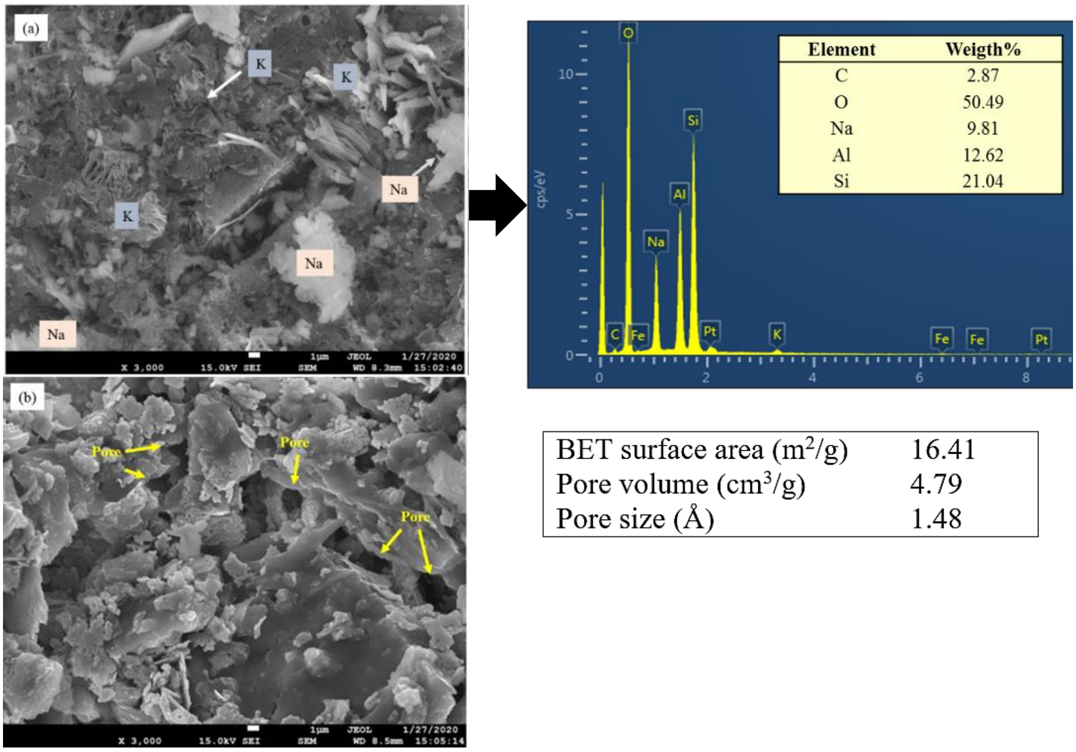

Element	Weigth%
C	2.87
O	50.49
Na	9.81
Al	12.62
Si	21.04

BET surface area (m^2/g)	16.41
Pore volume (cm^3/g)	4.79
Pore size (Å)	1.48

Figure 4.3 SEM/EDX of GEO8M5D (K: metakaolin, Na: sodium hydroxide from alkaline activator)

The EDX microanalysis was used to characterize the elemental composition of the metakaolin and geopolymer due to is morphological change observed in the synthesized geopolymer is due to the major elements such as carbon, oxygen, silicon, and aluminum, with proportion values of 2.87, 50.49, 21.04 and 12.62%, respectively.

The percentage of sodium elements 9.81% according to the alkali activator used in the geopolymerisation process. This finding is in agreement with the results reported by [93]. The BET surface area of metakaolin was 12.57 m^2/g, GEO8M5D at 16.41 m^2 /g, pore volume = 4.79 cm^3/g and pore size 1.48 Å, respectively. The results have been report [96]. The BET surface area of metakaolin from Thailand and geopolymer particles were 9.83 m^2/g and 20.36 m^2/g, respectively. The BET surface area and pore volume of geopolymer from fly ash was 29.00 m^2/g and 0.13 cm^3/g.

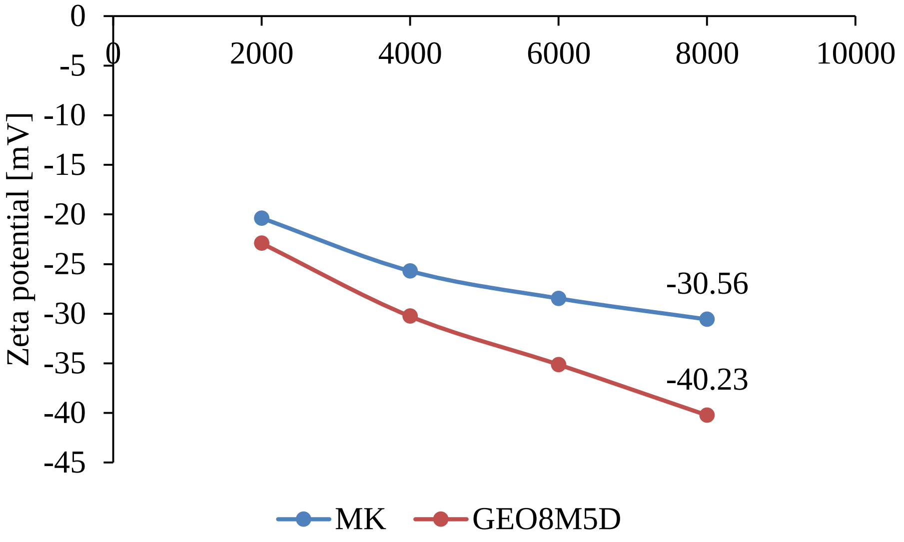

Figure 4.4 Zeta potential of MK and GEO8M5D with DI water at pH 5

Figure 4.4 contains the zeta potential obtained from MK and GEO8M5D at pH of 5 are -30.56 and -40.23 mV. The negative value was observed in the surface zeta potential. This behavior indicates that the surface of geopolymer is negatively charged higher than MK. Therefore, the compound is a good condition for the adsorption of the cationic dye existing in aqueous solution. Similar the literature by [98] and [99].

4.2 Adsorption efficiency of metakaolin and geopolymer

The adsorption efficiency of MK and GEO8M5D (8 M of NaOH) are shown in Table 4.2 and Figure 4.5. The adsorption efficiency were 76.46 and 95.00%, respectively. The specific BET surface area of metakaolin and metakaolin geopolymer was 12.57 and 16.41 m^2/g, respectively. Therefore, GEO8M5D powder had higher surface area than raw materials [100]. The geopolymer has better dye adsorption efficiency than MK, because the porous of geopolymer structure higher than MK. So, MK was developed of geopolymer for removal dye.

Table 4.2 Adsorption efficiency of metakaolin and geopolymer for MB removal

Adsorbents	Adsorption efficiency (%)	BET surface area (m^2/g)
MK	76.46±0.27	12.57
GEO8M5D	95.00±0.51	16.41

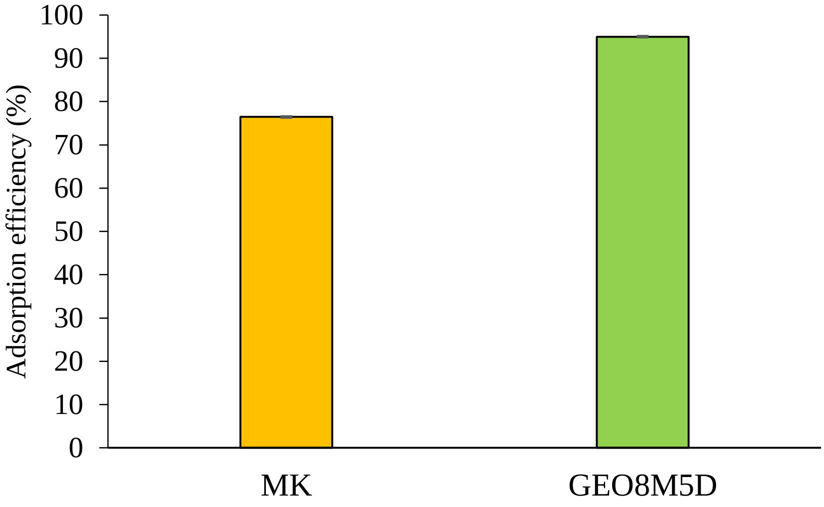

Figure 4.5 Adsorption efficiency of MK and GEO8M5D for MB removal

4.3 Optimization study

4.3.1 Effect of NaOH solution

The effect of NaOH concentrations and Na_2SiO_3 solution are important. The alkaline hydroxide is depended on the dissociation of aluminosilicates. The alkaline silicate acts as binder and alkaline activator are dispersant. The alkaline solution add amount of SiO_2 for the geopolymerization. These adsorbent characteristics can be tailored using alkali activation (geopolymerization). According to a results of [101], synthesis geopolymer with 8M solution of NaOH could remove clay and rice husk from MB aqueous solution well. El et al [93] used of NaOH 16 M and Na_2SiO_3 as an alkaline activator to synthesis geopolymer has been done. Wang et al [102] synthesis metakaolin was used as source material, NaOH and Na_2SiO_3 were used as alkali activators. Preparation of three sets of geopolymer samples subject different NaOH concentration from 8 to16 M. The effect of alkaline concentration on compressive strength was analyzed. NaOH concentrations at 12 and 16 M resulted in high 7 day compressive strengths. Finally, Luukkonen et al [103] , synthesis of geopolymer from metakaolin used difference alkali activator (8, 10 and 12 M NaOH). Adsorption capacities of NH_4^+ were investigated. The effect of NaOH concentrations on geopolymer properties has been investigated. NaOH concentrations was varied 6, 8, 10 and 12 M. 20 g/L of adsorbent dosage, 60 minutes of contact time and initial concentration at 300 ppm of MB . The adsorption performance increased with increasing the alkali concentration. Dissolution of silica and alumina from MK were greatly influenced by NaOH concentration where it has been completed that increasing molarity will increase the dissociation of the active species of raw material and yielding formation of more geopolymer gel network [104]. However, too high NaOH concentration may disrupt the geopolymerization process due to the excessive quantity OH^- ions which lead to inefficient reaction. The adsorption efficiency showed 95.17% of GEO8M5D.

The effect of alkali concentration on dye adsorption efficiency was shown in Table 4.3 and Figure 4.6. Therefore, the optimum concentration was GEO8M.

Table 4.3 The effect of NaOH concentration on dye adsorption efficiency

Samples	Adsorption efficiency (%)	q_e (mg/g)
GEO6M	91.82±0.61	30.23±0.07
GEO8M	95.17±0.20	31.75±0.03
GEO10M	96.68±0.12	32.98±0.01
GEO12M	96.59±0.19	33.00±0.08

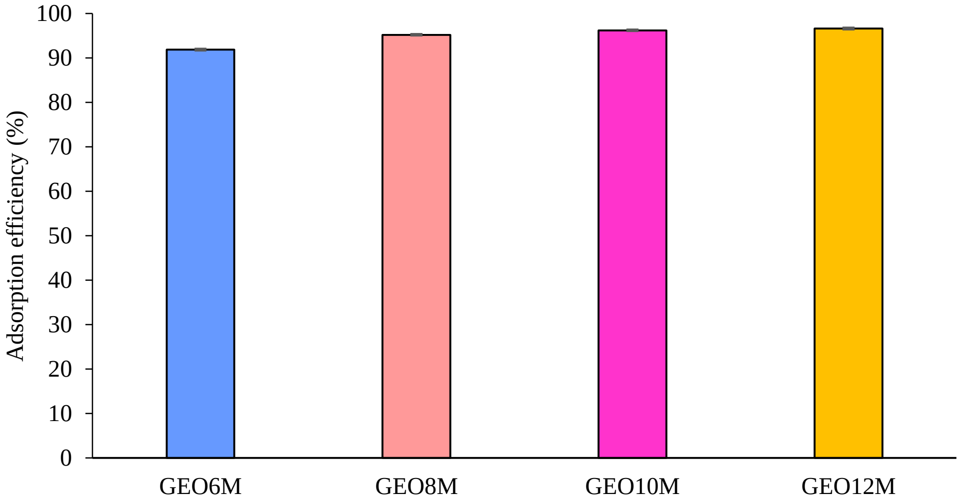

Figure 4.6 The effect of NaOH concentration on MB dye adsorption efficiency of geopolymer

4.3.2 Effect of curing time

The effect of curing time from geopolymer is direct mixing of aliminosilicate with alkaline solution. After mixing, geopolymer paste is compacted in molds, cover with a plastic film, cured in room temperature and avoid wide loss of moisture. Based on research of Lecomte et al [118], the normal and separate mixing did not lower the degree of geopolymerization of geopolymer from metakaolin. Nevertheless, separate mixing required additional water for mixing and hence detrimental to the mechanical strength. Therefore, the effect of cured time for geopolymer synthesis on geopolymer properties has been studied.

Table 4.4 The effect of cured time for geopolymer synthesis on dye adsorption efficiency of geopolymer

Curing time (Days)	Adsorption efficiency (%)	q_e (mg/g)
GEO3D	91.87±0.20	29.60±0.08
GEO5D	94.23±0.12	31.97±0.02
GEO7D	95.17±0.31	33.10±0.02

The cured time for geopolymer synthesis was varied from 3, 5 and 7 days. The result showed that the adsorption efficiency of 3, 5 and 7 days are 91.87, 94.23 and 95.17%, respectively. Therefore, the optimum cured times for geopolymer preparation was 5 days because the geopolymerisation reaction can completed at room temperature [105]. The adsorption efficiency was almost no change when increasing cure time as shown in Table 4.4 and Figure 4.7

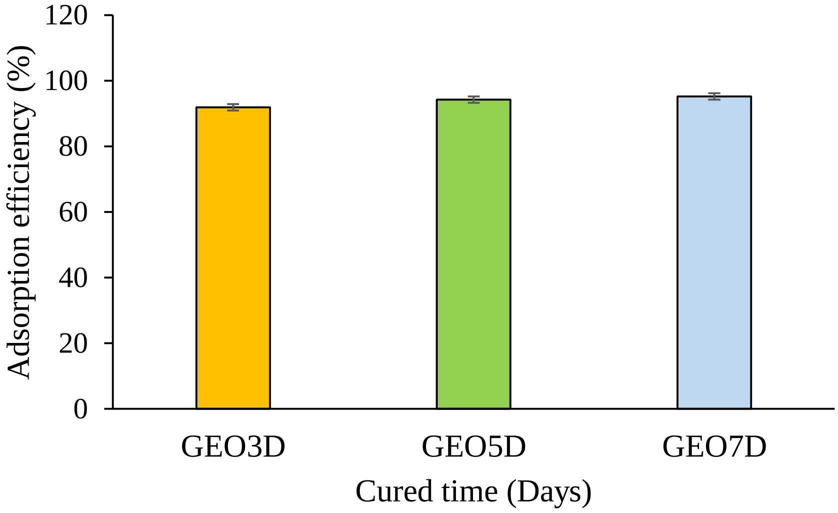

Figure 4.7 The effect of cured times for geopolymer synthesis on dye adsorption efficiency of geopolymer

4.3.3 Adsorption of dyes using geopolymer

The textile industry is main of the dyes and generates colored waste water with is capable of causing severe water pollution. The popular of dye was used by cationic and anionic. Because of its worldwide application in paper, letter and textile in dyeing and by virtue of being observed in the human. Other applications of geopolymer was used as an adsorbents for the removal of Brilliant green (BG), methyl orange (MO), and congo red (CR) from aqueous solution. The dosage of adsorbent was 20 g/L, 60 minutes of contact time and 300 ppm of concentration solution. The results were shown in Table 4.5, Figure 4.8.

Table 4.5 Adsorption efficiency on BG, CR and MO using GEO8M5D

Geopolymer using difference NaOH concentration (M)	Adsorption efficiency (%)			
	MB	BG	CR	MO
6	91.82±0.61	93.76±0.45	1.73±0.15	5.21±0.44
8	95.17±0.20	96.43±0.22	2.26±0.36	5.26±0.45
10	96.68±0.12	97.04±0.43	3.52±0.14	5.32±0.07
12	96.59±0.19	97.70±0.09	5.50±0.05	5.64±0.48

Figure 4.8 and 4.9 the adsorption efficiency of anionic dye were obtained. In Figure 4.8, the adsorption efficiency of congo red was shown around 1.80 to 6.0%. In Figure 4.10 the adsorption efficiency of methyl orange was shown 5.35%. Therefore, the removal of cationic dye and azo dye using geopolymer can higher efficiency.

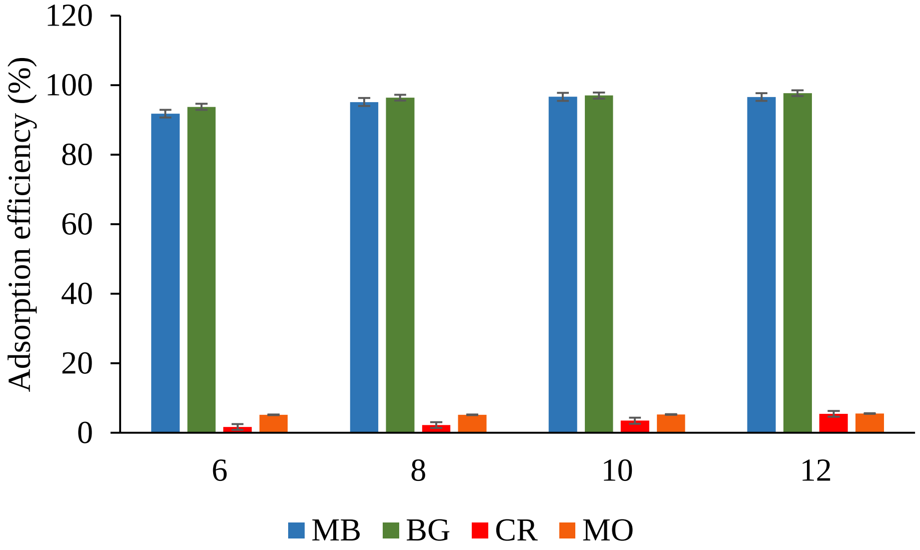

Figure 4.8 Adsorption efficiency of MB, BG, CR and MO using GEO8M5D

The adsorption efficiency of the geopolymer can adsorb with the cationic dyes. The adsorption efficiency between 91.82 to 96.59 and 93.76-97.70% of MB and BG, resprctively. The adsorption efficiency of the anion dye were adsorbed lower than

10%. The result showed that the zeta potential in Figure 4.9, the zeta potential was-30.56 and -40.23 mV of MK and GEO8M5D.

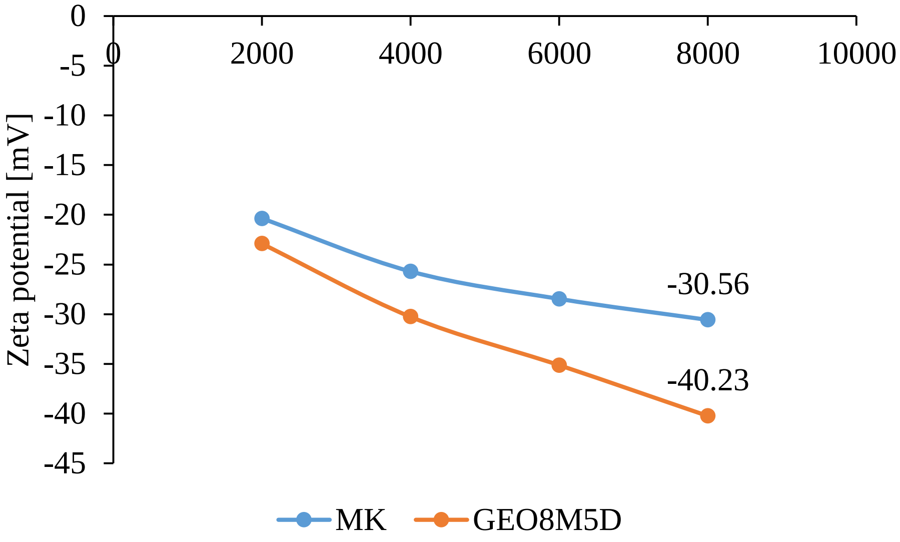

Figure 4.9 Zeta potenial of MK and GEO8M5D

So, the surface was shown negative value but the dye molecules of MB was positively charge. Consequently, the electrostatic repulsion increase between positively charge of cationic dye and negatively charge of surface adsorbent. With the increase in pH value is mainly according to the shape of cationic dye molecule as well as the pH value of the solution meaning strong attraction between H^+ and the positive charged cationic dye molecule. On the other hand, high solution of pH causing the surface of the geopolymer to become deprotonated and as a result the negative charge of the used geopolymer surface will be amplified. These result showed that a bonding between negative charge of adsorbent and positive charge of dye molecules and high removal of dye was seen [93] .

Therefore, the compound is a good condition for the adsorption of the cationic dye existing in aqueous solution. The adsorption for removal cationic dye using geopolymer from metakaolin and optimaized parameters were investigated by using MB dye.

4.4 Optimized parameters

4.4.1 Effect of pH

The pH is one of the important factors controlling the adsorption of dyes onto suspended particles . The effect of pH on the adsorption of MB using GEO8M5D was studied by changing initial solution pH values in the range from 2 to 10 at initial concentration 300 ppm, adsorbent dosage 20 g/L and 60 minutes of contact time.

The results are presented in Figure 4.10. The initial color of MB solution was deep blue. The color after adsorption was faded especially at pH 6 to 10.

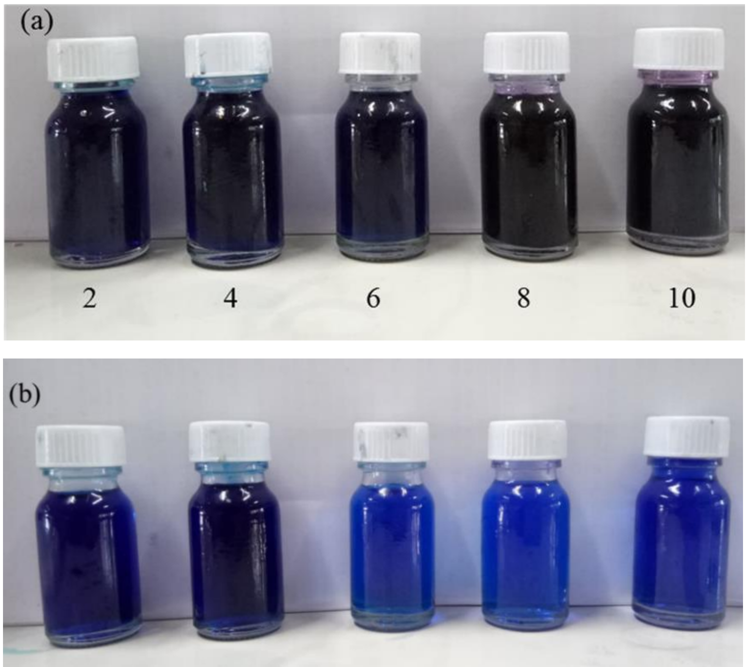

Figure 4.10 The color of solution different pH (a) before adsorption and (b) after adsorption

These result was shown that the surface charge and the degree of ionisation of adsorbate is greatly afected by pH parameter. In acidicpH, the surface of the GEO8M5D is surrounded by H^+ions, which decrease the interaction of the solute ions (MB^+) with the sites of the GEO8M5D material

For a better illustration of these results, it is required to determine experimentally the point of zero charge (pH_{PZC}). This is defined as the number of positive charges equal to the number of negative charges that exist on the surface of the adsorbent. The pH_{PZC} of the geopolymer is shown in Figure 4.11 and the pH_{PZC} value of the adsorbent found almost to be 8.57.

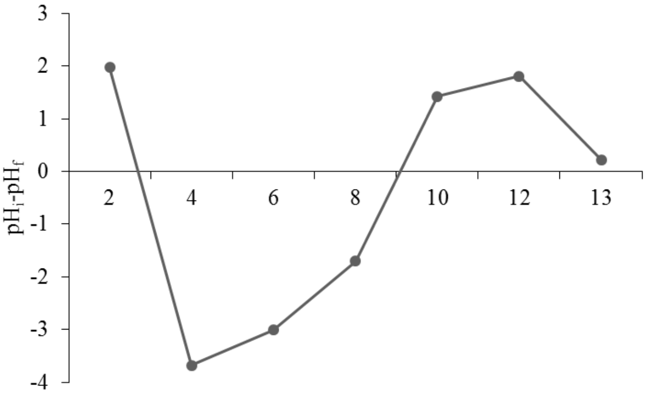

Figure 4.11 Point of zero charge (pH_{PZC}) of GEO8M5D

At pH = 2.23 to 6.16 < pH_{PZC} may be due to H^+ vies with MB, the sorbent surface takes up more H^+, reducing MB molecules bind on the sorbent surface.

At pH= 8.68 > pH_{PZC}, the adsorbent surface is negatively charged, the increasing electrostatic attraction between positive adsorbate species and adsorbent particles would lead to increase adsorption capacity of MB. Similar results were also reported by researcher [93].

Therefore, with increasing pH above pH_{pzc} , the removal of cationic dye by the geopolymer increased slightly. The removal increase can be explained by electrostatic attraction between the particles of the GEO8M5D, which is negatively charged, and the cationic dye, which is positively charged . These results show that the attraction between the GEO8M5D (negatively charged) and the MB (positively charged) depends on pH. The adsorption efficiency increases from 49.10 to 95.25% as pH increases from 2.23 to 8.68 then slowly decreased with pH of 10.20 (uptake 94.10%). The reuslt showed in Table 4.6 and Fugure 4.12.

Table 4.6 Effcet of initial pH solution

pH	Adsorption efficiency (%)	q_t (mg/g)
2.23	49.10± 0.92	16.24
4.34	87.69± 2.51	20.28
6.16	92.13± 0.05	30.20
8.68	95.25± 0.30	32.31
10.20	94.10± 0.02	31.54

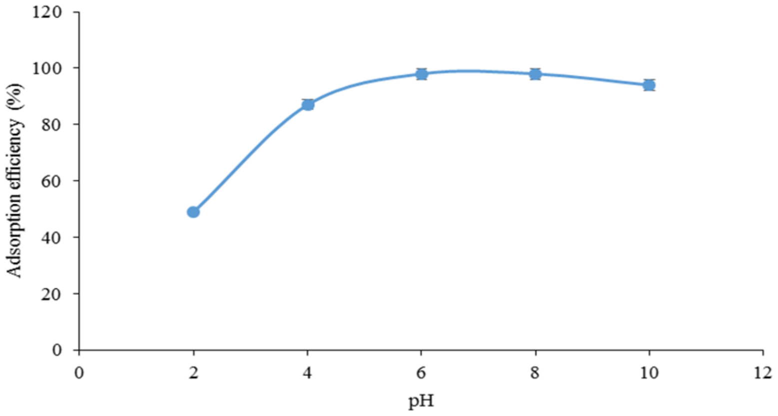

Figure 4.12 Effect of the different pH on the removal of MB dye

Low pH value (2.23-4.34) lead to increase in H^+ ion concentration in the system and the surface of the geopolymer carires positive charge by adsorbing H^+ ions. When increased with an increasing pH of 8.68, the adsorption efficiency increased because negatively charge on the surface area of GEO8M5D. At pH of 10.20, the adsorption efficiency slightly decreased due to the positive charge at the solution interface decreses and the adsorbent surface appears negatively. Thus, the adsorption of the dye molecules to the surface of the adsorbent reduced as pH was lowered. The result similar rerorted by Maleki et al. [36]

4.4.2 Optimum dosage

The effect of dosage on the removal of MB was studied using a series of 25 mL MB solution of 300 ppm containing a fixed contact time (60 minutes) of geopolymer, as shown in Table 4.7 and Figure 4.13.

Table 4.7 Effect of adsorbent dosage on adsorption efficiency

Dosage (g/L)	Adsorption efficiency (%)	q_e (mg/g)
10	81.48±0.25	27.17±0.35
20	95.77±0.31	31.94±0.07
40	96.01±0.02	32.02±0.15
80	99.00±0.01	33.01±0.02

The percentage removal of MB dye increased with the increase in dose of adsorbent. The mean percentage removal increased from 81.48 and 99.00 %. The adsorption capacity increased with an increasing 27.17 to 33.01 mg/g, the adsorption efficiency slightly increase before approach equilibrium at 95.77% of 20 g/L of dosage. This may be due to the increase in availability of surface active site resulting from the increased dose of the adsorbent. Considering the relationship between the optimal dosage and the MB removal, the optimal dosage for subsequent experiment was selected as 20 g/L (uptake 31.94 mg/g).

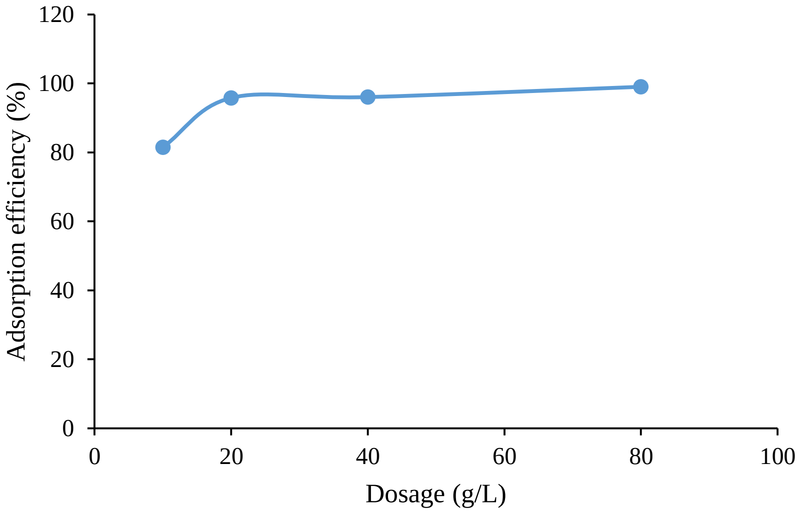

Figure 4.13 Effect of adsorbent dosage on adsorption efficiency of MB (C_0=300 ppm)

The similar results were earlier observed by Narumon Lertcumfu [106] and Pharatree Jaital [107], M.El Alouani and et al [93] and Maleki Ali et al [36]

Table 4.8 The Comparison of dosage removal by MB adsorptions

Adsorbents	Dosage (g/L)	q_e (mg/g)	References
MK- geopolymer	5.00	30.92	[106]
MK-geopolymer	1.00	43.48	[93]
MK-geopolymer	1.00	8.65	[36]
GEO8M5D	**20.00**	**31.94**	**This work**

By comparing the adsorption capacity described in Table 4.8. Lertcumfu et al studied MB removal by using MK-geopolymer. The adsorption capacity is 30.92 mg/g at an adsorbent dosage of 5.00 g/L. MB solution concentration was 200 ppm with 1440 minutes of contact time. The optimal dosage is lower than GEO8M5D. The adsorption capacity is nearly GEO8M5D. On the other hand, the highly MB solution concentration and contact time than GEO8M5D. Therefore, the optimal dosage of this work was shown high concentration of dye at 300 ppm.

4.4.3 Effect of contact time

The effect of contact time on the removal of MB was studied using a series of 25 mL MB solution of 300 mg/L containing a fixed amount of geopolymer, as shown in Table 4.9 and Figure 4.14. The mean percentage removal increased from 91.20 and 95.00 % when contact time was varied from 30 to 60 minutes and thereafter slightly change when increasing contact time to 120 minutes. The rate of dye removal is higher in the beginning due to free adsorption sites are more in the initial stage. The optimum contact time was 60 minutes. The adsorption capacity of geopolymer was increased with increasing contact time. The trend similar results were earlier observed by [106], [93], [36].

Table 4.9 Effect of adsorption time on adsorption efficiency of MB

Time (minutes)	Adsorption efficiency (%)	q_t (mg/g)
30	91.20±0.24	29.05±0.35
60	95.00±0.02	31.39±0.07
120	96.00±0.01	32.25±0.15
240	97.50±0.31	33.16±0.02

The process was divided into two step. The first step took 30 to 60 minutes to reach the relative adsorption equilibrium state called fast adsorption. This performance was due to the binding process between MB dye and the adsorption active sites, and functional groups on the GEO8M5D adsorbent. The absorption rate of the dye was controlled by the rate of the dye transported from the solution to the surface of the adsorbent particles. The second step was shown nearly equilibrium adsorption process. After 60 minutes of contact time, the relative increase in the removal extent of MB was slightly increased and with the increase of time. This performance was according to the binding process between MB dye and the adsorption active sites, and functional groups on the GEO8M5D adsorbent were gradually saturated. The absorption rate of the dye was controlled by the rate of the dye transported from the exterior to the interior pore sites of the adsorbent particles . Considering the relationship between the contact time and the MB removal, the contact time for subsequent experiments was selected as 60 minutes. The adsorption capacity for MB is 31.39 mg/g.

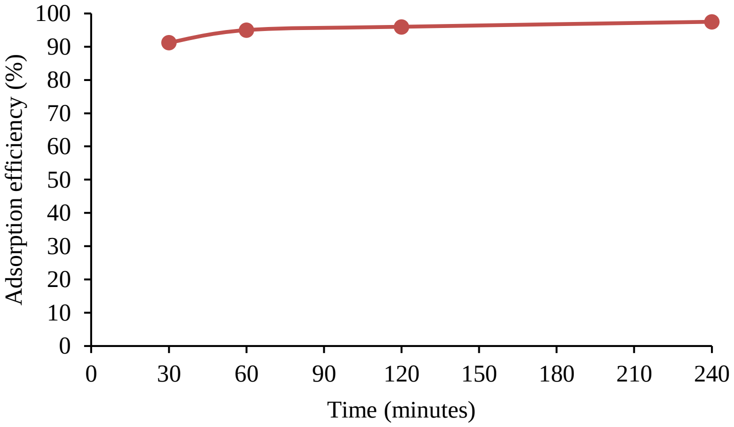

Figure 4.14 Effect of adsorption time on adsorption efficiency of MB (C_0=300 ppm)

By comparing the adsorption of contact time described in Table 4.10. El et al carried out a study on the removal of MB dye from aqueous solution at 120 minutes of contact time using by MK-geopolymer. He report that the adsorption capacity is 86.60 mg/g. The nearly equilibrium time here reported is higher than that of GEO8M5D (60 minutes). In this work showed lower contact time then others literatures reviews.

Table 4.10 Comparison of contact time removal by MB adsorptions

Adsorbents	**Contact time (minutes)**	**q_t(mg/g)**	**References**
MK- geopolymer	1440	30.92	[107]
MK-geopolymer	120	18.17	[93]
MK-geopolymer	1440	86.60	[36]
GEO8M5D	**60**	**31.39**	**This work**

4.4.4 Effect of initial concentration

The effect of initial concentration on the removal of MB was studied using a series of 25 mL MB solution of 300 to 550 ppm containing a fixed amount (20 g/L) and contact time (60 minutes) of geopolymer, as shown in Table 4.11 and Figure 4.15. The percentage removal of dye found to decrease with the increase initial dye concentration. The results showed that the percentage removal of dye decreases from 95.65 to 88.43%.

The adsorption capacity increased from 31.45 to 36.69 mg/g as the initial dye concentration increases from 300 to 550 ppm.

Table 4.11 Effect of initial concentration on adsorption efficiency

Concentration (ppm)	Adsorption efficiency (%)	q_t (mg/g)
300	95.65±0.24	31.45±0.25
350	94.36±0.59	32.14±0.12
400	91.64±0.57	33.47±0.02
450	90.45±0.21	34.23±0.36
500	89.27±0.12	35.17±0.14
550	88.43±0.56	36.69±0.03

At lower dye concentration, this may be due to unoccupied active sites on the adsorbent surface, when the initial concentration increases, the active sites required for adsorption of dye molecules disappear. The removal extent of dyes was decreased with an increase in the initial MB concentration due to the available active sites under high concentration of MB, but the adsorption capacity of MB solution on GEO8M5D increased with the increase of initial MB concentration. Similar results have been reported in literature by Lertcumfu et al, [106] M. El Alouani and et al [93] and Maleki Ali et al [36].

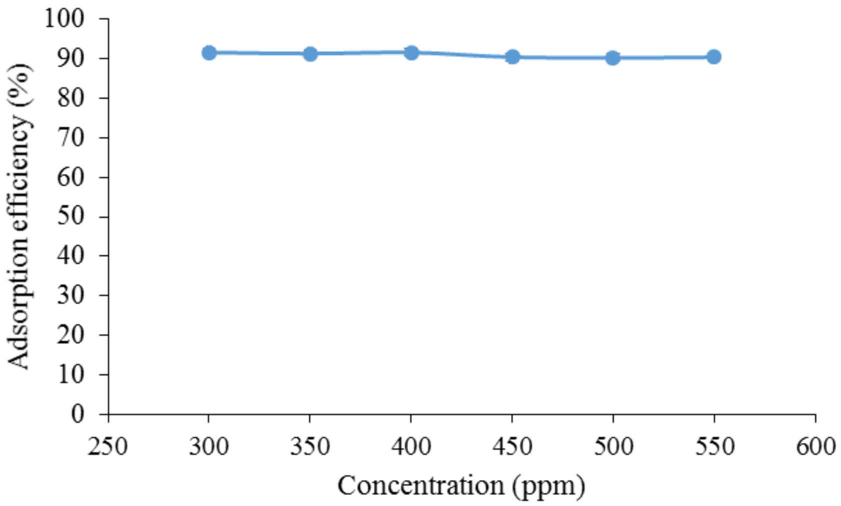

Figure 4.15 Adsorption efficiency of MB on effect of initial dye concentration

Similar trend on effect of initial concentration on adsorption of MB has been report by Lertcumfu et al. He report that the adsorption capacity of MK- based geopolymer of 39.20 mg/g at 200 ppm of initial concentration. Maleki et al reported that metakaolin based geopolymer for removed MB solution with adsorption capacity of 86.60 mg/g at 200 ppm of initial concentration. The adsorption capacity is higher than the adsorption capacity of GEO8M5D (31.45 mg/g). The different of adsorption capacity may be due to difference condition such as the concentration of NaOH Therefore, all of literature showed lower the initial concentration than GEO8M5D.

Table 4.12 Comparison of initial concentration removal MB dyes by difference adsorbents

Adsorbents	**Initial concentration (ppm)**	**q_e(mg/g)**	**References**
MK- geopolymer	200	30.48	[106]
MK-geopolymer	40	40.00	[93]
MK-geopolymer	200	86.60	[36]
GEO8M5D	**300**	**31.45**	**This work**

4.5 Isotherm studies

Isotherm studies to obtain the adsorption mechanism of the distribution between adsorbate and adsorbent, two different model, Langmuir and Freundlich were employed of to fit the data.

Langmuir Isotherm model was originally developed to explain and quantify sorption on a set of evident localized adsorption sites and has been used to describe both physical and chemical adsorption and monolayer adsorption. This model can be suppositions are following

(1) Molecule of adsorbate on define localized site and the fullness corresponds to full occupancy of these site.

(2) The adsorption site are all forcefully homogeneous, and there isn' t interaction between adsorbed molecules.

(3) Each active site interactions with only one adsorbate.

This model is expressed by the following equation 4.1:

$$\frac{C_e}{q_e} = \frac{1}{q_m K_e} + \frac{C_e}{q_m}, \tag{4.1}$$

When q_e is the amount of dye at equilibrium (mg/g), C_e is the equilibrium concentration of dye (mg/L), K_L is the Langmuir constant (L/mg) and q_m is amount of monolayer adsorption capacity (mg/g).

Freundlich Isotherm model is describing of the multilayer and heterogeneous adsorption molecule this surface equilibrium between fluid and a solid material. This model is demonstrated by Equation 4.2:

$$\log q_e = \log K_F + \frac{1}{n} \log C_e, \tag{4.2}$$

When K_F is adsorption capacity and is adsorption intensity; it also indicates the relative distribution of the energy and the heterogeneity of the adsorbate sites [108].

The essential features of the Langmuir isotherm can be explicated in terms of a dimensionless constant called separation factor (R_L, equilibrium parameter) which is determined by the following equation 4.3:

$$R_L = 1/1+ K_LC_o \tag{4.3}$$

Where C_0 (mg/ L) is the initial dye concentration and K_L (L/mg) is the Langmuir constant related to the energy of adsorption. In Table 4.13, were obtained the parameter of isotherm.

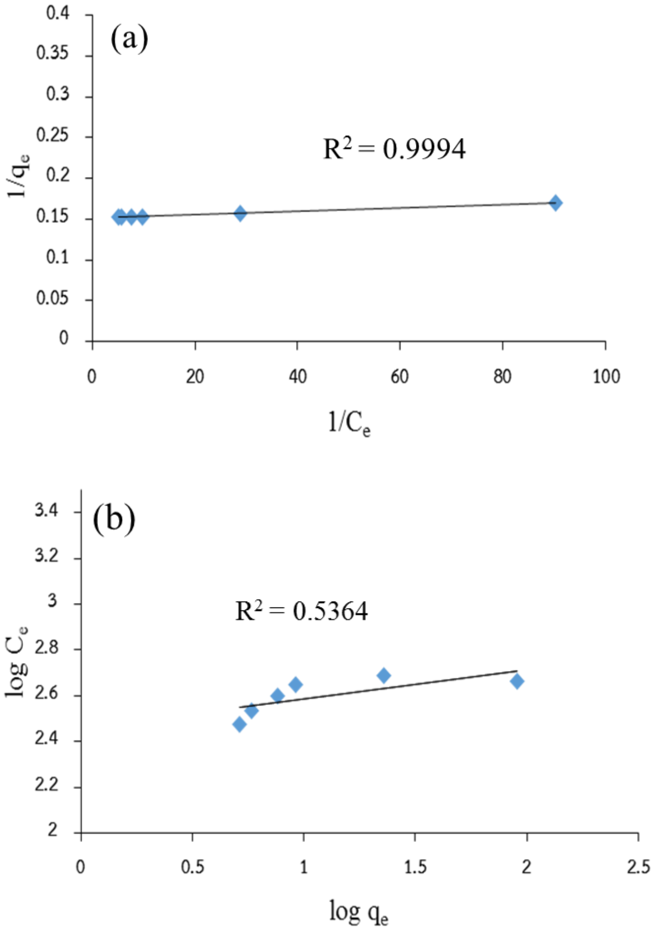

Figure 4.16 Adsorption isotherms for MB using geopolymer; (a) Langmuir isotherm (b) Freundlich isotherm.

Figure 4.16 represents the Langmuir and Freundlich, isotherm models. The constants calculated from the model equations (Langmuir and Freundlich are shown in Table 4.13.

Table 4.13 The parameter of adsorption of MB using Langmuir and Freundlich isotherm

Langmuir isotherm	Freundlich isotherm
R^2 = 0.9994	R^2 = 0.5364
q_e (mg/g) = 31.45	1/n = 0.1209
K_L = 0.0061	K_F = 0.0063
R_L = 0.7439	-

As observed, the value of R^2 obtained from the Langmuir isotherm equation (0.9994) was higher than that from the Freundlich (0.5364) isotherm equations. These results showed the adsorption could be well described by the Langmuir model. The adsorption occurred on the homogeneous surface as a monolayer, and the optimum monolayer adsorption capacity (q_e) was found to be 31.45 mg/g. The R_L value was obtained within the range $0 < R_L < 1$, indicating that the adsorption of cationic dye on the geopolymer material is favorable.

In addition, Table 4.14 presents a summary of the optimum adsorption capacity q_e and corresponded Langmuir isotherm of the developed adsorbents for MB dyestuff in the aqueous solution. All the literatures research showed isotherm model similarly trend of this works.

Table 4.14 Comparison of the obtained adsorption isotherm with the previously developed adsorbents in the literature

Adsorbents	**Isotherm**	**q_e (mg/g)**	**References**
FA-derived zeolites	Langmuir	4.26	[109]
NaOH-trated raw kaolin	Langmuir	16.34	[110]
Kaolin geopolymer	Langmuir	25.60	[111]
Phosphoric acid-based geopolymer	Langmuir	4.26	[112]
Coal-FA-geopolymer	Langmuir	50.70	[113]
FA-geopolymer		37.04	[12]
Biomass-geopolymer	Langmuir	15.40	[114]
MK-geopolymer	Langmuir	43.48	[93]
Geopolymer difference ratio Si/Al ;			
G-1	Langmuir	15.95	[115]
G-2		17.89	
G-3		20.22	
GEO8M5D	**Langmuir**	**31.45**	**This work**

4.6 Kinetic studies

It is important to be able to predict the rate at which contaminates are removed from aqueous solution in order to design adsorption treatment. The principle of the pseudo-first-order model is that the reaction rate is proportional to the number of ions remaining in the solution, summarizing that adsorption is controlled by diffusion step. It's concluded that the adsorption rate is proportional to the difference between the saturated concentration and the adsorption amount of GEO8M5D with time. The pseudo-second-order, which can be expressed as the reaction rate being proportional to the concentration of two reactants, concluding the adsorption is controlled by chemisorption steps.

Table 4.15 Kinetic parameters for adsorption of MB onto GEO8M5D

Parameters	Pseudo-first-order	Pseudo-second-order
R^2	0.7598	1
k	0.0070	0.3130
$q_{e(cal)}$ (mg/g)	43.52	31.39
$q_{e(exp)}$ (mg/g)	32.18	32.18

Table 4.15 and Figure 4.17 shows the pseudo-first-order and pseudo-second-order plots for adsorption of MB at various contact time at room temperature. The correlation coefficients (R^2) values obtained for the pseudo-first-order (0.7598) were lower than that of the pseudo-second-order (1). The experimental q_e ($q_{e(exp)}$)value did not agree with the calculated valued obtained from linear plot. This indicated that the adsorption of MB on to GEO8M5D does not follow pseudo-first-order. The suitability of pseudo- second-order was judged based on the R^2, which are a computation of goodness of fit. Pseudo-second- order rate constants k_2 (calculated from the intercept and slope) as well as linear regression R^2 summarized in Table 4.16 . The result show that R^2 for the pseudo-second-order are greater than those for pseudo-first-order, stipulating good agreement with the experimental data. It can be inferred that the pseudo-second-order ($R^2 = 1$) fits the adsorption data better than the first order model.

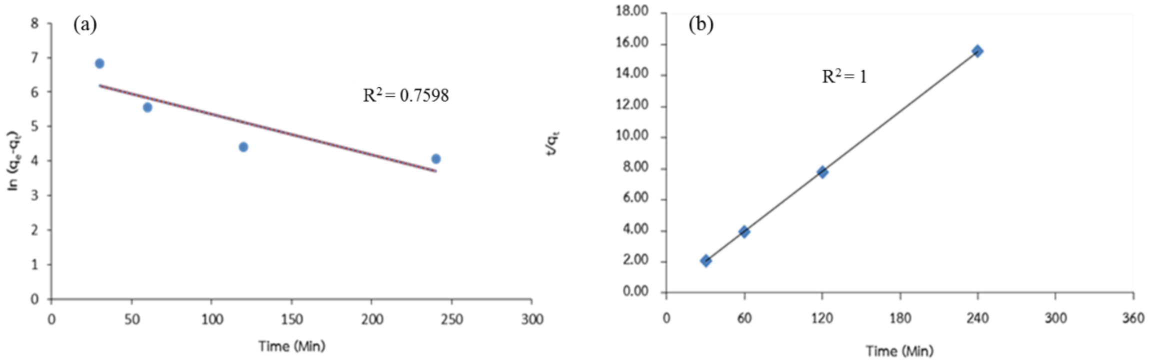

Figure 4.17 Adsorption kinetics of MB adsorption onto GEO8M5D; (a) pseudo-first-order and (b) pseudo-second-order

The results showed that the pseudo-second-order model can be used to explain the adsorption process of MB on GEO8M5D and demonstrated that chemisorption dominated the adsorption process. The adsorption process not only included the processes of the liquid film diffusion and the internal diffusion of mesopores, but also the chemisorption process with electrons shared and gained or loss of electrons between cationic dyes and functional group on the GEO8M5D surface. Furthermore, Table 4.16 presents a summary of pseudo-second-order and the adsorption capacity q_e of the developed adsorbents for MB dyestuff in the aqueous solution. The literature reviews was indicated that the pseudo-second-order.

Table 4.16 Comparison of the obtained kinetic model and the adsorption capacity with the previously developed adsorbents in the literature

Adsorbents	Kinetics	q_e (mg/g)	References
G-1	Pseudo-second-order	5.50	[115]
G-2		5.39	
G-3		5.64	
MK-geopolymer	Pseudo-second-order	39.20	[93]
AC-SLS	Pseudo-second-order	190.90	[116]
Kaolin-geopolymer	Pseudo-second-order	25.60	[111]
GEO8M5D	**Pseudo-second-order**	**31.25**	**This work**

The sialate geopolymer network consists of silicate and aluminate groups connected by covalent bond Si-O-Al-. The (Na^+) cations present in the structural cavities of the poly(sialate) balance the negative charge of Al^{3+} in coordination (IV) . During the adsorption phenomena, the removal of MB by the adsorbent can be explained by the interactions between the positive charge of MB^+ and the negative charge of Al tetrahedral (-Si-O-Al^--O-Si-O) in the metakaolin-based geopolymer (Figure 4.18) is proposed mechanism explains the chemisorption of MB by the GEO8M5D. Similar results were found in literature [19].

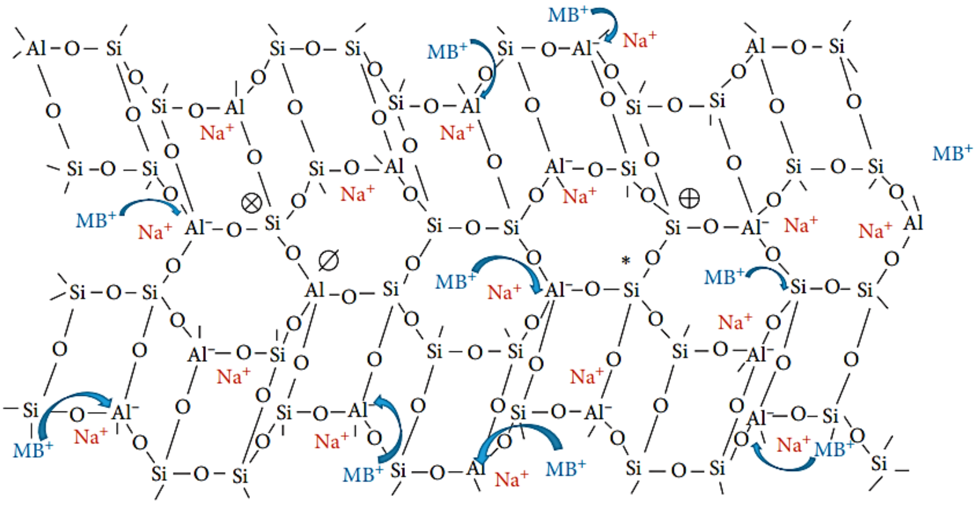

Figure 4.18 Proposed mechanism for adsorption of MB by GEO8M5D

4.7 Thermodynamics studies

The effect of temperature on dye removal was studied by varying temperatures (20, 30, 40 and 60°C). The values of thermodynamic parameters, enthalpy (ΔH°), gibbs energy change (ΔG°) and entropy change (ΔS°) of the adsorption process of the geopolymer were calculated from the slope and intercept of the plot of $\ln K_c$ versus 1/T (Figure 4.19).

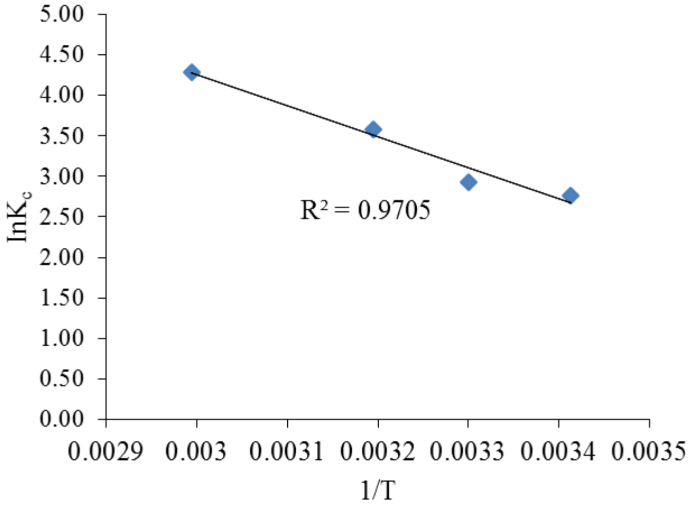

Figure 4.19 Enthapy and entropy change determination of the adsorption of MB by GEO8M5D

This indicated that the adsorption was a spontaneous endothermic process. The nagative ΔGº values, which can be seen from Table 4.17, corresponded the discolored process of MB on GEO8M5D in term of possibility and sponteneity. The positive ΔH° values 39.84 kJ/mol prove that the adsorption was an endothermic peocess. The positive Δ*S*° values indicate an irregular increase of the randomness at the adsorbate - adsorbent interface during the adsorption.

Table 4.17 Thermodynamic parameters for removal efficiency of MB on GEO8M5D

T(K)	**lnK$_c$**	**ΔG° (kJ/mol)**	**ΔH° (kJ/mol)**	**ΔS° (J/molK)**	**q$_e$ (mg/g)**
293	2.76	-6.72	39.84	162.49	31.51±0.02
303	2.93	-7.37			32.73±0.08
313	3.58	-9.30			33.20±0.01
333	4.29	-11.91			34.31±0.05

The adsorption capacity is 31.51 mg/g at 293 K. Similar phenomenon has been observed in the adsorption on developed adsorbents show in Table. 4.18.

Table 4.18 Comparison of the obtained thermodynamic with the previously developed adsorbents in the literature

Adsorbents	ΔG°	ΔH°	ΔS°	References
C4ABS C6ABS C8ABS	Spontaneous	Endothermic	Positively	[110]
Nano - zerovalent iron (nZVI)	Spontaneous	Endothermic	Positively	[108]
poly(AAc-SA-AM)/SH	Spontaneous	Endothermic	Positively	[117]
MK-geopolymer	Spontaneous	Endothermic	Positively	[93]
AC-SLS	Spontaneous	Endothermic	Positively	[116]
GEO8M5D	**Spontaneous**	**Endothermic**	**Positively**	**This work**

4.8 Regeneration test

The regeneration of geopolymer after dye adsorption was also performed. The possible reuse of the adsorption and to choose a suitable desorbated/regenerated was studied. The regeneration was obtained by calcined 400˚C for 2 hr. The FTIR spectra of pureMB , MB adsorbed on GEO8M5D and GEO8M5D after 1st cycles of calcined are shown in the Figures 4.20, respectively.

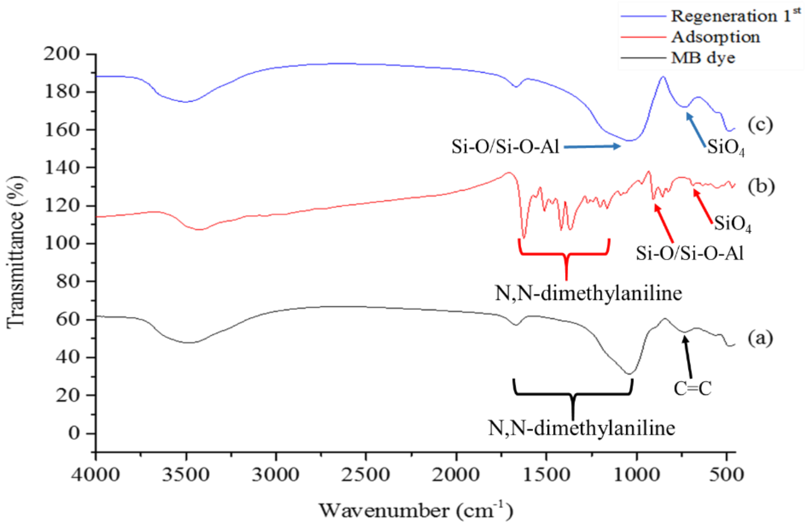

Figure 4.20 The peak of FT-IR;(a) MB dye; (b) Adsorption onto geoplymer and (c) after regeneration 1st cycles

For MB dye, from the range 1590 to 1294 cm^{-1} which represents aromatic ring structures in MB. This indicates destruction of polyaromatic structure in MB . Hence, N,N-dimethylaniline ($C_6H_5N(CH_3)_2$). The peak at 791 cm^{-1} is related to the C=C skeleton of the aromatic rings. Figure 4.19(b) shows strong signature of MB indicating the adsorption of MD on the surface of GEO8M5D. The FTIR spectrum of GEO8M5D without adsorbed dye moleculesis shown Figure 4.19 (c) for comparison. GEO8M5D are showed main FTIR band at 693 cm^{-1} (Si-O-Al/Si-O-Si stretching), 539 cm^{-1} (Tetrahedral aluminum stretching bands) are also show in metakaolin geopolymer high silica content in geopolymer structure as the SiO_4 bond. All the bands assignments are listed in Table 4.19.

Table 4.19 FTIR spectrum analysis

Materials	Bands (cm^{-1})	Assignments	Reference
GEO8M5D	1383	Si-O stretching	[37] [82]
	1017	Si-O stretching	
	692	Si-O-Al/Si-O/Si stretching	
	593	Bending vibration Si-O-Al	
MB dye	1591-1292	N,N-dimethylaniline	[119]
	791	C=C aromatic ring	
Adsorption	1590-1294	N,N-dimethylaniline	
	791	C=C aromatic ring	
	694	Si-O-Al/Si-O/Si stretching	
	592	Bending vibration Si-O-Al	
9th cycles	693	Si-O-Al/Si-O/Si stretching	
	539	Bending vibration Si-O-Al	

The sample was applied to remove MB under the conditions MB concentration 300 ppm and GEO8M5D dose 20 g/L in 25 mL solution (60 minutes of contact time) and the adsorption MB dye (C_0 = 300 ppm). Table 4.20, the percentage removal of MB dye decrease with the decrease in regenerate of adsorbent. The mean percentage removal decrease from 95.23 and 65.46 %. The adsorption capacity decreased with an decreasing 31.24 to 22.08 mg/ g. Truly, the thermal methods have been used for the regeneration of exhausted/spent zeolites. Sun et al investigated of regeneration zeolite by heating it at high temperatures (450 °C, 550 °C, and 650 °C); however, the optimal adsorption capacity (90 to100%) was achieved at 450 °C. Thermal treatment at higher temperature may cause the loss of the structure (framework) of zeolites, resulting in a decrease in their adsorption capacity.

4.20 MB uptake for GEO8M5D after multiple regeneration cycles

Number of cycles	Adsorption efficiency (%)	q_e (mg/g)
0	95.23±0.78	31.24±0.12
1	94.00±0.40	30.00±0.15
2	92.61±0.21	29.78±0.02
3	91.60±0.31	28.68±0.07
4	90.00±0.45	27.52±0.26
5	87.43±0.71	26.86±1.14
6	81.73±1.25	25.97±1.24
7	78.00±1.14	24.18±1.48
8	73.85±0.50	23.09±1.23
9	65.46±0.36	22.08±0.03
Cumulative q_e (mg/g)		**296.92**

The performance of geopolymer adsorbent was fermented after the 5th cycles, while induced slightly reduction on the MB uptake. At this stage the performance of the adsorbent decreaded were observed on uptake and removal efficiency up to the 9th cycle, showly the feasibility of reusing this rearranged adsorbent without any performance conciliated. The regeneration of adsorbent for removal MB dye has been significantly higher than geopolymer monolitic. Novais et al. [13], study the adsorption for removal MB dye used geopolymer monolitic and 5th cycles of regeneration at 50 ppm of MB dye concentration. The adsorption capacity and cumulative q_e showed at 31.10 mg/g and 78 mg/g, respectively after 5th cycles. The results of regeneration and reuse show that GEO8M5D can be used nine times, preserving the sameadsorption capacity being a cost–effective adsorbent and cumulative q_e up to 296.92 mg/g.

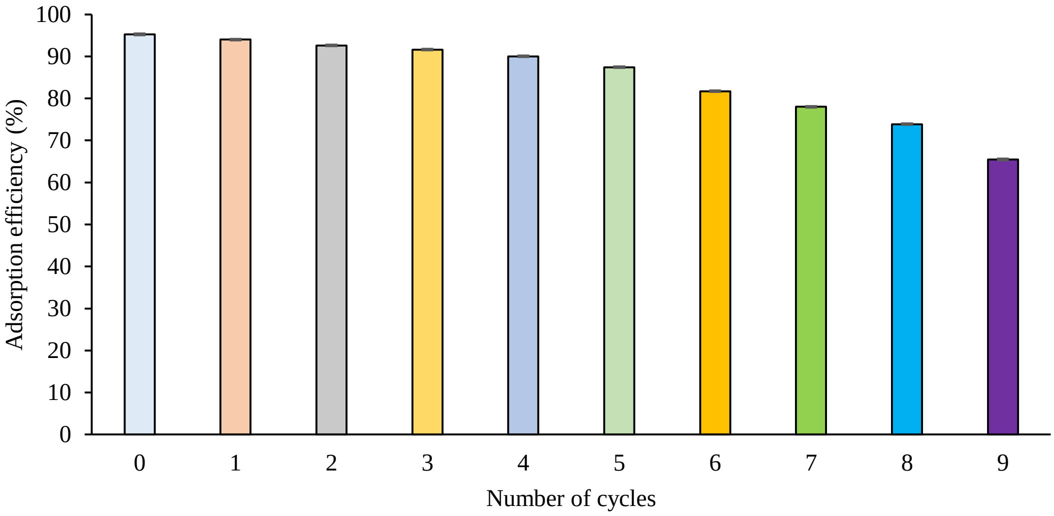

Figure 4.20 MB uptake for geopolymer after multiple regeneration cycles

The BET surface areas, pore volumes and pore sizes of the samples before and after thermal regenreration showed in Table 4.21.

Table 4.21 The BET surface areas, pore volumes and pore sizes of the sample of before and after calcined

Samples	BET surface areas	Pore volumes	Pore sizes
Before calcined	16.41	4.79	1.48
9th cycles	8.90	3.84	2.63

Before calcind, the sample showed higher value of BET surface area, pore volume and pore size than final of regeneration. The BET surface area, pore volume and pore size decreased with an increasing cycles of thermal regeneration.

Therefore, the next study to extract silica from RH used as Na_2SiO_3 for geopolymer precusor. The parameters such as the optimal dosage, contact time, isotherm, kinetic thermodynamic and regeneration of adsortption were studied.

4.9 Extract of silica from rice husk

The particles color showed in Figure 4.21. For Figure 4.21 (a), the particle showed a natural sheath that forms around rice grains. After calcined showed white silica powder form. The yields of silica from rice husk is 16%.

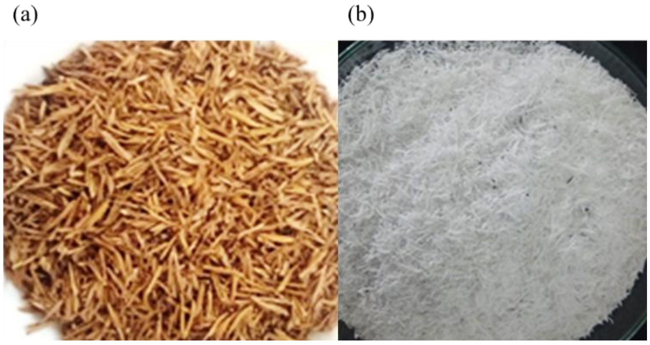

Figure 4.21 Particle color of (a) RH (b) Si-RH

The composition of Si-RH was investigated by XRF tecnique. The results showed pure silica is 99.30 % (Table 4.13). Afterthat, It can be prepared for Na_2SiO_3 (SiO_2 + NaOH) for geopolymer precursor. The alkali activator (Na_2SiO_3) from Si-RH was represented commercial.

Table 4.21 The composition of silica extract

Formula	Mass (%)
SiO_2	99.30
MgO	0.20
CaO	0.18
Fe_2O_3	0.11

The major chemical groups present in silica are identified by the FTIR spectra shown in Figure 4.21. The broad band at 3750 cm^{-1} was due to OH stretching. The broad band at 2500 was due to silanol hydroxyl groups. The peak between 1200 and 1050 cm^{-1} is associated with the Si-O-Si asymmetric band stretching and 690 cm^{-1} belongs to

Si-O-Si stretching modes. The FTIR analysis achieved here in this experiment is similar to those reported by other workers who carried out similar studies [120].

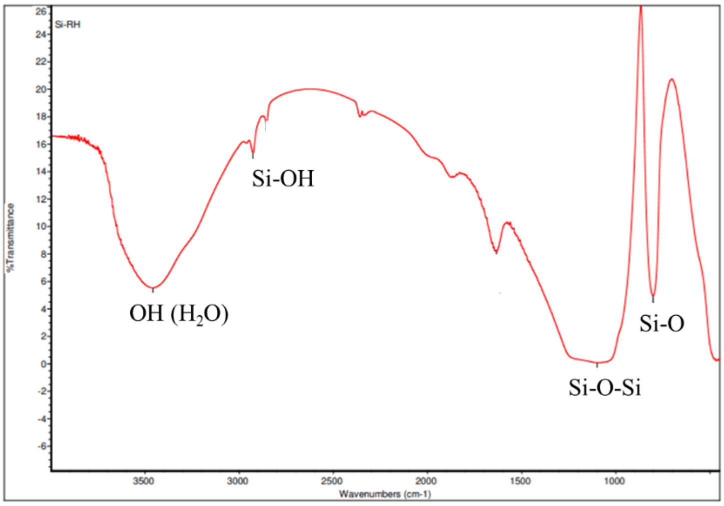

Figure 4.22 FTIR spectra for Si-RH

4.10 Characterization of GSiRH

The extraction of silica from rice husk was prepared for Na_2SiO_3 activator for geopolymer precursor. In this part, the adsorption efficiency and capacity used GSiRH compare with GEO8M5D. The XRD patterns for geopolymer are shown in Figure 4.23. The XRD patterns were shown crytalline and unchanged for composition. After the activation process, the main crsytalline in GSiRH was quartz . The crystalline phases were dissolved in the alkaline solution and aluminosilicates phases was formed in the surface of metakaolin by a slower geopolymerization. The present study suggests that the presence of silica has significant effect on the geopolymerisation reaction between alkaline solution and metakaolin. It has been widely accepted that geopolymerization compose of cross linked aluminate and silicate tetrahedral, where charge balance from aluminate is provided by hydrated Na^+ metal ions. So, the excess alkali was competent to migrate to the surface of the GSiRH during curing which then crystallized as NaOH. Similar findings were reported by [121].

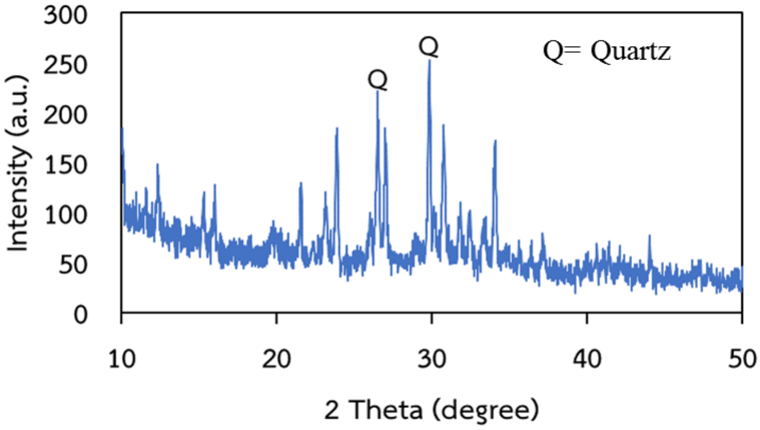

Figure 4.23 The XRD patterns of GSiRH

Figure 4.24 (a) showed FTIR of GSiRH. GSiRH showed several band at the region between 500 to 4000 cm^{-1}. Broad bands were shown in GSiRH at 3459 and 1652 cm^{-1} for the (-OH, H-O-H) stretching mode. On the other hand, one in peak situated at 1373 cm^{-1} was O-C-O stretching mode, indicating the presence of sodium carbonate. It is to the action in silicates. The peaks which were shown at 610 and 540 cm^{-1} consist of Si-O-Si and SiO_4 bending vibration of situ-synthesized silicate [122]. From Figure 4.24 can observed that intensity of most peak is similar for GEO8M.

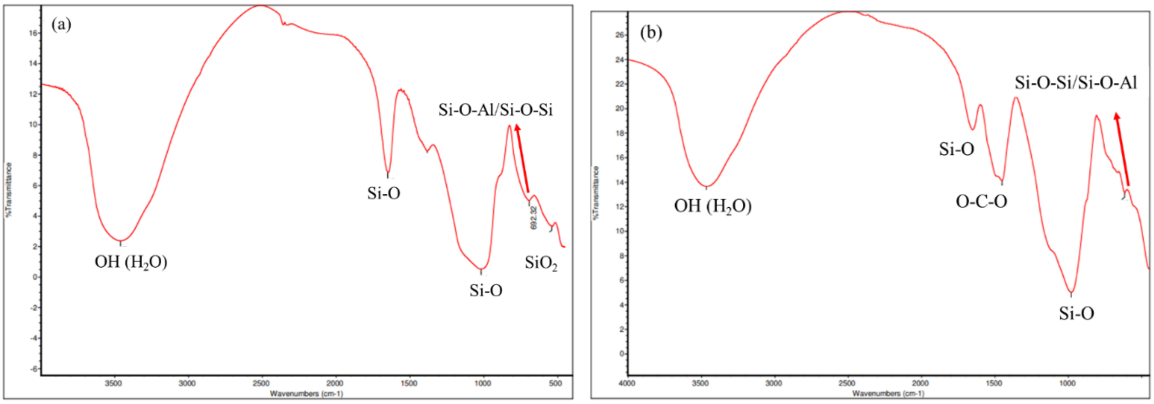

Figure 4.24 FTIR spectra of; (a) GEO8M5D and (b) GSiRH

Figure 4.25 shows the representtative SEM image of GSiRH . The surface morphology of the GSiRH is llustrated pore and roughness on the surface.This morphological change observed in the synthesized geopolymer is due to the dissolution of metakaolin aluminosilicates in the activator solution leading to the formation of aluminosilicate gel. EDX microanalysis was used to characterize the elemental composition of the GSiRH. According to the EDX analysis, the major elements were carbon, oxygen, and aluminum, with proportion values of 2.87, 50.49, and 12.62%, respectively.

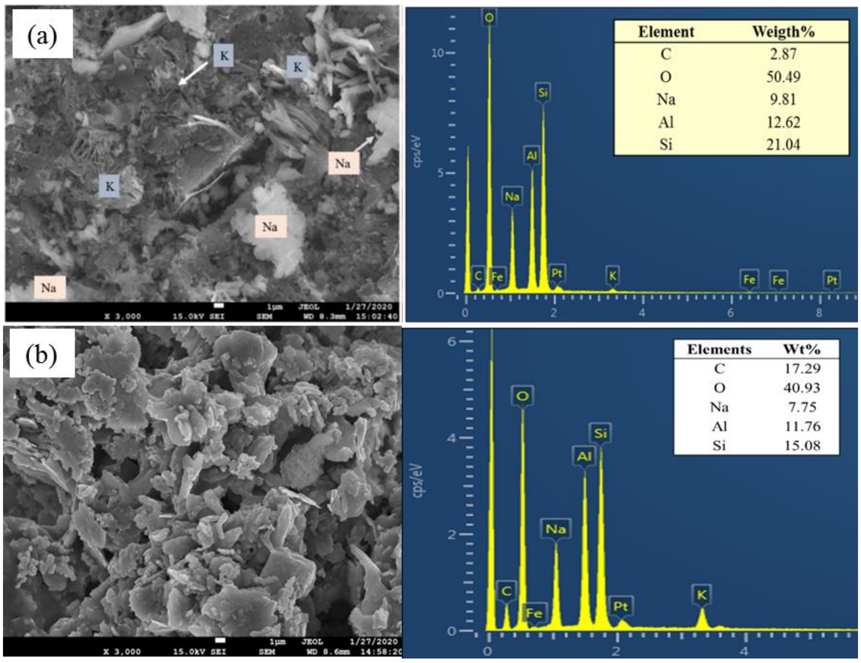

Element	Weigth%
C	2.87
O	50.49
Na	9.81
Al	12.62
Si	21.04

Elements	Wt%
C	17.29
O	40.93
Na	7.75
Al	11.76
Si	15.08

Figure 4.25 SEM-EDX microstructure of ; (a) GEO8M5D (b) GSiRH

As can be seen from the spectrum, the mainly weight percentage corresponds to carbon, oxygen, aluminium and silicon, which is clear due to the highly inorganic nature of the GSiRH, whereas the presence of carbon indicates the participation of organic fractions from silica, which are the factors causing the good flow behavior of the geopolymerisation The percentage of sodium elements is 9.81%; this is due to the alkali activator used in the geopolymerization process. The ratio of Si: Al showed 1.66 and 1.28 of GEO8M5D and GSiRH, respectively. The higher Si/Al ratio resulted in higher amount of Si-O-Si bonds in GEO8M5D and it was well known that Si-O-Si bonds were stronger than Si-O-Al bonds [121]

The BET surface area, pore volume and pore size were 13.99 m^2/g, 2.10 cm^3/g and 2.28 Å, respectively. The BET surface area of GSiRH lower than that showed in Table 4.22.

Table 4.22 The BET surface area between GEO8M5D and GSiRH

BET	GEO8M5D	GSiRH
BET surface area (m^2/g)	16.41	13.99
Pore volume (cm^3/g)	4.79	2.10
Pore size (Å)	1.48	2.28

4.11 Effect of alkaline solution of GSiRH

The effect of NaOH concentrations varied 6, 8, 10 and 12 M mixed silica. The results showed in Table 4.17 and Figure 4.23. The adsorption efficiency of geopolymer with G-6, G-8, G-10 and G-12 of 74.23, 78.67, 80.83 and 83.98%, respectively.

Table 4.23 The effect of NaOH concentration on dye adsorption efficiency

Samples	Adsorption efficiency (%)	q_e (mg/g)
G-6	74.23±0.12	18.48±0.02
G-8	78.67±0.11	20.25±0.01
G-10	80.83±0.03	21.38±0.21
G-12	83.98±0.24	22.54±0.30

The adsorption performance increased with increasing the alkali concentration. Because of dissolution silica and alumina from MK were greatly influenced by NaOH concentration where it has been completed that increasing molarity will increase the dissociation of the active species of raw material and yielding formation of more geopolymer gel network [104].

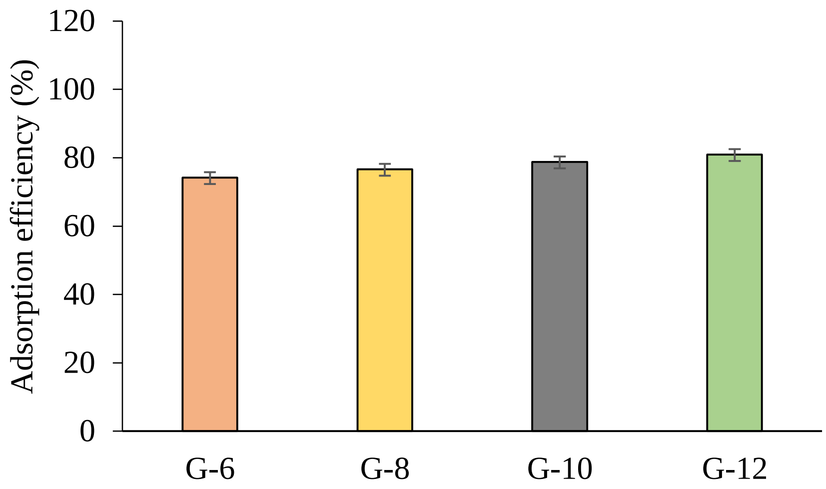

Figure 4.26 Effect of concentration of NaOH for prepared Na_2SiO_3 of adsorption efficiency

On the other hand, high concentraton of NaOH may disrupt the geopolymerization process due to the excessive quantity OH^- ions which lead to inefficient reaction. The optimum of concentration of NaOH on silica of geopolymer used G-6. Table 4.24 and Figure 4.27 were compared between GEO8M5D and GSiRH.

Table 4.24 The Comparison of adsorption efficiency removal by GEO8M5D and GSiRH

Adsorbents	Adsorption Efficiency (%)	q_e (mg/g)
GEO8M5D	95.17±0.02	31.12±0.51
GSiRH	74.23±0.13	18.48±0.25

The results showed that the adsorption efficiency of MB dye using GEO8M5D higher than GSiRH between range 95.17% (8 M) and 74.23% (6 M). Because the result demonstrated of the zeta potential that GEO8M5D (-40.23 mV) has a higher surface electronegativity than that of GSiRH (-32.56 mV). The enhanced electronegativity of GEO8M5D made it have a better electrostatic attraction and adsorption capacity to MB than GSiRH (Figure 4.28).

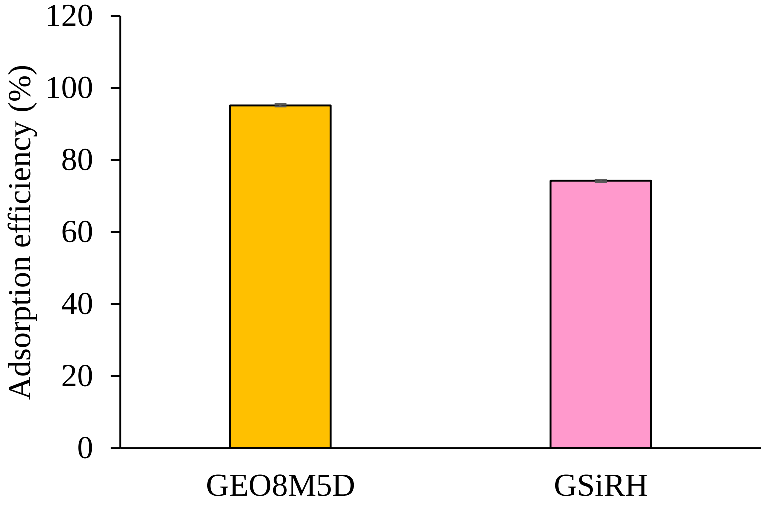

Figure 4.27 Adsorption efficiency compered between GEO8M5D and GSiRH

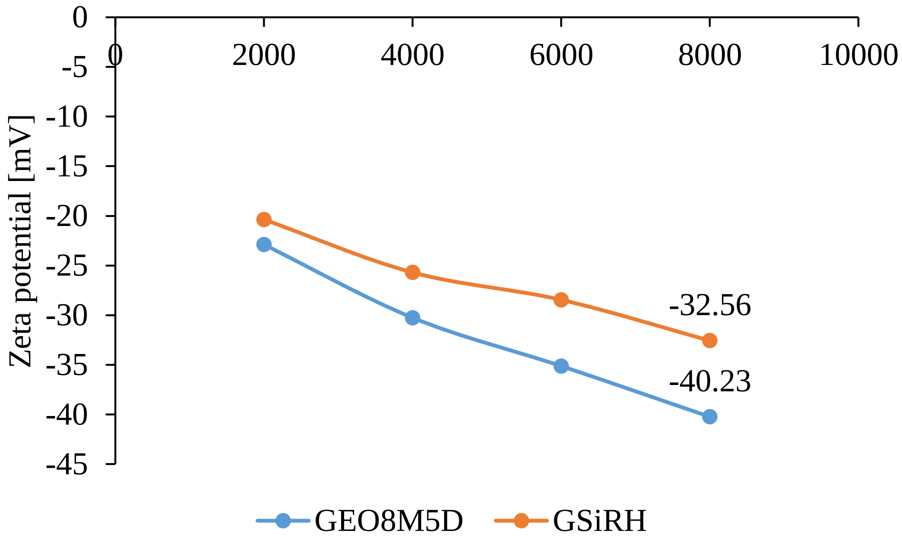

Figure 4.28 Zeta potential of GEO8M5D and GSiRH with DI water at pH 5

The surface charge and the degree of ionisation of adsorbate is greatly afected by pH parameter. In acidic pH, the surface of the GSiRH is surrounded by H^+ions, which decrease the interaction of the solute ions (MB^+) with the sites of the GEO8M5D material. For a better illustration of these results, it is required to determine experimentally the point of zero charge (pH_{PZC}). This is defined as the number of positive charges equal to the number of negative charges that exist on the surface of the adsorbent. The pH_{PZC} value of the adsorbent found almost to be 8.72 (Figure 4.32).

At pH = 2.02 to 6.14 < pH_{PZC} may be due to H^+ vies with MB, the sorbent surface takes up more H^+, reducing MB molecules bind on the sorbent surface.

At pH= 8. 72 > pH_{PZC}, the adsorbent surface is negatively charged, the increasing electrostatic attraction between positive adsorbate species and adsorbent particles would lead to increase adsorption capacity of MB. Similar results were also reported by GEO8M5D. So, increasing with pH above pH_{pzc} , the removal of cationic dye by the geopolymer increased slightly. The removal increase can be explained by electrostatic attraction between the particles of GSiRH, which is negatively charged, and the cationic dye, which is positively charged .

Therefore, it is interesting the development of GSiRH for removal MB dye. The parameters such as amount of dosage, contact time, initial concentration, isotherm, kinetic, thermodynamic and regeneration were investigated.

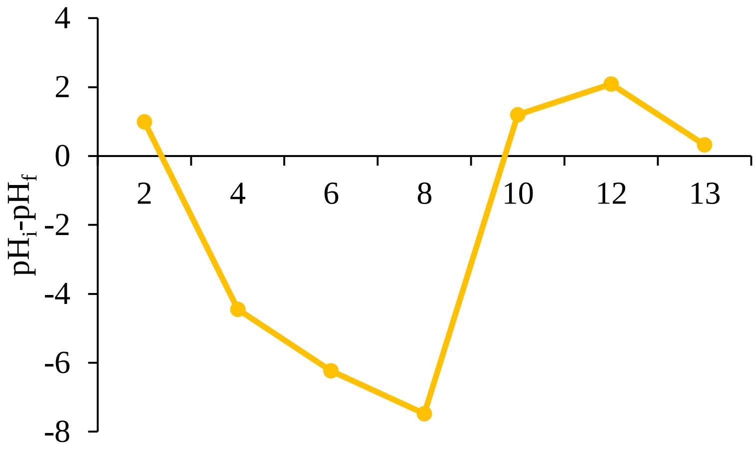

Figure 4.29 Point of zero charge (pH_{PZC}) of GSiRH

The composition of silica from fly ash was investigated by XRF tecnique. The results showed pure silica is 94.56 % (Table 4.25). The yield of silica is 16.13%. The pure silca and yield of silica from fly ash lower than RH. Afterthat, It can be prepared for Na_2SiO_3 (SiO_2 + NaOH) for geopolymer precursor (GFA).

Table 4.25 The composition of silica as an extraction from fly ash

Formula	Mass (%)	Molecule (%)
SiO_2	94.56	25.35
Al_2O_3	2.14	72.85
K_2O	1.99	1.16
Fe_2O_3	0.99	0.57

The alkali activator (Na_2SiO_3) from difference silica souces were compared commercial. The effect of adsorption efficiency of 3 adsorbent similary condition for MB removal was studied using a series of 25 mL MB solution of 300 ppm containing a fixed contact time (60 minutes) showed in Table 4.26 and Figure 4.30.

Table 4.26 Adsorption efficiency compered between GEO8M5D, GSiRH and GFA for MB removal

Adsorbents	Adsorption Efficiency (%)	q_e (mg/g)
GEO8M5D	95.17±0.02	31.12±0.51
GSiRH	78.67±0.13	20.25±0.21
GFA	29.20±1.31	5.63±0.02

The mean percentage removal are 95.17, 78.67 and 29.20% of GEO8M5D, GSiRH and GFA, respectively. For adsorption capacity are 31.12, 20.25 and 5.63 mg/g. The adsorption efficiency and capacity of GFA showed lower than GEO8M5D and GSiRH. The result suggested that, lower purity of silica from fly ash than silica from RH for prepared Na_2SiO_3.

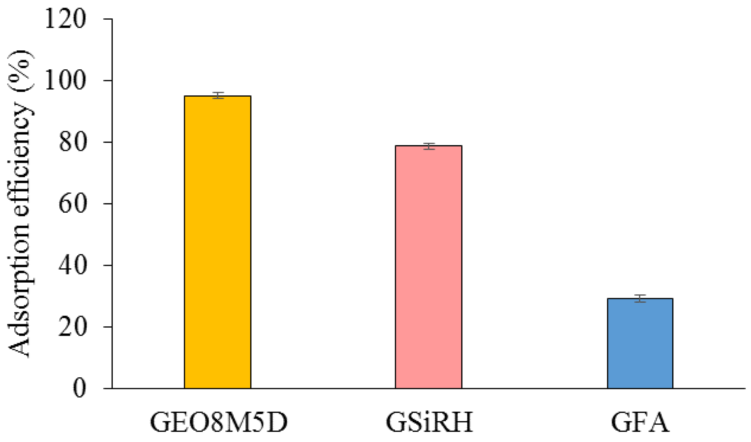

Figure 4.30 Adsorption efficiency compered between GEO8M5D, GSiRH and GFA

4.12 Optimized parameters

4.12.1 Optimal dosage

The effect of dosage on the removal of MB was studied using a series of 25 mL MB solution of 300 ppm containing a fixed contact time (60 minutes) of GSiRH, as shown in Table 4.27 and Figure 4.31.

Table 4.27 Effect of adsorbent dosage of GSiRH

Dosage (g/L)	Adsorption efficiency (%)	q_e (mg/g)
10	53.54±2.86	13.12±0.32
20	74.51±0.32	15.28±0.02
40	90.00±2.00	18.42±0.03
80	96.88±0.38	22.14±0.24

The percentage removal of MB dye increased with the increase in dose of adsorbent. The mean percentage removal increased from 53.54 to 96.88%. The adsorption capacity increased with an increasing 13.12 to 22.14 mg/g, the adsorption efficiency increase at 96.88% of 80 g/L of dosage. This result may attribute to the increasing number of binding site in the GSiRH for MB removal by increasing the quantity of adsorbent.

So, the optimum dosage was selected 40 g/L (uptake 90.00%). The adsorption capacity showed 18.42 mg/g.

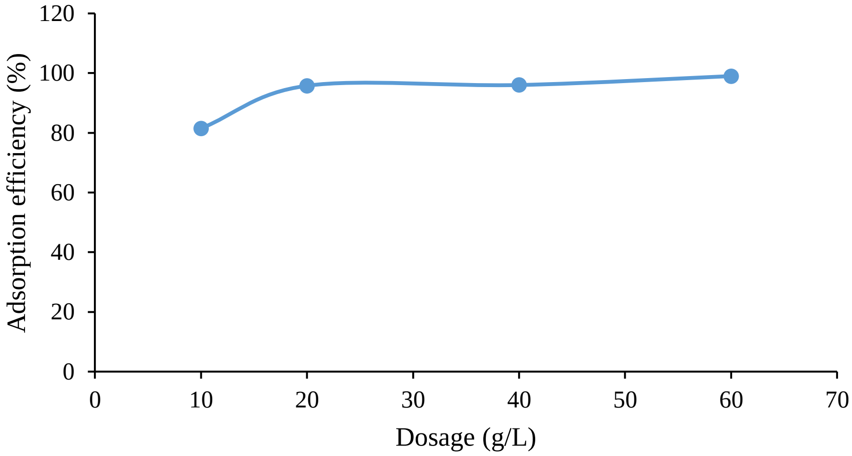

Figure 4.31 Effect of adsorbent dosage of GSiRH

Comparison of adsorption efficiency with GEO8M5D (q_e uptake 31.94 mg/g) and GSiRH (q_e uptake 18.42 mg/g) of MB using various adsorbent were report in Table 4.28 and Figure 4.32. The result of adsorption efficiency obtained GSiRH are closely GEO8M5D. Therefore, the result experimentally of GSiRH can represented than GEO8M5D for MB dye removal.

Table 4.28 Comparison of amount of dosage removal MB dyes by difference geopolymer

Dosage (g/L)	Adsorption efficiency (%)	
	GEO8M5D	GSiRH
10	81.48±0.25	53.54±2.86
20	95.77±0.31	74.51±0.32
40	96.01±0.02	90.00±2.00
80	99.00±0.01	96.88±0.38

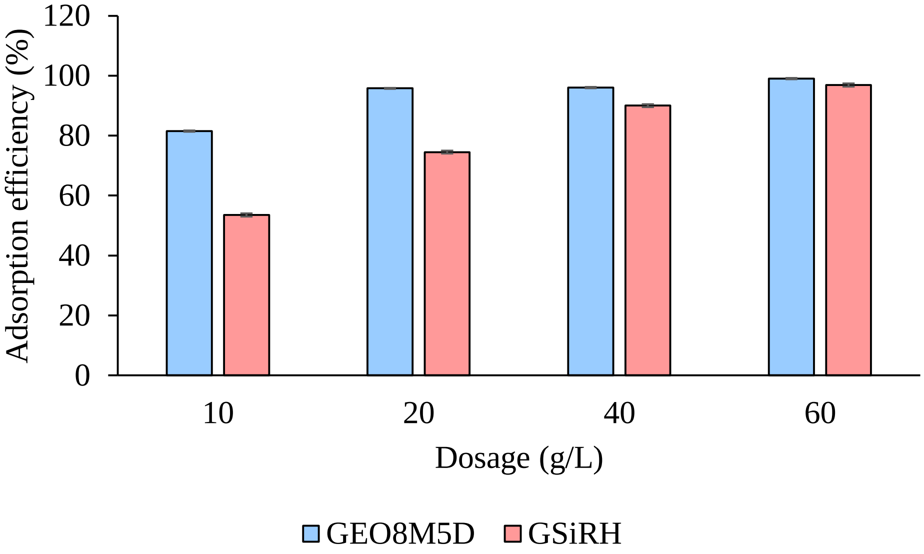

Figure 4.32 Comparison of the optimum dosage of adsorption efficiency

4.12.2 Effect of contact time

The effect of contact time on the removal of MB was studied using a series of 25 mL MB solution of 300 ppm containing a fixed amount of geopolymer (40 g/L), as shown in Table 4.29 and Figure 4.33.

Table 4.29 Effect of contact time of GSiRH MB removal

Time (minutes)	Adsorption efficiency (%)	q_t (mg/g)
30	84.25±0.15	15.57±0.12
60	91.76±0.21	18.24±0.01
120	93.70±0.01	19.07±0.01
240	96.56±0.05	21.14±0.14

The mean percentage removal increased from 84.25 and 96.56% when contact time was varied from 30 to 60 minutes and thereafter change when increasing contact time to 120 minutes. The adsorption capacity of geopolymer was increased with an increasing contact time from 15.57 to and 21.14.The rate of dye removal is higher in the beginning due to free adsorption sites are more in the initial stage. The trend similar results were earlier observed by GEO8M5D.

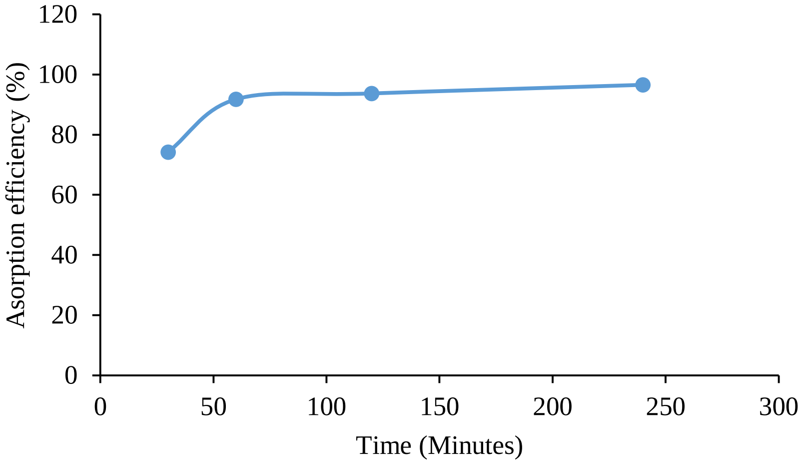

Figure 4.33 Effect of adsorption time on adsorption efficiency Of MB (C_0=300 ppm)

In addition, the fast adsorption at the initial stage may be due to the fact that a large number of surface sites are available for adsorption but after a lapse of time, the remaining surface sites are difficult to be occupied. The percentage of removal increased from 74.25 to 96.56% when contact time was varied from 30 to 60 minutes and thereafter slightly change of contact time to 60 minutes, the optimum of contact time is

60 minutes with 91.76% of adsorption efficiency. The adsorption capacity is 18.24 mg/g.

Table 4.30 Comparison of contact time removal MB dyes by difference geopolymer

Time (Minutes)	Adsorption efficiency (%)	
	GEO8M5D	GSiRH
30	91.20±0.28	84.25±0.15
60	95.00±0.12	91.76±0.21
120	96.51±0.25	93.70±0.01
240	97.50±0.02	96.56±0.05

Comparison of adsorption efficiency with GEO8M5D (q_e uptake 31.39 mg/g) and GSiRH (q_e uptake 18.24 mg/g) of MB using various adsorbent were report in Table 4.30 and Figure 4.34. The adsorption efficiency shows that GSiRH are closely GEO8M5D. Therefore, the result experimentally of GSiRH can represented than GEO8M5D for MB dye removal.

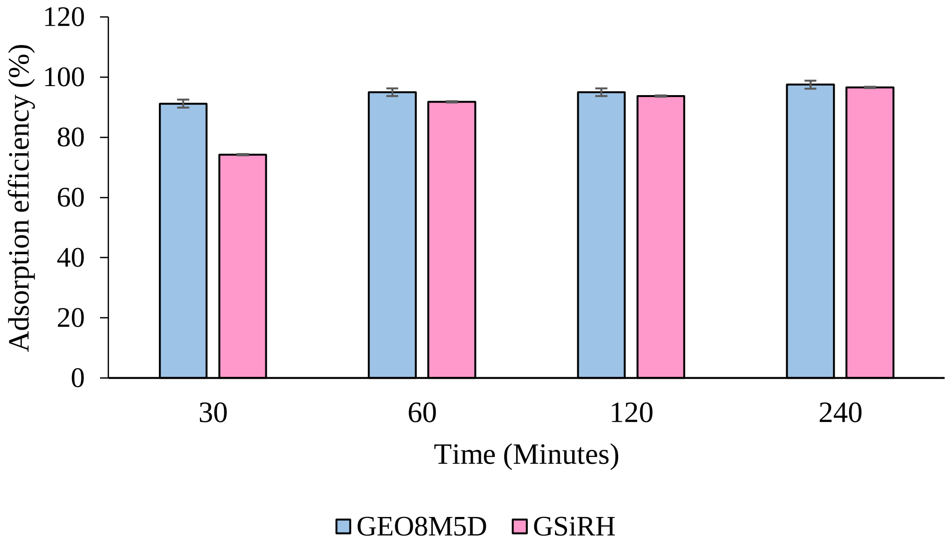

Figure 4.34 Adsorption efficiency of contact time of GEO8M5D and GSiRH

4.12.3 Effect of initial concentration

The effect of initial concentration on the removal of MB was studied using a series of 25 mL MB solution of 300 to 550 ppm containing a fixed amount (40 g/L) and contact time (60 minutes) of geopolymer, as shown in Table 4.31 and Figure 4.35. The percentage removal of dye found to decrease with the increase initial dye concentration. The results show that the percentage removal of dye decreases from 91.17 to 80.74%. The adsorption capacity increased from 18.78 to 22.61 mg/g as the initial dye concentration increases from 300 to 550 ppm.

Table 4.31 Effect of initial concentration on adsorption efficiency

Concentration (ppm)	**Adsorption efficiency (%)**	**q_e (mg/g)**
300	91.71±0.21	18.78±0.21
350	90.20±0.45	19.96±0.25
400	87.93±0.03	20.72±0.03
450	84.50±0.16	22.14±0.14
500	81.15±0.42	23.05±0.30
550	80.74±0.52	25.61±0.15

The results can explained, at lower dye concentration this may be due to unoccupied active sites on the adsorbent surface, when the initial concentration increases, the active sites required for adsorption of dye molecules disappear. The removal extent of dyes was decreased with an increase in the initial MB concentration due to the available active sites under high concentration of MB, but the adsorption capacity of MB solution on GSiRH increased with the increase of initial MB concentration. Similar trend on effect of initial dye concentration on adsorption of MB has been reported by GEO8M5D.

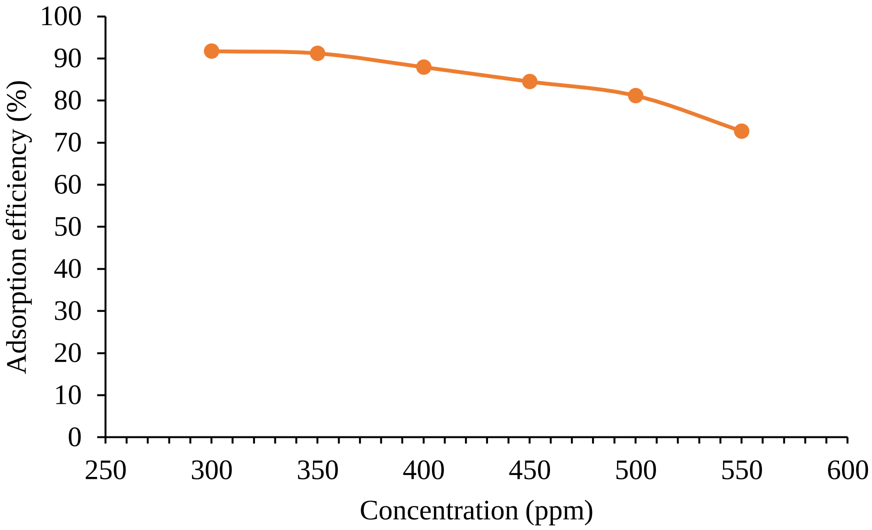

Figure 4.35 Adsorption efficiency of MB on effect of initial dye concentration

Comparison of adsorption efficiency with GEO8M5D (q_e uptake 31.45 mg/g) and GSiRH (q_e uptake 18.89 mg/g) of MB using various adsorbent were reported in Table 4.32. The result of adsorption efficiency trend of GSiRH are closely GEO8M5D. Therefore, the result experimentally of GSiRH can represented than GEO8M5D for MB dye removal.

Table 4.32 Comparison of initial concentration MB removal by GEO8M5D and GSiRH

Concentration (ppm)	**Adsorption efficiency (%)**	
	GEO8M5D	**GSiRH**
300	95.65±0.24	91.71±0.21
350	94.36±0.59	91.20±0.45
400	91.64±0.57	87.93±0.03
450	90.45±0.21	84.50±0.16
500	89.27±0.12	81.15±0.42
550	88.43±0.56	72.74±0.52

4.13 Isotherm studies

The isotherm results were obtained using the Langmuir and Freundlich isotherms. The Langmuir adsorption model is based on the assumption that adsorption energy is independent of surface coverage and constant, with no lateral interaction between the adsorbed molecules. The maximum adsorption occurs when surface covered by monolayer of adsorbate. The Langmuir adsorption isotherm can be use used to elucidate the adsorption of methylene blue from aqueous solutions.

The constants calculated from the model equations Langmuir and Freundlich are shown in Table 4.33 and Figure 4.36. As observed, the value of R^2 obtained from the Langmuir isotherm equation (0.9760) was higher than that from the Freundlich (0.8050) isotherm equations. These results showed the adsorption could be well described by the Langmuir model. The adsorption occurred on the homogeneous surface as a monolayer, and the optimum monolayer adsorption capacity (q_e) was found to be 18.89 mg/g. The R_L value was obtained within the range $0 < R_L < 1$, indicating that the adsorption of cationic dye on the geopolymer material is favorable.

Table 4.33 The parameter of adsorption of MB using Langmuir and Freundlich isotherm

Langmuir isotherm	**Freundlich isotherm**
R^2 = 0.976	R^2 = 0.805
q_e (mg/g) = 18.78	1/n = 0.1209
K_L = 0.0047	K_F = 0.0034
R_L = 0.6341	-

In addition, Table 4.33 presents a summary of the optimum adsorption capacity q_e and corresponded Langmuir isotherm of the developed adsorbents for MB dyestuff in the aqueous solution. The result showed isotherm model similarly trend of GEO8M5D.

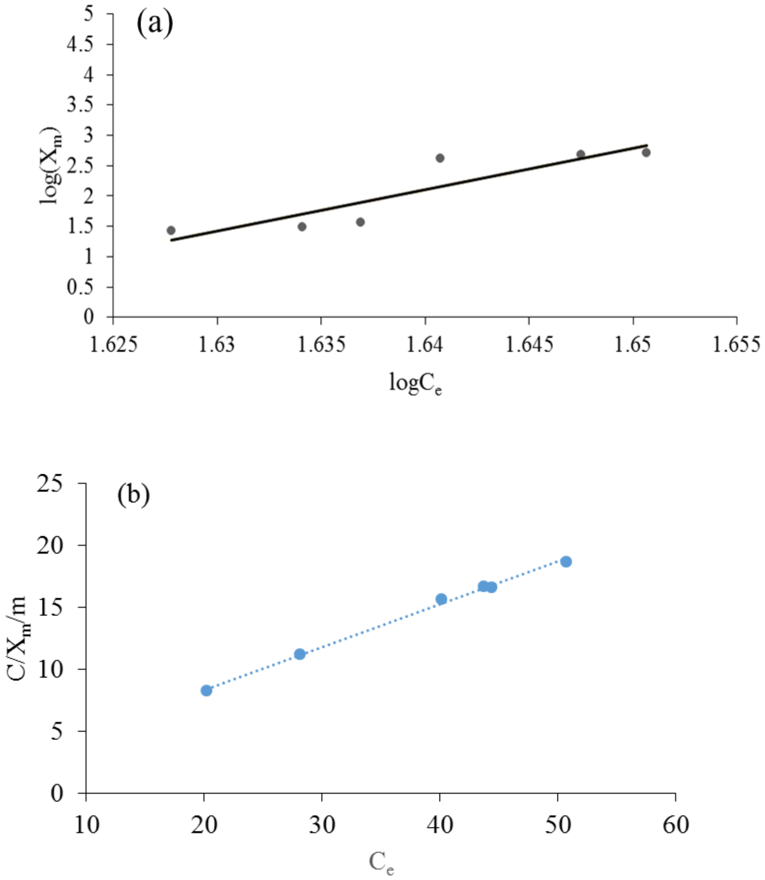

Figure 4.36 Adsorption isotherms for MB using geopolymer; (a) Freundlich isotherm (b) Langmuir isotherm

4.14 Kinetic studies

For the identification mechanism of GSiRH removal for MB dye, the kinetic models used pseudo-first-order and pseudo-second-order to examine the experimental. The results of both were obtained in Table 4.34 and Figure 4.37.

Table 4.34 Kinetic parameters for adsorption of MB onto GSiRH

Parameters	Pseudo-first-order	Pseudo-second-order
R^2	0.8330	0.9996
k	0.0012	0.2210
$q_{e(cal)}$ (mg/g)	38.62	18.24
$q_{e(exp)}$ (mg/g)	19.18	19.18

Table 4.25 shows the pseudo-first-order and pseudo-second-order plots for adsorption of MB at various contact time at room temperature. The (R^2) values obtained for the pseudo-first-order (0.8330) were lower than that of the pseudo-second-order (0.9996). The ($q_{e(exp)}$)value did not agree with the calculated valued showed from linear plot. This indicated that the adsorption of MB on to GSiRH does not follow pseudo-first-order. The suitability of pseudo-second-order was judged based on the R^2 value, which are a calculation of decency of fit. Pseudo-second-order rate constants k_2 (calculated from the intercept and slope) as well as linear regression R^2 summarized in Table 4.25 . The result show that R^2 for the pseudo-second-order are greater than those for pseudo-first-order, stipulating good agreement with the experimental data. It can be inferred that the pseudo-second-order (0.9996) fits the adsorption data better than the first order model.

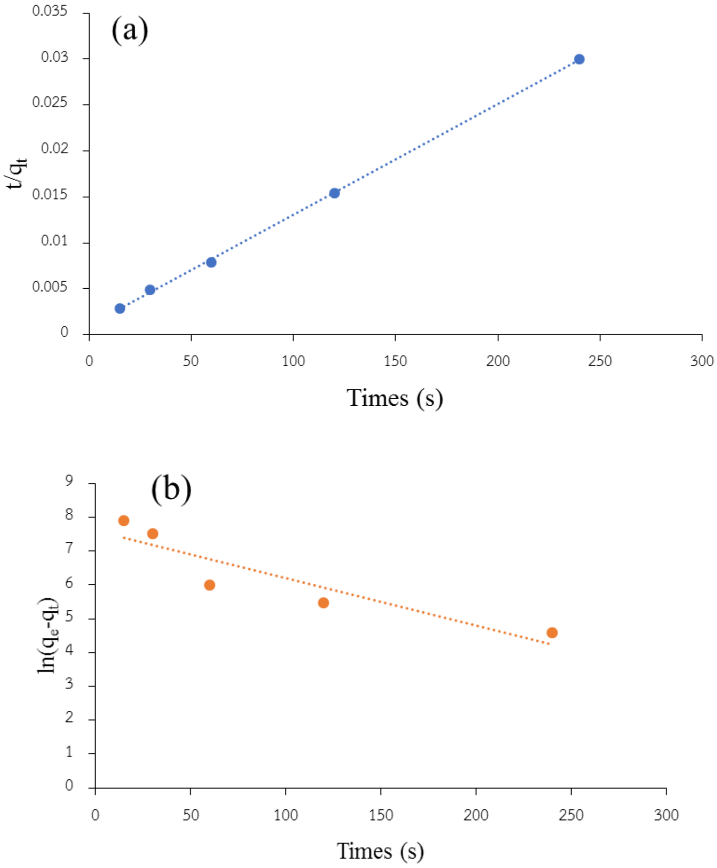

Figure 4.37 Adsorption kinetics of MB adsorption onto GSiRH ; (a) pseudo-first order and (b) pseudo-second-order

Therefore, the pseudo-second-order model can be used to explain the adsorption process of MB on GSiRH and demonstrated that chemisorption dominated the adsorption process. The adsorption process not only included the processes of the liquid film diffusion and the internal diffusion of mesopores, but also the chemisorption process with electrons shared and gained or loss of electrons between cationic dyes and functional group on the GSiRH surface. The literature reviews was indicated that the pseudo-second-order. A similar found in literature by Jawad et al [123] this result was corresponded of adsorption kinetic from GEO8M5D.

4.15 Thermodynamics studies

Effect of temperature on adsorption was studied by using temperature between range 20 to 60°C with initial concentration 300 ppm. The values of thermodynamic parameters, enthalpy (ΔH°), gibbs energy change (ΔG°) and entropy change (ΔS°) of the adsorption process of the geopolymer were calculated from the slope and intercept of the plot of $\ln K_c$ versus 1/T (Figure 4.38).

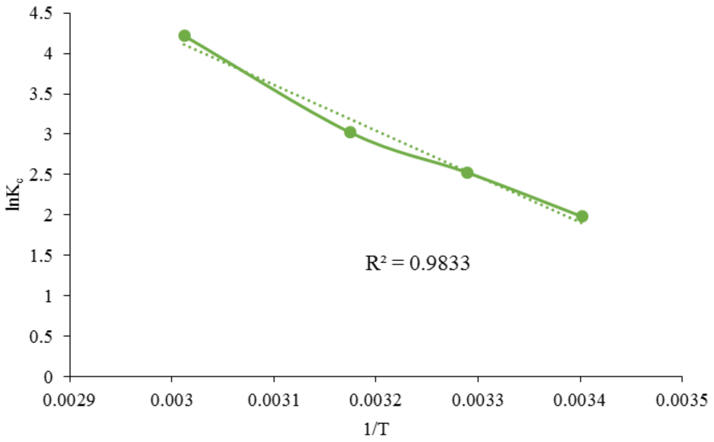

Figure 4.38 Enthapy and entropy change determination of the adsorption of MB by GSiRH

This indicated that the adsorption was a spontaneous endothermic process. The nagative ΔG° values, which can be seen from Table 4.26, corresponded the discolored process of MB on GSiRH in term of possibility and sponteneity.

This indicated that the adsorption was a spontaneous endothermic process. The negative ΔG° values, which can be seen from Table 4.35, corresponded the discolored process of MB on GSiRH in term of spontaneity. The positive ΔH° values 55.23 kJ/mol prove that the adsorption was an endothermic process. The positive Δ*S*° values indicate an irregular increase of the randomness at the adsorbate - adsorbent interface during the adsorption. This result was corresponded of adsorption thermodynamic from GEO8M5D.

Table 4.35 The distribution and adsorption constants and the thermodynamic parameters

T (K)	InK$_c$	ΔG°(kJ/mol)	ΔH°(kJ/mol)	ΔS°(J/molK)	q$_e$ (mg/g)
293	1.96	-4.80	55.23	98.23	18.41±0.03
303	2.82	-7.13			19.03±0.07
313	3.42	-8.96			20.26±0.05
333	4.01	-11.09			21.35±0.12

4.16 Regeneration test

The regeneration of GSiRH after MB adsorption was also performed.

The possible reuse of the adsorption and to choose a suitable desorbated/regenerated was compared with GEO8M5D . The regeneration was obtained by calcined 400˚C for 2 hr. The FTIR spectra of GSiRH and GSiRH after 1st cycles of calcined are shown in the Figure 4.39.

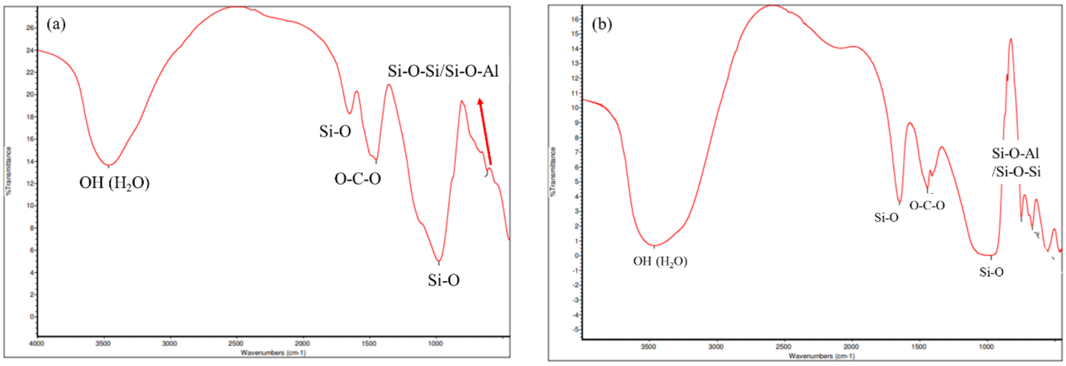

Figure 4.39 The peak of FT-IR; (a) GSiRH and (b) GSiRH after 1st cycles

Figure 4.39 (a), Broad bands were shown in GSiRH at 3459 cm^{-1} for the (-OH, H-O-H) stretching mode. On the other hand, one in peak situated at 1373 cm^{-1} was O-C-O stretching mode, indicating the presence of sodium carbonate. It is to the action in silicates. The peaks which were shown at 610 and 540 cm^{-1} consist of Si-O-Si and SiO_4 bending vibration of situ-synthesized silicate. Figure 39 (b), the peak after calcite showed similar GSiRH before calcite. It can be observed that intensity of most peak is similar for GEO8M. All the bands assignments are listed in Table 4.36.

Table 4.36 FTIR spectrum analysis

Materials	Bands (cm^{-1})	Assignments	Reference
GEO8M5D	1383	Si-O stretching	
	1017	Si-O stretching	[37]
	692	Si-O-Al/Si-O/Si stretching	[82]
	593	Si-O-Al Bending vibration	
GSiRH	3459	OH stretching	[122]
	1373	O-C-O stretching	
	610	Si-O-Al/Si-O/Si stretching	
	540	SiO_4 bending vibration	
1st cycles of GSiRH	3398	OH stretching	
	1256	O-C-O stretching	
	720-602	Si-O-Al/Si-O/Si stretching	
	520	SiO_4 bending vibration	

The adsorbent was performed using thermal regeneration methods. The sample was calcite at 400 ◦C for 2 hr. The sample was applied to remove MB under the conditions MB concentration 300 ppm and GSiRH dose 40 g/L in 25 mL solution (60 minutes of contact time) and the adsorption removal MB dye (Table 4.28).

Table 4.37 MB uptake for geopolymer after multiple regeneration cycles

Cycles	Adsorption efficiency (%)	q_e (mg/g)
0	92.28±1.11	18.98±0.12
1	80.52±1.51	16.88±0.05
2	65.17±0.48	14.87±0.17
3	60.25±0.40	11.52±0.11
4	45.33±2.04	9.67±0.21
Cumulative q_e (mg/g)		**71.92**

Table 4.37, the percentage removal of MB dye decrease with the decrease in regenerate of adsorbent. The mean percentage removal decrease from 92.28 and 45.33%. The adsorption capacity decreased with an decreasing 18.98 to 9.67 mg/g. The performance of GSiRH adsorbent was fermented after the 2nd cycles, while induced slightly reduction on the MB uptake. At this stage the performance of the adsorbent decreaded were observed on uptake and removal efficiency up to the fouth cycles. The results of regeneration and reuse showed that GSiRH can be used fouth times and cumulative q_e up to 71.92 mg/g. The BET surface areas, pore volumes and pore sizes of the samples before and after thermal regenreration showed in Table 4.38.

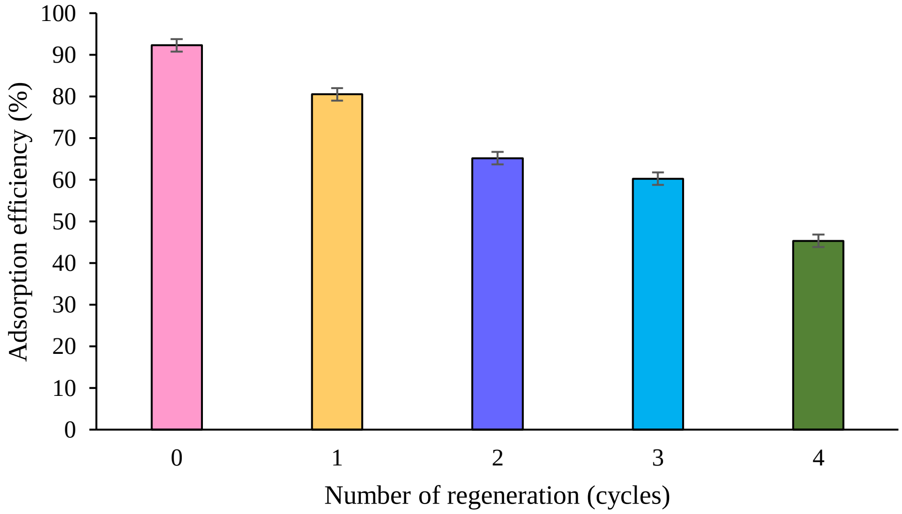

Figure 4.40 MB uptake for geopolymer after multiple regeneration cycles

Final of the regeneration, GSiRH showed lower value of BET surface area. The pore volume and pore size showed higher than GEO8M5D. The regeneration of adsorbent for removal MB dye has been significantly lower than GEO8M5D. The reasons may be due to the BET surface, pore volume and pore size that has changed. However, the possibility of GSiRH can compensated GEO8M5D.

Table 4.38 The BET surface area final regeneration

BET	**GEO8M5D (9th cycles)**	**GSiRH (4th cycles)**
BET surface area (m^2/g)	8.90	6.40
Pore volume (cm^3/g)	2.84	3.21
Pore size (Å)	2.63	3.02

Therefore, next part used to fly ash from power plan of Lampang province, Thailand for applications. Fly ash can be used as a new adsorbent without modification for the removal from aqueous solutions and study the optimum parameter were investigated. The characterizations of fly ash were analyzed by XRF, XRD and SEM-EDX.

4.17 Characterization of fly ash

The composition of fly ash was characterized by XRF techniques showed in Table 4.39. Fly ash contained mainly SiO_2 component, followed by CaO and K_2O components, while the Fe_2O_3 content is very low. Two classes of fly ash are defined by ASTMC618: Class F fly ash and Class C fly ash. The chief difference between these classes is the amount of calcium, silica, alumina, and iron content in the ash. The sample corresponded class F of ASTMC618 .

Table 4.39 The compositions of fly ash

Formula	Mass (%)	Molecule (%)
SiO_2	44.02	23.14
Al_2O_3	29.21	19.54
CaO	27.55	50.75
K_2O	24.18	0.26
Fe_2O_3	2.98	0.07

The XRD patterns of fly ash is given in Figure 4.41. The results of XRD analysis of the fly ash at 29, 30, 32, 39 and 40 ° indicated that quartz and mullite were the chief crystalline phase. The result was corresponded researches of Hsu et al [124].

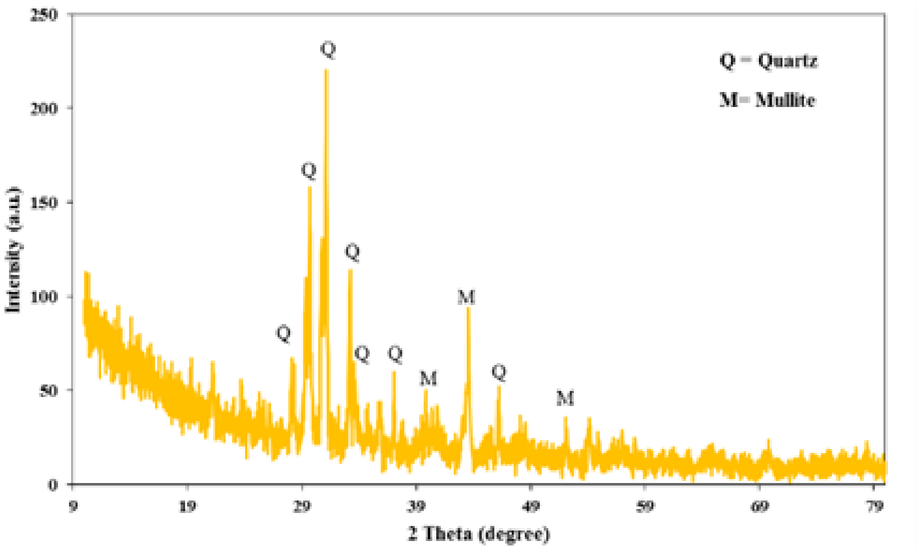

Figure 4.41 The XRD of fly ash

An infrared analysis was performed on fly ash. FTIR spectrum shown in Figure.4.42. FTIR spectrum showed signification change in position of peaks. The bands appeared in the regions of 1621 and 3409 cm^{-1} that were attributed to bending vibrations (H–O–H) and stretching vibrations O–H. The bands appeared in the regions of 457 and 734 cm^{-1} are due to the vibration mode Si-O-Al and Si–O–Si, respectively.

Which confirm the presence of mullite and quartz vibration mode Si-O-Al and Si–O–Si, respectively. Which confirm the presence of mullite and quartz.

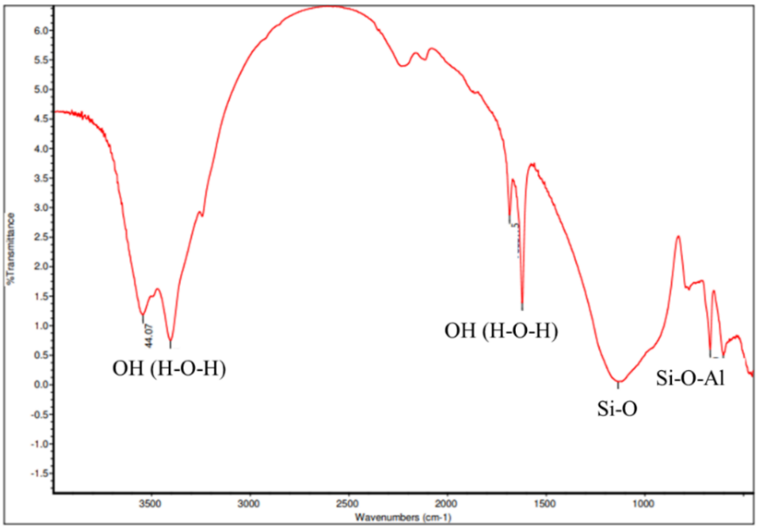

Figure 4.42 FTIR spectra of fly ash

The morphology of fly ash were analyzed by SEM shown in Figure 4.43. These image were obtained. The particle of surface was smooth spherical. The BET surface area, pore volume and pore size were 5.44 m^2/g, 1.25 cm^3/g and 1.38 Å, respectively.

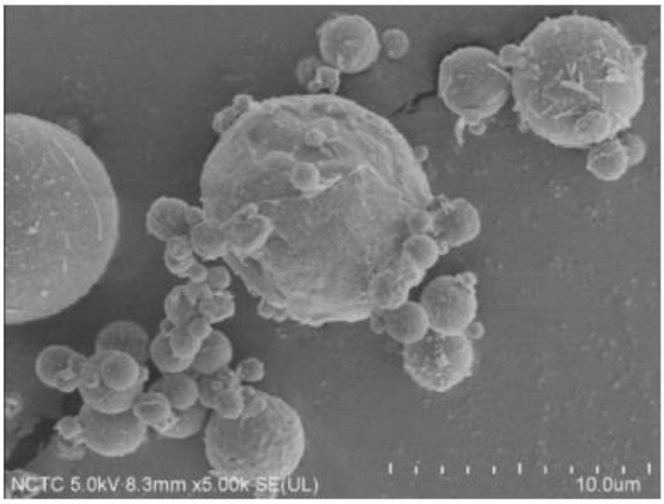

Figure 4.43 The morphology of fly ash observed by SEM image

4.18 The adsorption efficiency of dyes solution

The textile industry is main of the dyes and generates colored waste water with is capable of causing severe water pollution. The popular of dye was used by cationic. Because of its worldwide application in paper, letter and textile in dyeing and by virtue of being observed in the human. Fly ash was used as an adsorbents for the removal of MB and BG from aqueous solution. The dosage of adsorbent was 20 g/L, 60 minutes of contact time and 300 ppm of concentration solution.

Table 4.40 Adsorption efficiency on MB and BG using fly ash

Adsorbent	Dye	Adsorption efficiency (%)
Fly ash	MB	29.96±0.05
	BG	99.74±0.45

Table 4.40 and Figure 4.44 also shows that fly ash always has a high adsorption for BG than MB , which is probably due to the chemical structure. The molecular size of MB is much larger than BG prohibited it into the small pores of fly ash [70].

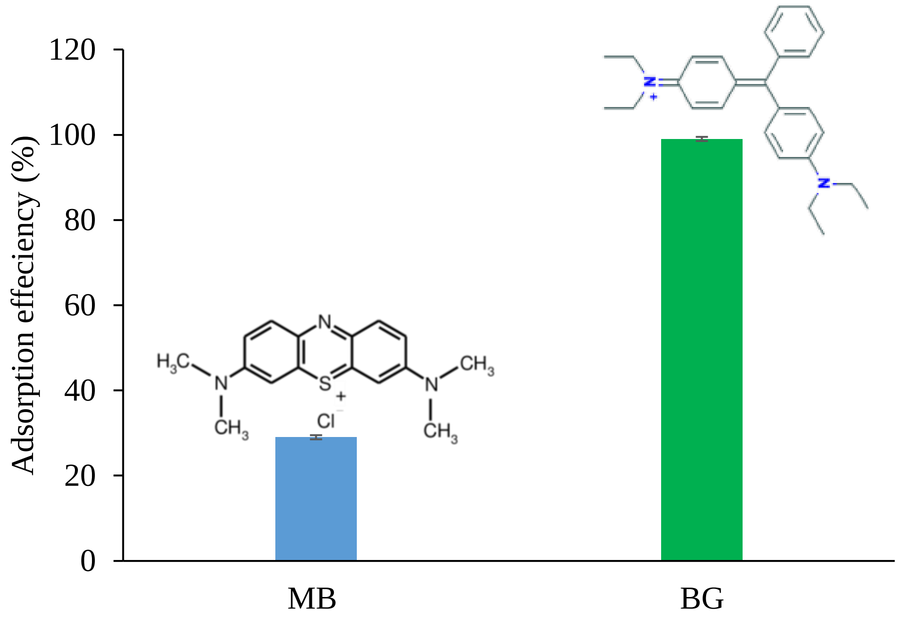

Figure 4.44 Adsorption efficiency for removal MB and BG dye using fly ash without modified

4.19 Optimized parameters

4.19.1 Optimal dosage

The effect of dosage on the removal of BG was studied using a series of 25 mL BG solution of 300 ppm containing a fixed contact time (60 minutes) of fly ash as shown in Table 4.41 and Figure 4.45.

Table 4.41 Effect of adsorbent dosage on adsorption efficiency

Dosage(g/L)	Adsorption efficiency (%)	q_e (mg/g)
2	78.80±0.16	75.02±0.12
4	93.50±0.02	78.14±0.05
6	99.90±0.01	91.45±0.12
8	99.91±0.04	91.74±0.11

The percentage removal of BG dye increased with the increase in dose of adsorbent. The mean percentage removal increased from 78.80 and 99.91 %. The adsorption capacity increased with an increasing 75.02 to 91.74 mg/g, the adsorption efficiency approach equilibrium at 99.90 % of 6 g/L of dosage. This may be due to the increase in availability of surface active site resulting from the increased dose of the adsorbent. Considering the relationship between the optimal dosage and the BG removal, the optimal dosage for subsequent experiment was selected as 4 g/L (uptake 78.14 mg/g).

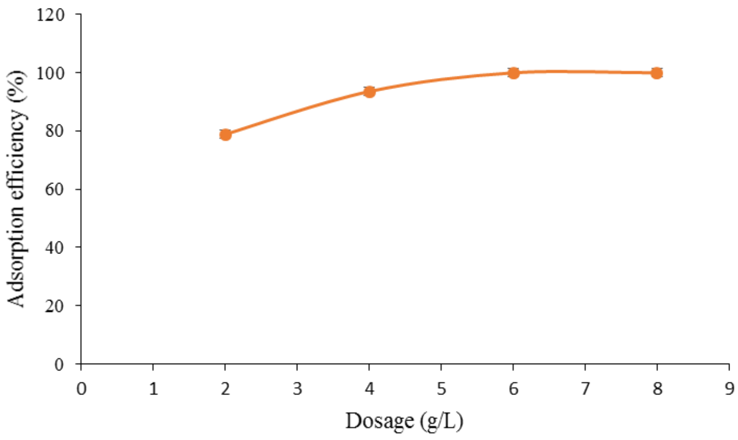

Figure 4.45 Effect of dosage on adsorption efficiency of BG (C_0=300 ppm, 25 mL).

4.19.2 Effect of contact time

The effect of contact time on the removal of BG was studied using a series of 25 mL BG solution of 300 mg/L containing a fixed amount of fly ash (4 g/L), as shown in Table 4.42 and Figure 4.46. The mean percentage removal increased from 83.60 and 95.12 % when contact time was varied from 5 to 15 minutes and thereafter slightly change when increasing contact time to 60 minutes. The rate of dye removal is higher in the beginning due to free adsorption sites are more in the initial stage. The optimum contact time was 30 minutes. The adsorption capacity of fly ash was increased with increasing contact time. The initial color of BG solution was deep green in 5 minutes. The color after adsorption was faded especially at 10 minutes and colorless at 15 to 60 mintues.

Table 4.42 Effect of Time on adsorption efficiency of BG

Time (minutes)	Adsorption efficiency (%)	q_t (mg/g)
5	83.60±0.01	67.43±0.02
10	85.06±0.04	70.66±0.01
15	89.53±0.14	74.43±0.30
30	93.50±0.21	78.94±0.10
60	95.12±0.23	82.14±0.15

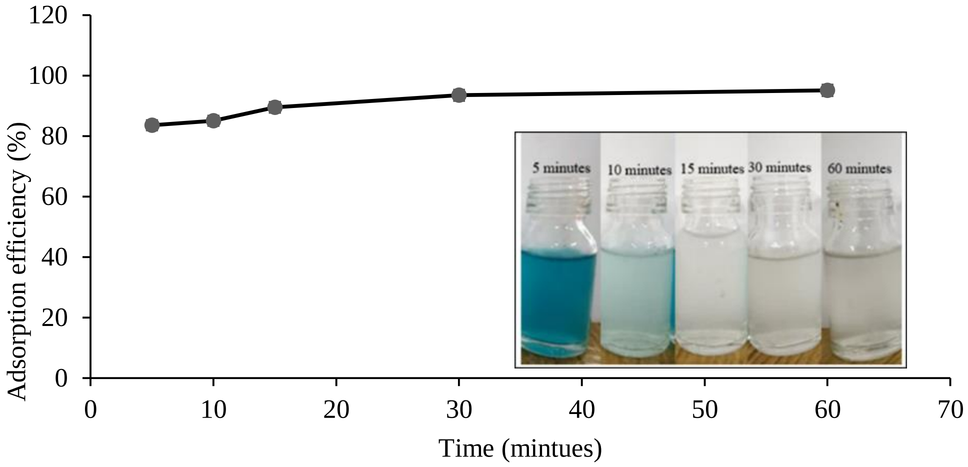

Figure 4.46 Effect of Time on adsorption efficiency of BG (dosage = 4 g/L, C_0=300 ppm, 25 mL)

The process was described into two step. The first step took 5 to 15 minutes to reach the relative adsorption equilibrium state called fast adsorption. This performance was due to the binding process between BG dye and the adsorption active sites, and functional groups on the fly ash adsorbent. The absorption rate of the dye was controlled by the rate of the dye transported from the solution to the surface of the adsorbent particles. The second step was shown closely equilibrium adsorption process. After 60 minutes of contact time, the relative increase in the removal extent of BG was slightly increased and with the increase of time. This performance was according to the binding process between BG dye and the adsorption active sites, and functional groups on fly ash adsorbent were gradually saturated. Considering the relationship between the contact time and the BG removal, the contact time for subsequent experiments was selected as 30 minutes. The adsorption capacity for BG is 78.94 mg/g.

4.19.3 Effect of initial concentration

The effect of initial concentration on the removal of BG was studied using a series of 25 mL BG solution of 300 to 550 ppm containing a fixed amount (4 g/L) and contact time (60 minutes) of fly ash, as shown in Table 4.43 and Figure 4.47. The percentage removal of dye found to decrease with the increase initial dye concentration. The results showed that the percentage removal of dye decreases from 93.36 to 82.07%.

The adsorption capacity increased from 78.93 to 90.37 mg/ g as the initial dye concentration increases from 300 to 550 ppm.

Table 4.43 Effect of initial concentration on adsorption efficiency

Concentration (ppm)	Adsorption efficiency (%)	q_e (mg/g)
300	93.36±0.05	78.93±0.18
350	92.00±0.22	80.62±0.06
400	90.52±0.32	82.50±0.50
450	87.14±0.06	84.12±0.23
500	86.43±0.15	87.43±0.14
550	82.07±0.41	90.37±0.16

At lower dye concentration, this might be due to unoccupied active sites on the adsorbent surface, when the initial concentration increases, the active sites required for adsorption of dye molecules disappear. The removal extent of dyes was decreased with an increase in the initial BG concentration due to the available active sites under high concentration of BG, but the adsorption capacity of BG solution on fly ash increased with the increase of initial BG concentration. Similar trends have been reported in work by GEO8M5D and GSiRH.

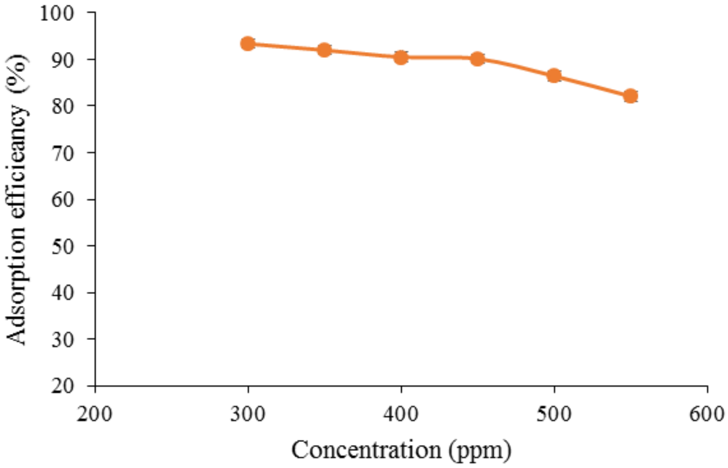

Figure 4.47 Adsorption efficiency of BG on effect of initial dye concentration

4.20 Isotherm studies

The isotherm results were obtained using the Langmuir and Freundlich isotherms. The Langmuir adsorption model is based on the assumption that adsorption energy is independent of surface coverage and constant, with no lateral interaction between the adsorbed molecules. The maximum adsorption occurs when surface covered by monolayer of adsorbate. The Langmuir adsorption isotherm can be use used to elucidate the adsorption of BG from aqueous solutions. The constants calculated from the model equations Langmuir and Freundlich are shown in Table 4.44 and Figure 4.48

Table 4.44 The parameter of adsorption of MB using Langmuir and Freundlich isotherm

Langmuir isotherm	**Freundlich isotherm**
R^2 = 0.9984	R^2 = 0.8004
q_e (mg/g) = 78.93	1/n = 0.2540
K_L = 0.0073	K_F = 0.0051
R_L = 0.5120	-

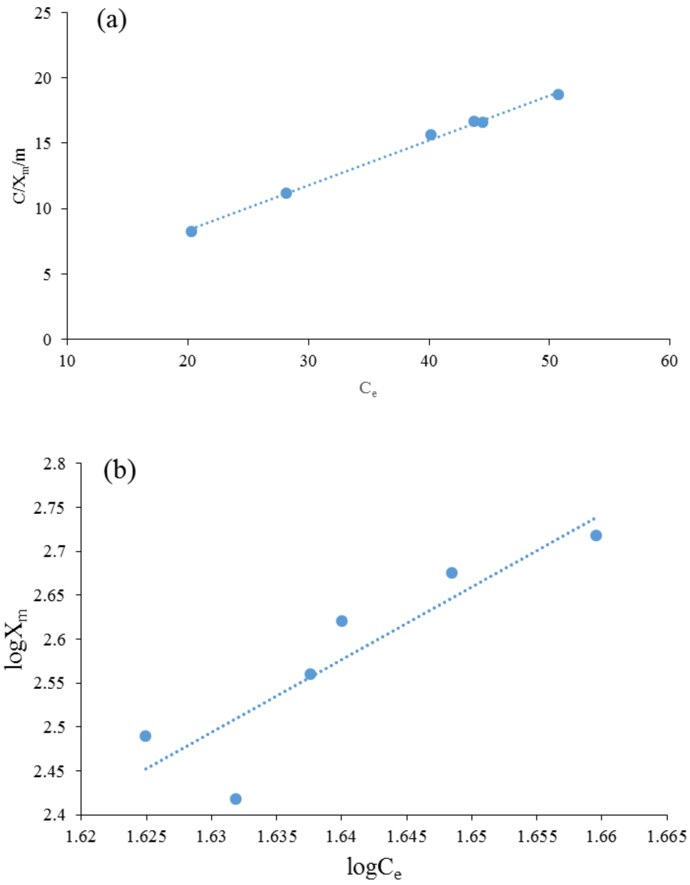

Figure 4.48 Adsorption isotherms for BG using fly ash: (a) Langmuir isotherm (b) Freundlich isotherm

As observed, the value of R^2 obtained from the Langmuir isotherm equation (0.9999) was higher than that from the Freundlich (0.6980) isotherm equations. These results showed the adsorption could be well described by the Langmuir model. The adsorption occurred on the homogeneous surface as a monolayer, and the optimum monolayer adsorption capacity (q_e) was found to be 78.93 mg/g. The R_L value was obtained within the range $0 < R_L < 1$, indicating that the adsorption of cationic dye on the geopolymer material is favorable. Similar trends have been reported in work by GEO8M5D and GSiRH.

4.21 Kinetic studies

It is important to be able to predict the rate at which contaminates are removed from aqueous solution in order to design adsorption treatment. The principle of the pseudo-first-order model is that the reaction rate is proportional to the number of ions remaining in the solution, summarizing that adsorption is controlled by diffusion step. It's concluded that the adsorption rate is proportional to the difference between the saturated concentration and the adsorption amount of fly ash with time. The pseudo-second-order, which can be expressed as the reaction rate being proportional to the concentration of two reactants, concluding the adsorption is controlled by chemisorption steps.

Table 4.45 Kinetic parameters for adsorption of BG onto fly ash

Parameters	Pseudo-first-order	Pseudo-second-order
R^2	0.8004	0.9999
k	0.0150	0.4211
$q_{e(cal)}$ (mg/g)	100.24	78.94
$q_{e(exp)}$ (mg/g)	80.32	80.32

Table 4.45 and Figure 4.49 shows the pseudo-first-order and pseudo-second-order plots for adsorption of BG at various contact time at room temperature. The correlation coefficients (R^2) values obtained for the pseudo-first-order (0.8004) were lower than that of the pseudo-second-order (1).

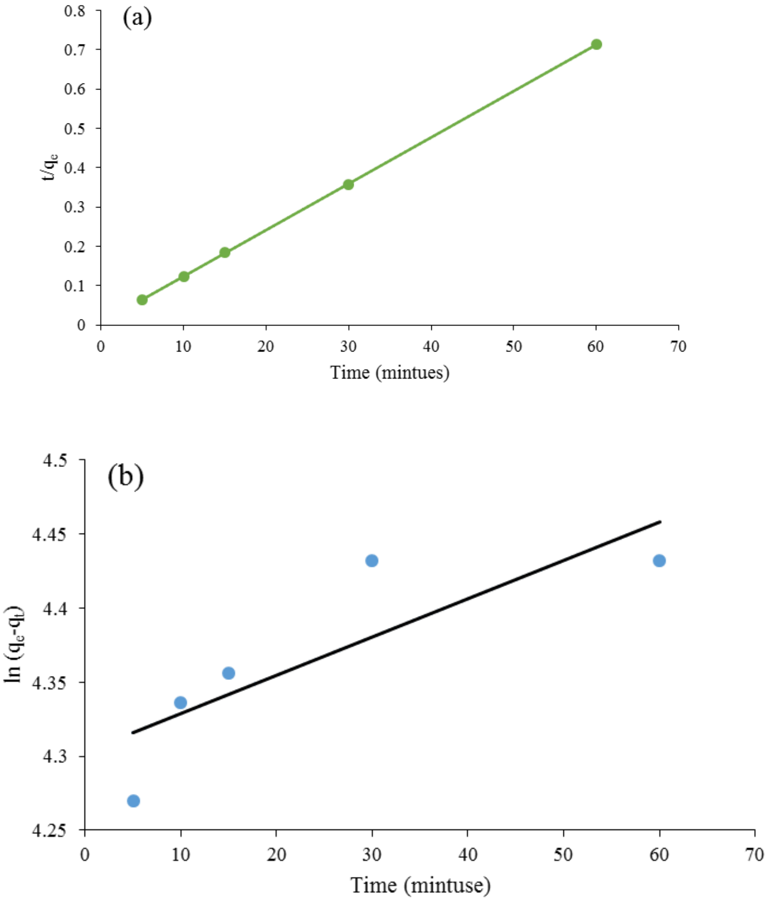

Figure 4.49 Model of adsorption kinetics: (a) pseudo-first-order and (b) pseudo second-order

The experimental q_e ($q_{e(exp)}$)value did not agree with the calculated valued obtained from linear plot. This indicated that the adsorption of BG on to fly ash does not follow pseudo-first-order. The suitability of pseudo- second- order was judged based on the R^2, which are a computation of goodness of fit. Pseudo- second- order rate constants k_2 (calculated from the intercept and slope) as well as linear regression R^2 summarized in Table 4.35. The result show that R^2 for the pseudo-second-order are greater than those for pseudo-first-order, stipulating good agreement with the experimental data. It can be inferred that the pseudo-second-order ($R^2 = 0.9999$) fits the adsorption data better than the first order model.

Similar trends have been reported in work by GEO8M5D and GSiRH.

4.22 Thermodynamics studies

The effect of temperature on dye removal was studied by varying temperatures (20, 30, 40 and 60°C). The values of thermodynamic parameters, enthalpy (ΔHº), gibbs energy change (ΔGº) and entropy change (ΔSº) of the adsorption process of the geopolymer were calculated from the slope and intercept of the plot of $\ln K_c$ versus 1/T (Figure 4.50).

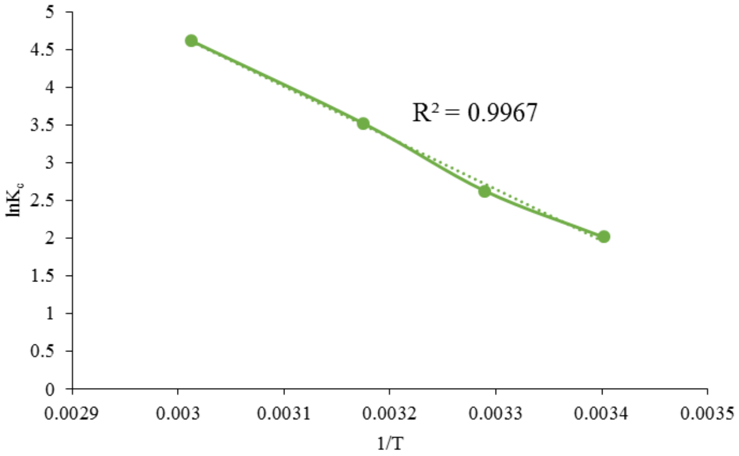

Figure 4.50 Enthapy and entropy change determination of the adsorption of BG using fly ash

This indicated that the adsorption was a spontaneous endothermic process. The nagative ΔGº values, which can be seen from Table 4.46, corresponded the discolored process of MB on GEO8M5D in term of possibility and sponteneity. The positive ΔH° values 60.96 kJ/mol prove that the adsorption was an endothermic peocess. The positive Δ*S*° values indicate an irregular increase of the randomness at the adsorbate - adsorbent interface during the adsorption. The adsorption capacity is 78.25 mg/g at 293 K. Similar trends have been reported in work by GEO8M5D and GSiRH.

Table 4.46 Coefficients of adsorption thermodynamic

T(K)	$\ln K_c$	ΔG° (kJ/mol)	ΔH° (kJ/mol)	ΔS° (J/molK)	q_e (mg/g)
293	1.981	-4.84	60.96	100.26	78.25
303	2.52	-6.37			79.21
313	3.02	-7.91			82.36
333	4.22	-11.64			83.14

4.23 Regeneration test

The regeneration of geopolymer after dye adsorption was also performed. The possible reuse of the adsorption and to choose a suitable desorbated/regenerated was studied. The regeneration was obtained by calcined 400˚C for 2 hr. The FTIR spectra of fly ash after 1st cycles of calcined regenerated is shown in the Figures 4.51, respectively.

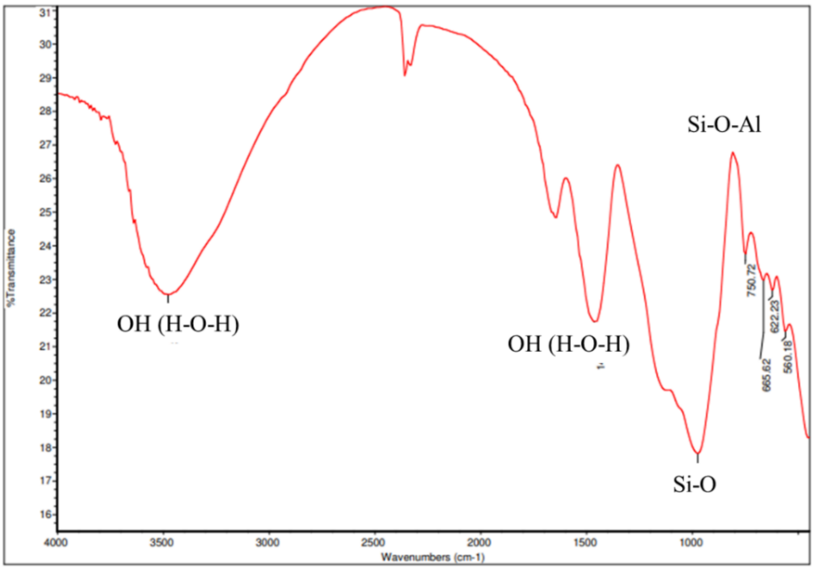

Figure 4.51 The peak of FT-IR of fly after regeneration 1st cycles

The FTIR spectrum shown in Figure.4.54 and all the band assignments are listed in Table 4.46. Figure 4.51 (a), FTIR spectrum showed signification change in position of peaks. The bands appeared in the regions of 1630 and 3702 cm^{-1} that were attributed to bending vibrations (H–O–H) and stretching vibrations O–H. The bands appeared in the regions of 720 to 532 cm^{-1} are due to the vibration mode Si-O-Al and Si–O– Si, respectively. The FTIR of 1st calcined showed similarly band of fly ash before calcite.

Table 4.47 FTIR spectrum analysis

Materials	Bands (cm^{-1})	Assignments	Reference
Fly ash	3406	stretching vibrations O–H	[12]
	1621	bending vibrations H–O–H	
	1235	Si-O stretching	
	734-457	Si-O-Al/Si-O/Si stretching	
1st calcined	3702	stretching vibrations O–H	
	1630	bending vibrations H–O–H	
	1123	Si-O stretching	
	720 - 532	Si-O-Al/Si-O/Si stretching	

Fly ash was applied to remove BG under the conditions BG concentration 300 ppm and fly ash dose 4 g/L in 25 mL solution (60 minutes of contact time) and the adsorption BG dye (C_0 = 300 ppm).

Table 4.48 BG uptake for geopolymer after multiple regeneration cycles

Number of cycles	Adsorption efficiency (%)	q_e (mg/g)
0	93.40±0.13	78.90±0.01
1	79.52±0.24	60.12±0.36
2	62.84±1.21	58.17±0.14
3	42.33±0.23	29.01±0.64
Cumulative q_e (mg/g)		**227.10**

Table 4.47, the percentage removal of BG dye decrease with the decrease in regenerate of adsorbent. The mean percentage removal decrease from 93.40 and 42.33%. The adsorption capacity decreased with an decreasing 78.90 to 29.01 mg/g. The performance of BG adsorbent was fermented after the 1st cycles, while induced

reduction on the BG uptake. At this stage the performance of the adsorbent decreaded were observed on uptake and removal efficiency up to the third cycles. The results of regeneration and reuse showed that fly ash can be used fouth times and cumulative q_e up to 227.10 mg/g.

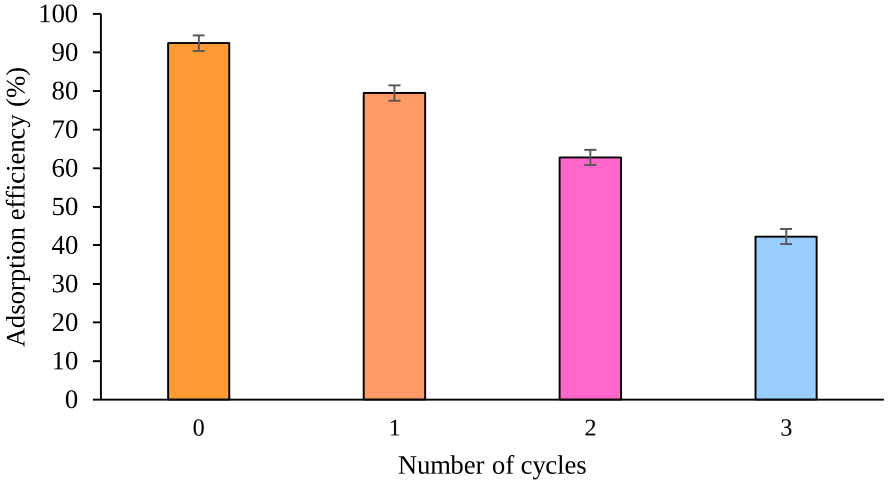

Figure 4.52 BG uptake for fly ash after multiple regeneration cycles

The BET surface areas, pore volumes and pore sizes of the samples before and after thermal regenreration showed in Table 4.48.

Table 4.49 The BET surface areas, pore volumes and pore sizes of the sample of before and after calcined

Samples	BET surface areas	Pore volumes	Pore sizes
Before calcined	5.44	1.25	1.38
3rd cycles	2.10	4.50	3.23

Before calcined, the sample showed higher value of BET surface area, pore volume and pore size than final of regeneration. The BET surface area, pore volume and pore size decreased with an increasing cycles of thermal regeneration.

4.24 Application of geopolymer

The importance of removing dissolved heavy metals from water is a primary concern for society because heavy metals represent a risk to both public and environmental health. Heavy metals are toxic and carcinogenic, and they can easily enter the food chain. According to the Environmental Protection Agency (EPA), heavy metals are considered priority pollutants and must be removed or reduced from any water body that may or may not come into contact with the environment [125]. According to Pollution Management or PCD reported limit of heavy metal from water. The limit of Zn(II), Cr(III) and Cd(II) are 0.50, 0.03 and 0.70 ppm of respectively.

Therefore, it is interesting used geopolymer for heavy metal removal from solution such as Cr(III), Zn(II) and Cd(II). The adsorption efficiency, Initial concentration at 50 ppm, dosage at 4 g/L and 60 minutes of contact time were investigated. The results of adsorption efficiency were shown in Table 4.49 and Figure 4.53.

Table 4.50 The adsorption efficiency of heavy metal solution

Heavy metal solution	Adsorption efficiency (%)	q_e (mg/g)
Cd(II)	93.48±0.51	75.14±0.13
Zn(II)	92.86±0.11	46.12±0.02
Cr(III)	90.68±0.48	60.18±0.25

The initial final concentration of after adsorption of Cr(III), Zn(II) and Cd(II) are 5.21, 4.01, 3.26 ppm, respectively. The adsorption efficiency of Cr(III), Zn(II) and Cd(II) are 90.68, 92.86 and 93.48%, respectively.

The relationship, attraction force between adsorbent and metals ion, is influenced by the size of cation; the smaller the hydrated radius, the greater the relationship [126]. In this work, GEO8M5D can reduced heavy metal from solution at 50 ppm concentration.

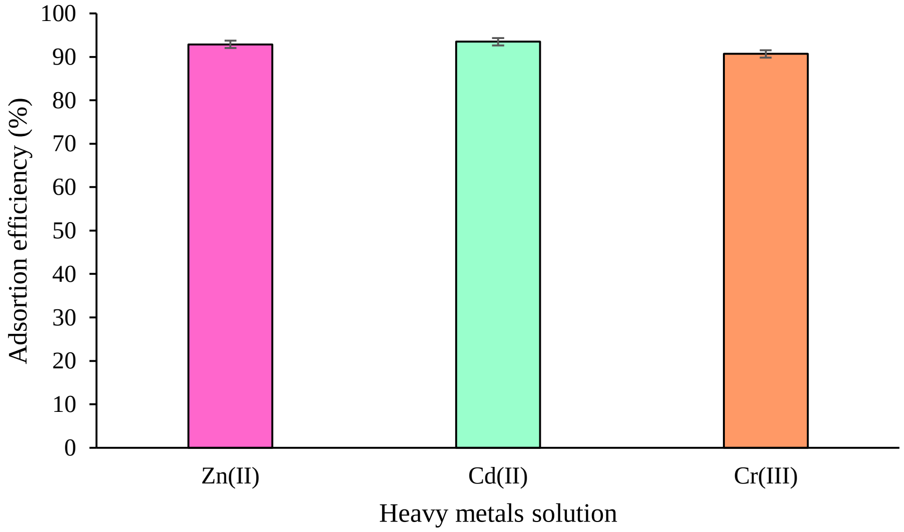

Figure 4.53 The adsorption efficiency of heavy metal solution

CHAPTER 5

DISCUSSION AND CONCLUSION

5.1 Conclusions

Recent researches in geopolymer materials have focused on the synthesis of building materials. However, the problem made cleaning of wastewater interest for development of new adsorbent materials. Therefore, the present thesis would give an potential application for geopolymers and fly ash. The following conclusions can be drawn from the results of the experiments in this study:

5.1.1 The synthetic GEO8M5D from metakaolin has been demonstrated as an adsorbent for the removal of the MB dye. The optimal alkaline solution was 8M of NaOH at 5 days of cured time . At initial concentration at 300 ppm MB solution at pH 8.0, the equilibrium time at 60 minutes and optimal dosage is 20 g/L with the adsorption efficiency at 95 % (uptake 31 mg/g). The best-fit with Langmuir isotherm was obtained monolayer adsorption. Kinetic study showed that the adsorption followed pseudo-second –order, which can be expressed as the reaction rate being proportional to the concentration of two reactants, concluding the adsorption is controlled by chemisorption steps. The results indicated that geopolymer has high potential to be used as a low-cost adsorbent for the removal of MB from aqueous solutions. The regeneration of adsorbent were observed on uptake and removal efficiency up to the 9th cycle and 296.92 mg/g of cumulative q_e, slowly the feasibility of reusing this rearranged adsorbent without any performance conciliated.

5.1.2 The study to extract silica from RH and fly ash used as Na_2SiO_3 forgeopolymer precusor. The yields of silica from RH and fly ash are similarly 16 and 16.13%, respectively. The purity of silica powder from RH higher than that of fly ash are 99.30 and 94.56%. The adsorption efficiency of GEO8M5D, GSiRH and GFA are 95.17, 78.67 and 29.20, respectively. The adsorption efficiency and capacity of GFA showed lower than

GEO8M5D and GSiRH. Thus, Na_2SiO_3 obtained from extracted silica from RH for geopolymer preparation could be used as a replacement of Na_2SiO_3 commercial .

5.1.3 The study to extract silica from RH used as Na_2SiO_3 for geopolymer preparation for the removal of the MB dye . The optimal alkaline solution was 6M of NaOH and cured time was 5 days. The initial concentration at 300, the equilibrium time at 60 minutes and optimal dosage is 40 g/L with the adsorption efficiency more than 90.00 % (uptake 18.48 mg/g). The best-fit Langmuir isotherm was obtained monolayer adsorption. Kinetic study showed that the adsorption followed pseudo-second –order. The adsorption is controlled by chemisorption steps. The results indicated that geopolymer has high potential to be used as a low-cost adsorbent for the removal of MB from aqueous solutions. The capacity mass of geopolymer resulting from the adsorption process was 16.88 mg/g (80.52%) during the 1st cycle and the 4th of cycle was 9.67 mg/g and 71.92 mg/g of cumulative $q_{e.}$ The similarly results of contact time was 60 minutes for both adsorbent (95% of adsorption efficiency). Table 5.1 shows some reported adsorption capacities of MB dye using metakaolin based geopolymer.

Table 5.1 Comparison of adsorption capacities of MB by metakaolin based geopolymer

Adsorbents	q_e (mg/g)	References
MK- geopolymer	30.92	[106]
MK-geopolymer	80.65	[36]
GEO8M5D	**31.94**	**This work**
GSiRH	**18.48**	**This work**

By comparing the adsorption capacity explained in Table 5.1. Lertcumfu et al studied MB removal by using MK-geopolymer. The adsorption capacity is 30.92 mg/g at an adsorbent dosage of 5.00 g/L. MB solution concentration was 200 ppm with 1440 minutes of contact time. Finally, Maleki et al studied MB removal by using MK-geopolymer. The adsorption capacity is 30.92 mg/g at an adsorbent dosage of 1.00 g/L. MB solution concentration was 200 ppm with 1440 minutes of contact time. All the literatures review used the lower than that of MB solution concentration and contact time of GEO8M5D and GSiRH.

5.2.3 The present study obtained the adsorption of BG dye from aqueous solution by using fly ash. Mae Moh fly ash from power plant in Lampang province, Thailand has been demonstrated as an excellent adsorbent not modified for removal of the BG cationic dye. At initial concentration at 300 mg/L, the equilibrium time of 30 minutes and the optimal dosage is 4 g/L with the adsorption efficiency was 93.00 % (q_e uptake mg/g).The best-fit Langmuir isotherm was obtained monolayer adsorption. Kinetic study showed that the adsorption followed pseudo-second –order. The adsorption is controlled by chemisorption steps. Therefore, it material was interesting because the results indicated that fly ash without modified has high potential to be used as a low-cost adsorbent for the removal of BG from aqueous solutions. The adsorption efficiency of recycles was between demonstrated 93.40 to 42.30% up to 3rd cycles and 227.10 mg/g of cumulative q_e

All the result of removal cationic dye were similarly obtained of thermodynamic process. The negative value of gibbs energy change ΔG^o indicates that the process is spontaneous and the positive value of $\Delta H°$ indicate that the adsorption of the dye was endothermic. Positive $\Delta S°$ values indicate an irregular increase of the randomness at the adsorbate - adsorbent interface during the adsorption.

5.1.4 Other application of geopolymer from metakaolin was used removal heavy metal from solution. The result of adsorption efficiency of Cr(III), Zn(II) and Cd(II) are 90.68, 92.86 and 93.48%, respectively. Our results thus that an adsorbent samples can be removed heavy metal from solution at 50 ppm of concentration. According to Pollution Management or PCD reported limit of heavy metal from water.

The limit showed 0.50, 0.03 and 0.70 ppm of Zn(II), Cr(III) and Cd(II) respectively. The sample successfully utilized for the adsorption of cationic dye and heavy metal from solutions.

5.2 Recommendation for future work

5.2.1 This investigated optimum condition for adsorption of cationic dye and heavy metal by geopolymers and fly ash should be applied in treatment of real wastewater sample.

5.2.2 The crystalline size of adsorbent should be calculated from XRD.

5.2.3 Adsorption of fly ash and pure BG should be analyzed from FTIR .

5.2.4 The morphology of fly ash should be analyzed from SEM-EDX.

5.2.5 The preparation of Na_2SiO_3 from fly ash should be increased amount of dosage of silica powder. Baceuse purity of silica from fly ash have lower than RH.

REFERENCES

REFERENCES

[1] Kocaoba, S.O. and et al. " Kinetics and equilibrium studies of heavy metal ions Removal by use of natural zeolite", **Desalination.** 2007(214): 1-10; August, 2007.

[2] Kushwaha, A. K. and et al. "Removal of cationic methylene blue and malachite green dyes from aqueous solution by waste materials of Daucus carota", **Journal of Saudi Chemical Society.** 2014(18): 200-207; July, 2014.

[3] Oplatowska, M. and et al. "The potential for human exposure, direct and indirect, to the suspected carcinogenic triphenylmethane dye brilliant green from green paper towels", **Food and Chemical Toxicology.** 2011(49): 1870-1876; August, 2011.

[4] Central equipment division. "มาตรฐานน้ำทิ้ง", http://thaienvironmentblog.com. December 15, 2019.

[5] Electricity Generating Authority of Thailand. **Liqnite Byproduct Business**. https://www.egat.co.th/en/business-operation/egat-service-business/byproduct-business. December 15, 2019.

[6] Adriano, G.S. and et al . "Effect of curing temperature, activator solution composition and particle size in Brazilian fly-ash based geopolymer production", **Materials Research.** 2019(22): 1-12; June 2019.

[7] Ngamcharussrivichai, C. and et al. "Adsorptive removal of thiophene and benzothiophene over zeolites from Mae Moh coal fly ash", **Fuel**. 2008(87): 2347 - 2351; August, 2008.

[8] Nabil, B. and et al. "Development of ternary blends for high- performance concrete", **Materials Journal.** 2004(101): 19-29; January, 2004.

[9] Murmu, A. L. and et al. "Towards sustainable bricks production: An overview", **Construction and Building Materials**. 2018(165): 112-125; March, 2018.

REFERENCES (CONTINUED)

[10] El, S. G. and et al. "Removal of methylene blue and crystal violet from aqueous solutions by palm kernel fiber", **Desalination.** 2011(272): 225-232 ; May, 2011.

[11] Mishra, A. and et al. "Utilization of fly ash in adsorption of heavy metals from wastewater", **Toxicological & Environmental Chemistry**. 2008(90): 1091-1097; January, 2008.

[12] El, A.M. and et al. "Removal of cationic dye - methylene blue - from aqueous solution by adsorption on fly ash-based geopolymer", **Journal of Materials and Environmental Science**. 2018(9): 32-46; January, 2018.

[13] Novais, R. M. and et al. "Synthesis of porous biomass fly ash-based geopolymer spheres for efficient removal of methylene blue from wastewaters", **Journal of Cleaner Production**. 2019(207): 350-362; October, 2019.

[14] Mužek, M. N. and et al. "Fly ash-based geopolymeric adsorbent for copper ion removal from wastewater", **Desalination and Water Treatment**. 2013(52): 2519 - 2526; May, 2013.

[15] Patthra, P. and et al. "Extracting silica from biomass fly ash by using alkaline hydrothermal treatment and silica precipitation by using organic acids", **The Journal of KMUTNB.** 2018(28): 175-182; Junuary, 2018.

[16] Gao, M. and et al. "A novel approach to extract SiO_2 from fly ash and its considerable adsorption properties", **Materials & Design.** 2017(116): 666 - 675; February, 2017.

[17] Chungsangunsit, T. and et al. "Environmental assessment of electricity production from rice husk: A case study in Thailand", **International Energy Journal**. 2005(6): 47-55; June, 2005.

[18] Chandrasekhar, S. ad et al. "Effect of calcination temperature and heating rate on the optical properties and reactivity of rice husk ash", **Journal of Materials Science**. 2006(41): 7926-7933; July, 2006.

REFERENCES (CONTINUED)

[19] Davidovits, J. and et al. “Geopolymeric concretes for environmental protection”, **Journal of thermal analysis.** 1990 (12): 30-39; March, 1990.

[20] Provis, J. L. and et al. “Do geopolymers actually contain nanocrystalline zeolites a reexamination of existing results”, **Chemistry of Materials.** 2005(17): 3075-3085; May, 2005.

[21] Saidi, N. and et al. “Effect of Composition on structure and mechanical properties of metakaolin based PSS-geopolymer”, **International Journal of Material Sciences**. 2013(3), 145-151; December, 2013.

[22] Davidovits, J. “30 years of successes and failures in geopolymer applications market trends and potential breakthroughs”, **Geopolymer 2002 Conference**. 2002: 1 - 16; January, 2002.

[23] Nasvi, M. C. M. and et al. “The permeability of geopolymer at down-hole stress conditions: Application for carbon dioxide sequestration wells”, **Applied Energy**. 2013(102): 1391 - 1398; February, 2013.

[24] Zhang, Z. and et al. “Preparation and characterization of a reflective and heat insulative coating based on geopolymers”, **Energy and Buildings.** 2015(87): 220-225; January, 2015.

[25] Duxson, P. and et al. “Geopolymer technology: the current state of the art”, **Journal of Materials Science**. 2007(42): 2917-2933; December, 2006.

[26] Barbosa, T. R. and et al. “Preparation of mesoporous geopolymer using metakaolin and rice husk ash as synthesis precursors and its use as potential adsorbent to remove organic dye from aqueous solutions”, **Ceramics International**. 2018(44): 416-423; January, 2018.

[27] Da'na, E. and et al. “Adsorption of heavy metals on functionalized-mesoporous silica: A review”, **Microporous and Mesoporous Materials.** 2017**(**247): 145 157; July, 2017.

REFERENCES (CONTINUED)

[28] Fumba, G. “Equilibrium and kinetic adsorption studies of methyl orange from aqueous solutions using kaolinite, metakaolinite and activated geopolymer as low cost adsorbents”, **Journal of Academia and Industrial Research**. 2014(3): 156-163; September, 2014.

[29] Lü, L. and et al.“Equilibrium and Kinetic Modeling of Pb(II) Biosorption by a chemically modified orange peel containing cyanex 272”, Journal of Chemical & Engineering Data. 2010(55): 4147-4153; July, 2010.

[30] Tan, I. A. and et al. “Adsorption of basic dye on high-surface-area activated carbon prepared from coconut husk: Equilibrium, kinetic and thermodynamic studies”, **Journal of Hazardous Materials.** 2008(154): 337-346; June, 2008.

[31] Cheng, S. and et al. “Comparison of activated carbon and iron/cerium modified activated carbon to remove methylene blue from wastewater”. **Journal of environmental sciences (China).** 2018(65): 92-102; April, 2018.

[32] Merouani, S. and et al. “Influence of bicarbonate and carbonate ions on sonochemical degradation of rhodamine B in aqueous phase”, **Journal of Hazardous Materials.** 2009 (175): 593-599; October, 2019

[33] Lesmana, S. O. and et al. “Studies on potential applications of biomass for the separation of heavy metals from water and wastewater”, **Biochemical Engineering Journal**. 2009(44): 19-41; April, 2009.

[34] Barbosa, V. F. and et al. “Synthesis and thermal behaviour of potassium sialate geopolymers”, **Materials Letters**. 2003(57): 1477-1482; February, 2003.

[35] Bhosale, G. S. and et al. “Kinetics of ozonation of phenol and substituted phenols”, **Industrial & Engineering Chemistry Research.** 2019(58): 7461-7466; April, 2019.

[36] Maleki, A. and et al. “Adsorbent materials based on a geopolymer paste for dye removal from aqueous solutions”, **Arabian Journal of Chemistry**. 2020(13): 3017 - 3025; January, 2020.

REFERENCES (CONTINUED)

[37] Boukhemkhem, A. and et al. “Improvement adsorption capacity of methylene blue onto modified Tamazert kaolin”, **Adsorption Science & Technology**. 2017(35): 753 -773; January, 2017.

[38] Neto, V. and et al. “Equilibrium and kinetic studies in adsorption of toxic metal ions for wastewater treatment”, **A Book on Ion Exchange, Adsorption and Solvent Extraction**. 2013(3): 145-182; December, 2013.

[39] Chemistry. **Factors affecting adsorption of gases on solids**. https://byjus.com/chemistry/factors-affecting-the-extent-of-adsorption. January, 2020.

[40] Ahmaruzzaman, M. “A review on the utilization of fly ash”, **Progress in Energy and Combustion Science.** 2010(36): 327-363; June, 2010.

[41] Rees, C. and et al. “In situ ATR-FTIR study of the early stages of fly ash geopolymer gel formation". **Langmuir: the ACS journal of surfaces and colloids**. 2007(23): 9076-9082; July, 2007.

[42] Hardjito, D. and et al. “Fly ash-based geopolymer concrete”, **Australian Journal of Structural Engineering**. 2017(6): 77-86; January, 2015.

[43] Comrie, D. C. and et al. “Composite cold ceramic geopolymer in a refractory application”, **Advances in Ceramic Matrix Composites IX**. 2004(153): 211-225; January, 2004.

[44] Zhang, Z. and et al. **“**Potential application of geopolymers as protection coatings for marine concrete: I. Basic properties”, **Applied Clay Science.** 2010 (49): 1-6; June, 2010.

[45] Al-Harahsheh, M. and et al. “ Fly ash based geopolymer for heavy metal removal: A case study on copper removal”, **Journal of Environmental Chemical Engineering.** 2015(3): 1669-1677; September, 2015.

REFERENCES (CONTINUED)

[46] Ge, Y. and et al. "Facile fabrication of green geopolymer/alginate hybrid spheres for efficient removal of Cu(II) in water: Batch and column studies", **Chemical Engineering Journal.** 2017(311): 126-134; March, 2017.

[47] El Alouani, M. and et al. "Removal of cationic dye - methylene blue- from aqueous solution by adsorption on fly ash-based geopolymer", **Journal of Materials and Environmental Science.** 2018(9): 32-46; January, 2018.

[48] Zhang, Y. J.and et al. " A facile and low-cost synthesis of granulated blast furnace slag-based cementitious material coupled with Fe_2O_3 catalyst for treatment of dye wastewater", **Applied Catalysis B: Environmental.** 2013(138): 9-16; July, 2013.

[49] Zhang, Y. and et al. "A new graphene/geopolymer nanocomposite for degradation of dye wastewater", **Integrated Ferroelectrics.** 2016(171): 38-45; May, 2016.

[50] Cheng, T. and et al. "The heavy metal adsorption characteristics on metakaolin-based geopolymer", **Applied Clay Science.** 2012(56): 90–96; February, 2012.

[51] Lee, N. K. and et al. "Adsorption characteristics of cesium onto mesoporous geopolymers containing nano-crystalline zeolites", **Microporous and Mesoporous Materials.** 2017(242): 238-244; April, 2017.

[52] O'Connor, S. and et al. "Ion exchange in the charge-balancing sites of aluminosilicate inorganic polymers", **J. Mater. Chem.** 2010(20): 10234-1024 ; October, 2010.

[53] Nontoxichub**. Dyeing Safely: Overview.** https://www.nontoxichub.com/dyeing**.** January, 2020.

[54] Dyeing Process. **Classification of dyes.** https://textilelearner.blogspot.com/2011/07/dyeing-process-different-types-of-dye1720.html. January, 2020.

REFERENCES (CONTINUED)

[55] Lenntech BV. **Chemical properties of chromium - health effects of chromium – environmental effects of chromium**. https://www.lenntech.com/periodic/elements/cr.htm. January, 2020.

[56] Wikipedia. **Cadmium**. https://en.wikipedia.org/wiki/Cadmium. January, 2020.

[57] Wikipedia. **Zinc**. https://en.wikipedia.org/wiki/Zinc_toxicity. January, 2020.

[58] Varga, G. "The structure of kaolinite and metakaolinite", **Epitoanyag - Journal of Silicate Based and Composite Materials.** 2007 (59): 6-9; January, 2007.

[59] Xu, H. and et al. "Geopolymerisation of multiple minerals", **Minerals Engineering**. 2002(15) : 1131-1139; December, 2002.

[60] Liew, Y. M. and et al. "Processing and characterization of calcined kaolin cement powder", **Construction and Building Materials.** 2012(30): 794-802 ; May, 2012.

[61] Lecomte, I. and et al. "Synthesis and characterization of new inorganic polymeric composites based on kaolin or white clay and on ground-granulated blast furnace slag", **Journal of Materials Research.** 2011(18): 2571-2579; January, 2011.

[62] Zhang, H. and et al. "Fiber reinforced geopolymers for fire resistance applications", **Procedia Engineering**. 2014(71): 153-158; December, 2014.

[63] Chris, W. **Power plants (power stations)**. https://www.explainthatstuff.com/powerplants.html. January, 2020.

[64] Wikipedia. **Rice hull.** https://en.wikipedia.org/wiki/Rice_hulls. January, 2020.

[65] Van, B. and et al. "Freundlich Isotherm", **Encyclopedia of Membranes**. 2015: 1-2; December, 2015.

[66] Langmuir, I. "The adsorption of gase on plane surfaces of glass, mica and platinum", **Journal of the American Chemical Society**. 1918(40): 1361-1403; September, 1918.

REFERENCES (CONTINUED)

[67] Plazinski, W. and et al. “Modeling of sorption kinetics: the pseudo-second order equation and the sorbate intraparticle diffusivity”, **Adsorption.** 2013(19): 1055-1064; March, 2013.

[68] Özcan, A. and et al. “Modification of bentonite with a cationic surfactant: An adsorption study of textile dye Reactive Blue 19”, **Journal of Hazardous Materials**. 2007(140): 173-179; March, 2007.

[69] Salman, M. and et al. “Adsorption of humic acid on bentonite”, **Applied Clay Science**. 2007 (38): 51-56; December, 2007.

[70] Wang, S. and et al. “Removal of dyes from aqueous solutions using fly ash and red mud”, **Water Research**. 2005(39): 129-138; February, 2005.

[71] Wongyai, K. and et al. “A geochemistry study of arsenic speciation in overburden from Mae Moh Lignite Mine, Lampang, Thailand”, **Environmental earth sciences.** 2010(70): 2047-2053; January, 2010.

[72] Mane, V. and et al. “Kinetic and equilibrium isotherm studies for the adsorptive removal of brilliant green dye from aqueous solution by rice husk ash”, **J Environ Manage.** 2007(84): 390–399; September, 2007.

[73] Mane, V. and et al. “Use of bagasse fly sh as an adsorbent for the removal of brilliant green dye from aqueous solution”, **Dyes and Pigments - DYE PIGMENT**. 2007 (73): 269-278; December, 2007.

[74] Yao, X. and et al. “Geopolymerization process of alkali-metakaolinite characterized by isothermal calorimetry”, **Thermochimica Acta**. 2009(493): 49-54; September, 2009.

[75] Rovnanik, P. and et al. “Effect of curing temperature on the development of hard structure of metakaolin-based geopolymer”, **Construction and Building Materials.** 2010(24): 1176-1183; July, 2010.

REFERENCES (CONTINUED)

[76] White, C. and et al. “The Effects of Temperature on the Local Structure of Metakaolin-Based Geopolymer Binder: A Neutron Pair Distribution Function Investigation”, **Journal of the American Ceramic Society**. 2010(93): 3486-3492; July, 2010.

[77] Zhang, Z. and et al. “Quantitative kinetic and structural analysis of geopolymers. Part 1. The activation of metakaolin with sodium hydroxide”, **Thermochimica Acta**. 2012(539): 23–33; July, 2012.

[78] Ferrero, F. and et al. “Dye removal from aqueous solution using coal fly ash for continuous flow adsorption”, **Clean Technologies and Environmental Policy.** 2015(17): 1907-1915; January, 2015.

[79] Khan, M. and et al. “Effective removal of methylene blue from water using phosphoric acid based geopolymers: synthesis, characterizations and adsorption studies’’, **RSC Advances**. 2015(5): 61410-61420; July, 2015.

[80] Malkawi, A. B. and et al. “Effects of alkaline solution on properties of the HCFA geopolymer mortars”, **Procedia Engineering.** 2016(148): 710-717; December, 2016.

[81] Jackson, P. and et al. “Effect of Initial cure time on toughness of geopolymer matrix composites”, **Ceramics International**. 2017(43): 9884-9890; September, 2017.

[82] Kara, İ. And et al. “Metakaolin based geopolymer as an effective adsorbent for adsorption of zinc(II) and nickel(II) ions from aqueous solutions”, **Applied Clay Science**. 2017(139): 54-63; April, 2017.

REFERENCES (CONTINUED)

[83] Noda L.C. and et al. “Effect of NaOH concentration and curing regime on geopolymer”, **Revista IBRACON de Estruturas e Materiais**. 2017(10): 1174-1181; November, 2017.

[84] Barbosa, T. et al. “Preparation of mesoporous geopolymer using metakaolin and rice husk ash as synthesis precursors and its use as potential adsorbent to remove organic dye from aqueous solutions”, **Ceramics International.** 2017(44): 416-423; September, 2017.

[85] Ge, Y. “Facile fabrication of green geopolymer/alginate hybrid spheres for efficient removal of Cu(II) in water: Batch and column studies”, **Chemical Engineering Journal.** 2016(311): 126-134; November, 2016.

[86] Azarsa, P. et al. “Freeze-thaw performance characterization and leachability of potassium-based geopolymer concrete”, **Journal of Composites Science**. 2020(4): 1-18; April, 2020.

[87] Arslan, A. A. and et al. “Influence of wetting-drying curing system on the performance of fiber reinforced metakaolin-based geopolymer composites”, **Construction and Building Materials**. 2019(225): 909-926; November, 2019.

[88] Maleki, A. and et al. “A green, porous and eco-friendly magnetic geopolymer adsorbent for heavy metals removal from aqueous solutions”, **Journal of Cleaner Production.** 2019(215): 1233-1245; April, 2019.

[89] Cai, J. and et al. “Thermal and compressive behaviors of fly ash and metakaolin-based geopolymer”, **Journal of Building Engineering**. 2020(30): 101307; January, 2020.

[90] Cai, J. and et al. “Electrical resistivity of fly ash and metakaolin based geopolymers”, **Construction And Building Materials**. 2020(234): 1-9; January, 2020.

REFERENCES (CONTINUED)

[91] Hua, P. and et al. “Adsorption of acid green and procion red on a magnetic geopolymer based adsorbent: Experiments, characterization and theoretical treatment”, **Chemical Engineering Journal.** 2020(383): 123113; March, 2020.

[92] Lecomte, I. and et al. “Synthesis and characterization of new inorganic polymeric composites based on kaolin or white clay and on ground-granulated blast furnace slag”, **Journal of Materials Research**. 2011(18): 2571-2579; January, 2011.

[93] El A.M. and et al. “Preparation, characterization, and application of metakaolin-based geopolymer for removal of methylene blue from aqueous solution”, **Journal of Chemistry.** 2019: 2-14; April, 2019.

[94] Rahier, H. and et al. “Reaction mechanism, kinetics and high temperature transformations of geopolymers”, **Journal of Materials Science**. 2006(42): 2982-2996; December, 2006.

[96] Oyelude, E. and et al. “Removal of malachite green from aqueous solution using pulverized teak leaf litter: equilibrium, kinetic and thermodynamic studies”, **Chemistry Central Journal.** 2018(12): 1-10; December, 2018.

[97] López, F. and et al. “Metakaolin-based geopolymers for targeted adsorbents to heavy metal ion separation”, **Journal of Materials Science and Chemical Engineering**. 2014(2): 16-27; January, 2014.

[98] Geng, H. and et al. “Effect of pre-dispersing metakaolin in water on the properties, hydration, and metakaolin distribution in mortar”, **Frontiers in Materials.** 2019(6): 1-10; May, 2019.

[100] Onutai, S. and et al. “Fast microwave syntheses of fly ash based porous geopolymers in the presence of high alkali concentration”, **Ceramics International.** 2016(42): 9866-9874; June, 2016.

REFERENCES (CONTINUED)

[101] Mbuvi, H. and et al. “Adsorption kinetics and isotherms of methylene blue by geopolymers derived from common clay and rice husk ash”, **International Journal of Materials and Chemistry**. 2017 (7): 87-97; December, 2017.

[102] Wang, J. and et al. “The Effect of Alkali on Compressive of Metakaolin Based Geopolymeric Cement”, **Advanced Materials Research**. 2012(554): 327-330; July, 2012.

[103] Luukkonen, T. and et al. “Optimization of the metakaolin geopolymer preparation for maximized ammonium adsorption capacity”, **Journal of Materials Science**.2017(52): 9363-9376; August, 2017.

[104] Olivia, M. and et al. “Properties of fly ash geopolymer concrete designed by Taguchi method”, **Materials & Design - MATER DESIGN**. 2011(36): 191-198; January, 2011.

[105] Poowancum, A. and et al. “Development of Room Temperature curing geopolymer from calcined water-treatment-sludge and rice husk ash”, **RILEM Bookseries**. 2015(10): 291-297; May, 2015.

[106] Lertcumfu, N. and et al. “Characterization of metakaolin-based materials for dye adsorption from aqueous solution”, **Solid State Phenomena**. 2018(283): 88-94; September, 2018.

[107] Pathania, D. and et al. “Removal of methylene blue by adsorption onto activated carbon developed from ficus carica bast”, **Arabian Journal of Chemistry**. 2017(10): Febuary, 2017.

[108] Boparai, H. and et al. “Kinetics and thermodynamics of cadmium ion removal by adsorption onto nano zerovalent iron particles”, **Journal of Hazardous Materials.** 2011(186): 458-465; February, 2011.

[109] Woolard, C. and et al. “Evaluation of the use of modified coal ash as a potential sorbent for organic waste streams”, **Applied Geochemistry**. 2002(17): 1159-1164; August, 2002.

REFERENCES (CONTINUED)

[110] Ghosh, D. and et al. “Adsorption of methylene blue on kaolinite”, **Applied Clay Science**. 2002(20): 295-300; February, 2002.

[111] Yousef, R. and et al. “The influence of using Jordanian natural zeolite on the adsorption, physical, and mechanical properties of geopolymers products”, **Journal of Hazardous Materials**. 2009(165): 379-387; June, 2009.

[112] Khan, M. I. and et al. “Effective removal of methylene blue from water using phosphoric acid based geopolymers: synthesis, characterizations and adsorption studies”, **RSC Advances**. 2015(5): 61410-6142; July, 2015.

[113] Liu, Y. and et al. “A facile method for preparation of floatable and permeable fly ash-based geopolymer block”, **Materials Letters**. 2016(185): 370-373; December, 2016.

[114] Novais, S. and et al. “Phosphorus removal from eutrophic water using modified biochar”, **The Science of the total environment**. 2018(633): 825-835; August, 2018.

[115] Mbuvi, H. “Adsorption kinetics and isotherms of methylene blue by geopolymers derived from common clay and rice husk ash”, **International Journal of Materials and Chemistry** 2017(7): 87-97; December, 2017.

[116] Kuang, Y. and et al. “Adsorption of methylene blue in water onto activated carbon by surfactant modification”, **Water**. 2020(12): 1-19; Febuary, 2020.

[117] Singh, T. and et al. “Kinetics and thermodynamics of cationic dye adsorption onto dry and swollen hydrogels poly(acrylic acid-sodium acrylate-acrylamide) sodium humate”, **Desalination and Water Treatment**. 2015(53): 3668-3680; December, 2015.

[118] Chen, M. and et al. “Adsorption kinetics and thermodynamics of methylene blue onto p-tert-Butyl-calix[4,6,8]arene-Bonded silica gel”, **Journal of Chemical & Engineering Data**. 2010(55): 5109-5116; September, 2010.

REFERENCES (CONTINUED)

[119] Mazlan, N. and et al. “Geopolymer: A review on physical properties of inorganic aluminosilicate coating materials”, **Materials Science Forum**. 2014(803): 367 373; August, 2014.

[120] Jembere, A. “Studies on the synthesis of silica powder from rice husk ash as reinforcement filler in rubber tire tread part: replacement of commercial precipitated silica”, **International Journal of Materials Science and Applications**. 2017(6): 87-97; March, 2017.

[121] He, P. and et al. “Effects of Si/Al ratio on the structure and properties of metakaolin based geopolymer”, **Ceramics International**. 2016(42): 14416-14422; October, 2016.

[122] Kumar, B. and et al. “Adsorption of malachite green in aqueous solution onto sodium carbonate treated rice husk”, **Korean Journal of Chemical Engineering**. 2015(32): 1655-1666; March, 2015.

[123] Jawad, A. H. and et al. “Tunable Schiff’s base-cross-linked chitosan composite for the removal of reactive red 120 dye: Adsorption and mechanism study”, **International Journal of Biological Macromolecules**. 2020(142): 732-741; January, 2020.

[124] Hsu, T.C. “Adsorption of an acid dye onto coal fly ash”, **Fuel**. 2008(87): 3040-3045; October, 2008.

[125] Román, P.B. anf et al. “Plant growth-promoting traits in rhizobacteria of heavy metal-resistant plants and their effects on brassica nigra seed germination”, **Pedosphere**. 2017(27): 511-526; May, 2017.

[126] Hawari, A. H. and et al. “Effect of the presence of lead on the biosorption of copper, cadmium and nickel by anaerobic biomass”, **Process Biochemistry**. 2007(42): 1546-1552; November, 2007.

APPENDICES

APPENDICES A

Silica content and instruments

Table A.1 The percentages of silica content extract from rice husk

NO	Weight of rice husk (g)	Weight of silica content (g)	Recovery (%)
1	35.355	4.556	13.00
2	36.839	5.236	14.57
3	79.353	10.901	13.69
4	29.551	4.8487	17.00
5	30.605	4.5741	15.96

Figure A.1 The extraction of silica using rice husk

Table A 2 The percentages of Silica content extract from fly ash

NO	Weight of fly ash (g)	Weight of silica content (g)	Recovery (%)
1	20.2145	3.3376	16.68
2	20.1458	3.1254	15.51
3	20.2369	3.1896	15.76
4	20.1247	3.3147	16.47
5	20.1385	3.2654	16.21

Instruments

1. UV-Visible spectrophotometer

The determination of dye concentration before and after batch adsorption by adsorbent were performed by using a Perkin-Elmer UV-Visible spectrophotometer as shown in Figure A.2. The maximum absorbance of each dye was listed in Table A.3.

Figure A.2 Image of UV-Visible spectrophotometer

Table A.3 The maximum absorbance of dyes

Dyes	Absorbance (nm)
Brilliant green	625
Methylene blue	665
Congo red	498
Methyl orange	465

2. Atomic Absorption Spectrophotometer

The determination of heavy metal concentration before and after batch adsorption by adsorbent were performed by using Atomic Absorption Spectrophotometer (AAS) model AAnalyte 800, equipped with flame burner head and air/acetylene as flame as shown in Figure A.3. Standard technique was used to determine the amount of Zn (II), Cd (II) and Cr (III) ion.

Figure A.3 Image of Atomic absorption spectrophotometer

3. pH meter

A Metrohm 713 pH meter equipped with a glass electrode, Model 6.0238.000 (Metrohm) was used for all pH measurements.

4. Magnetic stirrer

A JENWAY hotplate and magnetic stirrer model 1000 from UK was used for perturbation in the adsorption step.

APPENDICES B

Publications

National conferences

วรางคณา กิตติวงศ์วิศาล, พรพรรณ พึ่งโพธิ์, ปาจรีย์ ถาวรนิติ , เขมกร โกมลศิริสุข, และ สายสมร ลำลอง, การกำจัดสีย้อมเมทิลีน บลู โดยใช้จีโอพอลิเมอร์เป็นตัวดูดซับที่มีประสิทธิภาพสูง, งานประชุมวิชาการ ม.อบ. วิจัย ครั้งที่ 13, 2019, 77-85.

International conferences

Kittiwongwisan, **W.**; Pungpo, P. ; Prajuabsuk, M.; Sattayakul, D.; Deshativong, J. ; Kamsri, P.; Gomonsirisuk, K.; Thavorniti, P. and Lumlong, S. Utilization of fly ash for industrial dyes removal, *Pure and Applied Chemistry International Conference 2020, February*. 13-14, 2020, 46-50**.**

การกำจัดสีย้อมเมทิลีน บลู โดยใช้จีโอพอลิเมอร์เป็นตัวดูดซับที่มีประสิทธิภาพสูง

วรางคณา กิตติวงศ์วิศาล[1] พรพรรณ พึ่งโพธิ์[1] ปาจรีย์ ถาวรนิติ [2] เขมกร โกมลศิริสุข[2] สายสมร ลำลอง[1*]
[1] คณะวิทยาศาสตร์ มหาวิทยาลัยอุบลราชธานี
[2] ศูนย์เทคโนโลยีโลหะและวัสดุแห่งชาติ สำนักงานพัฒนาวิทยาศาสตร์และเทคโนโลยีแห่งชาติ (สวทช)
*E-mail : g3936619@hotmail.com

บทคัดย่อ

งานวิจัยนี้ได้ศึกษาการสังเคราะห์จีโอพอลิเมอร์ (geopolymer) เพื่อใช้เป็นตัวดูดซับสีย้อมประจุบวกเมทิลีน บลู (methylene blue) โดยเตรียมจากจากดินขาวระนอง (Ranong kaolin) แล้วพิสูจน์เอกลักษณ์ด้วยเทคนิค *X-ray diffraction* (*XRD*) และ *X-ray fluorescence* (*XRF*) ศึกษาพารามิเตอร์ที่เหมาะสมในการดูดซับ คือ ปริมาณตัวดูดซับ เวลาในการดูดซับ รวมถึงศึกษาไอโซเทอร์ม จลนศาสตร์ และ อุณหพลศาสตร์ของการดูดซับ พบว่าที่ความเข้มข้นสีเริ่มต้น 300 มิลลิกรัมต่อลิตร ปริมาณตัวดูดซับที่เหมาะสม คือ 20.00 กรัมต่อลิตร เวลาที่เหมาะสม คือ 60 นาที ให้ประสิทธิภาพการดูดซับสีย้อมมากกว่า 90 % ไอโซเทอร์มการดูดซับเป็นแบบแลงเมียร์ ไอโซเทอร์ม จลนศาสตร์ในการดูดซับสอดคล้องกับปฏิกิริยาอันดับสองเสมือน (pseudo second-order) ศึกษาอุณหพลศาสตร์พบว่าการเปลี่ยนแปลงเอนโทรปี ($\Delta S°$) มีค่า 162.49 J/molK มีค่าเป็นบวก แสดงให้เห็นว่ากระบวนการดูดซับทำให้ระบบมีความไม่เป็นระเบียบเพิ่มขึ้น เอนทาลปี ($\Delta H°$) มีค่าเท่ากับ 39.84 kJ/mol มีค่าบวก แสดงว่ากระบวนการดูดซับเป็นปฏิกิริยาดูดความร้อน และ พลังงานอิสระกิบส์ ($\Delta G°$) ของการดูดซับมีค่าเป็นลบ แสดงว่าการดูดซับสีย้อมประจุบวกเป็นการดูดซับเกิดขึ้นได้เอง การศึกษานี้แสดงให้เห็นว่าจีโอพอลิเมอร์ที่สังเคราะห์ได้เป็นตัวดูดซับที่น่าสนใจและมีราคาถูกในการกำจัดสีย้อมเมทิลีน บลูจากน้ำเสียได้

คำสำคัญ : เมทิลีน บลู จีโอพอลิเมอร์ ดินขาว

Removal Methylene Blue Dyes from Aqueous Solution Using Geopolymer as a Highly Potential Adsorbent

Warangkana Kittiwongwisan, [1] Pornpan Pungpo, [1]Pajaree Thavorniti, [2] Khemmakorn Gomonsirisuk, [2]
and Saisamorn Lumlong[1*]

[1]*Department of Chemistry, Faculty of Science, Ubon Ratchathani University, Ubon Ratchathani, 34190, Thailand*
[2]*Division of Chemistry, Faculty of Science, Nakhon Phanom University, Nakhon Phanom, 48000, Thailand*
[3]*National Metal and Materials Technology Center, NSTDA, 111 Thailand Science Park,*
Klong Luang, Pathum Thani, Thailand 12120
**E-mail:* *g3936619@hotmail.com*

Abstract

The aim of this work is to synthesize geopolymers as adsorbent for cationic dye (methylene blue) removal. Geopolymers were prepared from Ranong kaolin. Geopolymer characteristics were determined by *X-Ray diffraction* (*XRD*) และ *X-ray fluorescence* (*XRF*). The optimum parameters for adsorption including adsorbent dosage and adsorption time were investigated. Isotherm, kinetics and thermodynamic of adsorption were also studied. The results indicated that at initial dye concentration at 300 mg/L, the optimum dosage of geopolymer is 20.00 g/L and the optimum adsorption time is 60 minutes with adsorption efficiency of more than 90 %. The adsorption isotherm of cationic dyes onto geopolymer agrees well with the Langmuir isotherm and kinetic process corresponded well to pseudo-second order model. Moreover, for the thermodynamic properties of the adsorption, the positive value of ΔS^{o} (+162.49 J/molK) revealing that adsorption process increased randomness in the system. Positive ΔH^{o} (+39.84 KJ/mol) means endothermic reaction. Negative ΔG^{o} indicated spontaneous adsorption of the cationic dye. These results indicate that the synthetic geopolymer is a promising and low-cost adsorbent for removing dye from wastewater.

Keywords : METHYLENE BLUE, GEOPOLYMER, KAOLIN

บทนำ

จีโอพอลิเมอร์ (geopolymer) เป็นวัสดุใหม่ที่สามารถนำมาใช้เป็นตัวดูดซับสีย้อมได้ โดยจีโอพอลิเมอร์เป็นวัสดุที่มีรูพรุน ประกอบด้วยอะลูมิโน-ซิลิเกต ได้จากการกระตุ้นด้วยด่าง โดยประจุบวก ได้แก่ Li^+, Na^+, K^+ และ Cs^+ (Nanavati et al., 2017) โดยจีโอพอลิเมอร์สามารถสังเคราะห์ได้จากหลากหลายแหล่ง เช่น ดินขาว, ดินตะกอนน้ำประปา และเถ้าลอย (Cheng et al., 2012 ; Davidovits et al., 1991) นอกจากนี้จีโอพอลิเมอร์ยังถูกใช้เป็นตัวดูดซับ เนื่องจากมีต้นทุนต่ำ มีสมบัติทางกลและทางกายภาพที่ยอดเยี่ยม กระบวนการสังเคราะห์มีการใช้พลังงานต่ำและเป็นมิตรกับสิ่งแวดล้อม ส่วนใหญ่นำมาใช้ในการดูดซับสีย้อมจากน้ำเสีย (Sivamani et al., 2009) อุตสาหกรรมการย้อมสีเป็นหนึ่งในอุตสาหกรรมที่มีการใช้น้ำมากที่สุด น้ำทิ้งที่ออกมาจากอุตสาหกรรมการย้อมจะมีสารเคมีและสารผสมต่าง ๆ และน้ำทิ้งต้องได้รับการบำบัดอย่างเหมาะสมก่อนที่จะปล่อยลงสู่แหล่งน้ำ แต่น้ำทิ้งจากโรงย้อมสีนั้นยากต่อการบำบัด (Yagub et al., 2014) เช่น เมทิลีน บลู (methylene blue) ซึ่งเป็นสีประจุบวกโดยโครงสร้างสีย้อมเมทิลีน บลู แสดงดังรูปที่ 1 เมทิลีน บลู เป็นสีที่ใช้กันมากที่สุดในการย้อมผ้าไหม (Deng et al., 2011) แม้ว่าเมทิลีนบลูจะไม่ถือว่าเป็นสีย้อมที่เป็นพิษมาก แต่ก็สามารถทำให้เกิดผลกระทบที่เป็นอันตราย เช่น อาเจียน อัตราการเต้นของหัวใจที่เพิ่มขึ้น ท้องเสีย ช็อก ดีซ่าน อัมพาตและเนื้อร้ายเนื้อเยื่อในมนุษย์ (Chen et al., 2011) ดังนั้น สีเมทิลีน บลูที่ควรได้รับการบำบัดก่อนปล่อยออกมา

รูปที่ 1 โครงสร้างของสีย้อมเมทิลีน บลู

ในงานวิจัยนี้ได้ทำการสังเคราะห์จีโอพอลิเมอร์จากดินขาวระนองเผาที่อุณหภูมิ 600 °C ใช้เป็นตัวดูดซับสารละลายสีย้อมเมทิลีน บลู โดยวิธี batch method โดยศึกษาปริมาณที่เหมาะสม เวลาที่เหมาะสมในการดูดซับสีย้อม รวมทั้งศึกษาไอโซเทอร์มที่เหมาะสมใช้ในการอธิบายแบบจำลองการดูดซับ, จลนศาสตร์ที่ใช้ในการอธิบายอัตราเร็วในการดูดซับ และอุณหพลศาสตร์สามารถใช้ประมาณค่าคงที่สมดุล การเปลี่ยนแปลงพลังงานอิสระของการดูดซับ สามารถนำไปประยุกต์ใช้ในอุตสาหกรรมต่อไปได้

วิธีการวิจัย

สารเคมี

sodium hydroxide (commercial grade) บริษัท อิตัลมาร์ (ปะเทศไทย) จำกัด
sodium silicate (commercial grade) บริษัท อิตัลมาร์ (ปะเทศไทย) จำกัด

การสังเคราะห์จีโอพอลิเมอร์

เผาดินขาวระนองที่อุณหภูมิ 600 °C เป็นเวลา 2 ชั่วโมง ผสม alkali solution โดยใช้อัตราส่วน NaOH : Na_2SiO_3 เท่ากับ (2:3) ผสมให้เป็นเนื้อเดียวกัน จากนั้นผสมกับดินขาวระนองเผาในอัตราส่วนของแข็ง : ของเหลว เท่ากับ 1:1 ผสมให้เป็นเนื้อเดียวกันแล้วเทลงบนแม่พิมพ์ ทำการไล่ฟองอากาศ พันด้วยฟิล์มถนอมอาหาร และบ่มเป็นเวลา 5 วันที่อุณหภูมิห้อง จากนั้นจึงบดให้เป็นผงร่อนด้วยตะแกรงขนาด 250 เมช ได้จีโอพอลิเมอร์มีลักษณะดังรูปที่ 2

รูปที่ 2 จีโอพอลิเมอร์

การพิสูจน์เอกลักษณ์

ศึกษาโครงสร้างผลึกด้วยเทคนิค X-ray diffraction (XRD, Exported by X'Pert SW) ใช้ Cu Kα รัศมี (λ = 1.5406 Å) ที่ 40 kV และ 30 mA

วิเคราะห์องค์ประกอบของธาตุด้วยเทคนิค X-ray fluorescence (XRF) ด้วยเครื่อง ED-XRF (HORIBA, XGT-5200)

ศึกษาปริมาณที่เหมาะสมในการดูดซับ

ศึกษาปริมาณที่เหมาะสมในการดูดซับสีย้อมเมทิลีน บลู แปรปริมาณตัวดูดซับที่ 10.00, 20.00, 40.00 และ 80.00 กรัมต่อลิตร โดยความเข้มข้นสีย้อมเริ่มต้น 300 มิลลิกรัมต่อลิตร เวลาในการดูดซับ 60 นาที กรอง แล้วนำสารละลายมาวัดค่าการดูดกลืนแสงด้วยเครื่อง UV-visible spectrophotometer ที่ λ_{max} = 665 นาโนเมตร ทำซ้ำ 3 ครั้ง นำมาคำนวณเปอร์เซ็นต์ประสิทธิภาพการดูดซับคำนวณได้จากสมการที่ 1

$$\textbf{เปอร์เซ็นต์ประสิทธิภาพการดูดซับ} = ([A_0]-[A_t])/[A_0]\times 100\% \qquad (1)$$

เมื่อ [A_0] คือ ความเข้มข้นก่อนการดูดซับ (มิลลิกรัมต่อลิตร)
[A_t] คือ ความเข้มข้นหลังการดูดซับ (มิลลิกรัมต่อลิตร)

ศึกษาเวลาที่เหมาะสมในการดูดซับ

ศึกษาเวลาที่เหมาะสมในการดูดซับสีย้อมเมทิลีน บลู แปรเวลาในการดูดซับที่ 30, 60, 120 และ 240 นาที โดยความเข้มข้นสีย้อมเริ่มต้น 300 มิลลิกรัมต่อลิตร ปริมาณตัวดูดซับ 20.00 กรัมต่อลิตร กรอง แล้วนำสารละลายมาวัดค่าการดูดกลืนแสงด้วยเครื่อง UV-visible spectrophotometer ที่ λ_{max} = 665 นาโนเมตร ทำซ้ำ 3 ครั้ง นำมาคำนวณเปอร์เซ็นต์ประสิทธิภาพการดูดซับ

ศึกษาไอโซเทอร์มการดูดซับ

ศึกษาไอโซเทอร์มการดูดซับ ใช้ปริมาณตัวดูดซับ 20.00 กรัมต่อลิตร เวลา 60 นาที แปรความเข้มข้นของสารละลายสีย้อมเมทิลีน บลู 300, 350, 400, 450, 500 และ 550 มิลลิกรัมต่อลิตร กรอง แล้วนำสารละลายมาวัดค่าการดูดกลืนแสงด้วยเครื่อง UV-visible spectrophotometer ที่ λ_{max} = 665 นาโนเมตร ทำซ้ำ 3 ครั้ง นำความเข้มข้นของสีย้อมก่อนและหลังการดูดซับ นำไปเขียนกราฟลอการิทึม (logarithm) โดยให้ความเข้มข้นของสีย้อมหลังการดูดซับเปนแกนนอนและปริมาณของสีย้อมที่ถูกดูดซับตอน้ำหนักของตัวดูดซับเปนแกนตั้ง เส้นโคงที่เกิดจากการลากผานจุดที่ไดจากการทดลอง โดยใช้ฟรอยลิช ไอโซเทอร์ม (Freundlich isotherm) จากสมการที่ (2) และ (3) (Freundlich, 1906):

$$q_e = k_F C^{1/n} \qquad (2)$$

$$\log (q_e) = \log (k_F) + (1/n)\log (C_e) \qquad (3)$$

เมื่อ k_F คือ ค่าคงที่ฟรอยลิช คำนวณได้จาก slope ใต้กราฟ (มิลลิกรัมต่อกรัม)

ศึกษาไอโซเทอร์มแบบแลงเมียร์ (Langmuir isotherm) ซึ่งป็นการทำนายระหว่างตัวดูดซับและตัวถูกดูดซับแบบชั้นเดียว (monolayer) สามารถคำนวณและพล็อตกราฟได้จากสมการที่ (4) (Langmuir,1918):

$$C_e/q_e = 1/q_m b + C_e/q_m \qquad (4)$$

เมื่อ C_e คือ ความเข้มข้นที่สมดุล (มิลลิกรัมต่อลิตร) , q_e คือ น้ำหนักตัวดูดซับที่สมดุล (มิลลิกรัมต่อกรัม), q_m คือ น้ำหนักตัวดูดซับที่มากที่สุด (มิลลิกรัมต่อกรัม) และ b คือ ค่าคงที่แลงเมียร์ เมื่อเขียนกราฟระหว่าง C_e/q_e กับ C_e ค่า q_m และ b หาได้จากความชัน (slope) และจุดตัดแกน (intercept)

ศึกษาจลนศาสตร์การดูดซับ

ศึกษาจลนศาสตร์การดูดซับ ใช้ปริมาณตัวดูดซับ 20.00 กรัมต่อลิตร ความเข้มข้นของสารละลายสีย้อมเมทิลีน บลู 300 มิลลิกรัมต่อลิตร แปรเวลาในการดูดซับ 30, 60, 120 และ 240 นาที กรอง แล้วนำสารละลายมาวัดค่าการดูดกลืนแสงด้วยเครื่อง UV-visible spectrophotometer ที่ λ_{max} = 665 นาโนเมตร ทำซ้ำ 3 ครั้ง นำความเข้มข้นของสีย้อมก่อนและหลังการดูดซับมาคำนวณว่าสอดคล้องกับปฏิกิริยาอันดับหนึ่งเสมือน (pseudo first-order) และ ปฏิกิริยาอันดับสองเสมือน (pseudo-second-order) สามารถคำนวณทั้งสองปฏิกิริยาได้จากสมการที่ (5) และ สมการที่ (6)

สมการปฏิกิริยาอันดับหนึ่งเสมือน ; $\log (q_e - q_t) = \log q_e - ((k_{01}/2.303)t)$ (5)

สมการปฏิกิริยาอันดับสองเสมือน ; $t/q_t = (1/k_{12}q_e^{2}) + (1/q_e)t$ (6)

โดย k_{01} คือ ค่าคงที่จลนศาสตร์อันดับหนึ่งเสมือน, (1/วัน) k_{12} คือ ค่าคงที่จลนศาสตร์อันดับสองเสมือน, (กรัมต่อมิลลิกรัมต่อวัน) q_e คือ การดูดซับสีย้อมเมทิลีน บลู ณ เวลาที่สมดุล (มิลลิกรัมต่อกรัม) q_t คือ การดูดซับสีย้อมเมทิลีน บลู ณ เวลาใดๆ (มิลลิกรัมต่อกรัม) และ t คือ เวลา (วัน)

ศึกษาอุณหพลศาสตร์การดูดซับ

ศึกษาอุณหพลศาสตร์การดูดซับ ใช้ปริมาณตัวดูดซับ 20.00 กรัมต่อลิตร ความเข้มข้นของสารละลายสีย้อมเมทิลีน บลู 300 มิลลิกรัมต่อลิตร เวลาในการดูดซับ 60 นาที แปรอุณหภูมิ 293, 303, 313 และ 333 เคลวิน กรอง แล้วนำสารละลายมาวัดค่าการดูดกลืนแสงด้วยเครื่อง UV-visible spectrophotometer ที่ λ_{max} = 665 นาโนเมตร ทำซ้ำ 3 ครั้ง ได้ข้อมูลความเข้มข้นของสีย้อมก่อนและหลังการดูดซับ นำผลที่ได้จากการทดลองของอุณหภูมิที่ใช้ในการดูดซับสีย้อมที่มีผลต่อการดูดซับของจีโอโพลิเมอร์มาแทนค่าในตัวแปรของสมการ Van't Hoff คือ $\ln K_c = -\frac{\Delta H^{\circ}}{RT} + \frac{\Delta S^{\circ}}{R}$ นำค่าที่ได้ไปสร้างกราฟโดยที่แกน X คือ 1/T และแกน Y คือ $\ln K_c$ จากสมการเส้นตรงที่ได้ จุดตัดแกน Y คือ $\frac{\Delta S^{\circ}}{R}$ และ K_c คือค่าคงที่สมดุลซึ่งได้จากการหา $K_c = \frac{C_{ads}}{C_e}$ เมื่อ C_{ads} คือ ความเข้มข้นที่สมดุลของตัวถูกดูดซับ (มิลลิกรัมต่อลิตร) เมื่อได้ค่า K_c แล้วจากนั้นคำนวณหา ΔG° ที่มีผลต่อการดูดซับได้จากสมการ $\Delta G^{\circ} = -RT \ln K_c$

ผลการวิจัย

พิสูจน์เอกลักษณ์ของตัวดูดซับ

พิสูจน์เอกลักษณ์โดยเทคนิค XRF เพื่อวิเคราะห์องค์ประกอบของธาตุ จากดินขาวระนองเผา 600 °C เป็นเวลา 2 ชั่วโมง แสดงดังตารางที่ 1 มีองค์ประกอบหลัก คือ SiO_2 และ Al_2O_3

ตารางที่ 1 องค์ประกอบของธาตุในดินขาวระนองเผา

Formula	Mass (%)	Molecule (%)
Al_2O_3	35.975	25.325
SiO_2	60.993	72.855
K_2O	1.531	1.167
Fe_2O_3	1.288	0.579
ZnO	0.005	0.005
As_2O_5	0.011	0.003
Rb_2O	0.113	0.043
Y_2O_3	0.056	0.018
Ir_2O_3	0.028	0.005

เมื่อวิเคราะห์หาโครงสร้างผลึกด้วยเทคนิค XRD ของดินขาวระนอง พบพีค kaolinite ที่ 10°, 25° และ 26.5° พีคที่ 27° เป็นพีคของ quartz (SiO_2) ส่วนที่ 9° และ 12° เป็นพีคของ illite ดังรูปที่ 3(a) สำหรับดินขาวระนองหลังเผาที่ 600 °C ยังคงพบพีคของ kaolinite, quartz และ illite แต่มีความเป็นผลึกน้อยกว่าดินขาวระนองก่อนเผา ดังรูปที่ 3(b) ส่วนจีโอพอลิเมอร์พบ quartz และ kaolinite มี XRD pattern คล้ายกับดินขาวระนองหลังเผา ดังรูปที่ 3(c)

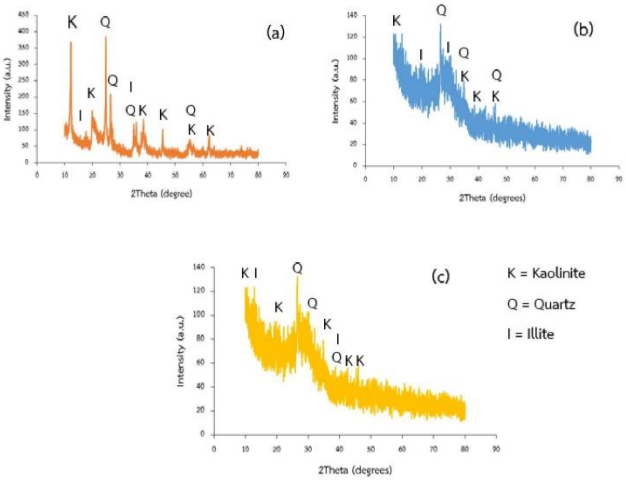

รูปที่ 3 XRD patterns ของ : (a) ดินขาวระนอง (b) ดินขาวระนองหลังเผา และ (c) จีโอพอลิเมอร์

การหาพารามิเตอร์ที่เหมาะสม

ปริมาณตัวดูดซับที่เหมาะสม

ศึกษาปริมาณที่เหมาะสมในการดูดซับที่ปริมาณตัวดูดซับตั้งแต่ 10.00- 80.00 กรัมต่อลิตร พบว่าเมื่อเพิ่มตัวดูดซับจาก 10.00 เป็น 20.00 กรัมต่อลิตร ส่งผลให้มีประสิทธิภาพการดูดซับเพิ่มมากขึ้น ทั้งนี้เพราะรูพรุนในจีโอพอลิเมอร์สามารถดูดซับสีย้อมเมทิลีน บลู ได้มากขึ้น สอดคล้องกับงานวิจัยของ Khodaie et al., 2013 แต่เมื่อเพิ่มปริมาณตัวดูดซับเป็น 40.00 กรัมต่อลิตร ประสิทธิภาพการดูดซับไม่แตกต่างกันอย่างมีนัยสำคัญ แสดงว่าเริ่มเข้าสู่สมดุลที่ปริมาณจีโอพอลิเมอร์ 20.00 กรัมต่อลิตร มีประสิทธิภาพการดูดซับคือ 95.00±0.23% ดังนั้น จึงเลือกปริมาณที่เหมาะสมคือ 20.00 กรัมต่อลิตร ดังรูปที่ 4

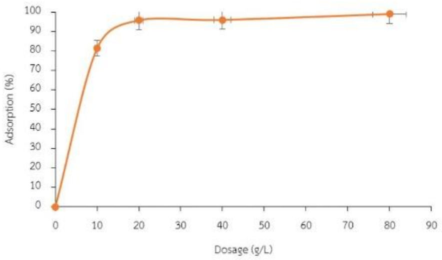

รูปที่ 4 ประสิทธิภาพการดูดซับสีย้อมเมทิลีน บลู ความเข้มข้นสีย้อมเริ่มต้น 300 มิลลิกรัมต่อลิตร ด้วยจีโอพอลิเมอร์จากดินขาวระนอง แปรปริมาณตัวดูดซับตั้งแต่ 10.00-80.00 กรัมต่อลิตร

เวลาที่เหมาะสมในการดูดซับ

ศึกษาเวลาในการดูดซับที่ 30, 60, 120 และ 240 นาที พบว่าระบบเข้าสู่สภาวะสมดุล ที่เวลา 60 นาที เนื่องจากเมื่อเพิ่มเวลาในการดูดซับเป็น 2 เท่า คือ 120 นาที ประสิทธิภาพการดูดซับไม่เปลี่ยนแปลงอย่างมีนัยสำคัญ เมื่อระบบเข้าสู่สภาวะสมดุลอัตราการดูดซับและคายซับเท่ากัน เมื่อระบบเข้าสู่สมดุลจะไม่สามารถดูดซับโมเลกุลของสีย้อมเพิ่มได้อีก สอดคล้องกับงานวิจัยของ Derakhshan et al., 2013 ดังนั้นเวลาที่เหมาะสมในการดูดซับสีย้อมเมทิลีน บลู คือ เวลา 60 นาที เนื่องจากการดูดซับเริ่มเข้าสู่สมดุล มีประสิทธิภาพการดูดซับคือ 95.00±0.38% ดังรูปที่ 5

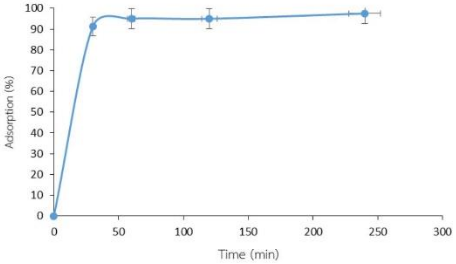

รูปที่ 5 ประสิทธิภาพการดูดซับสีย้อมเมทิลีน บลู ความเข้มข้นสีย้อมเริ่มต้น 300 มิลลิกรัมต่อลิตร ด้วยจีโอพอลิเมอร์จากดินขาวระนอง แปรเวลาในการดูดซับตั้งแต่ 30-240 นาที

ไอโซเทอร์มการดูดซับ

ศึกษาไอโซเทอร์มโดยใช้สมการระหว่างแลงเมียร์ ไอโซเทอร์ม และ ฟรอยลิช ไอโซเทอร์มแสดงในรูปที่ 6 ค่า R^2 โดย ฟรอยลิช ไอโซเทอร์ม มีค่า $R^2 = 0.5364$ และ แลงเมียร์ ไอโซเทอร์มมีค่า $R^2 = 0.9994$ พบว่าค่า R^2 ของแลงเมียร์ไอโซเทอร์มีค่าเข้าใกล้ 1 ซึ่งมีความน่าเชื่อถือมากกว่า ดังนั้น การดูดซับระหว่างตัวดูดซับคือจีโอพอลิเมอร์ และ สีย้อมเมทิลีน บลู จึงเป็นการดูดซับแบบชั้นเดียว (Li et al., 2013)

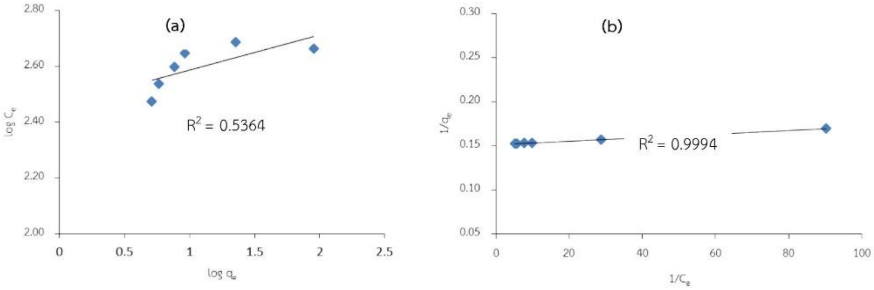

รูปที่ 6 ไอโซเทอร์มการดูดซับ : (a) ฟรอยลิช ไอโซเทอร์ม (b) แลงเมียร์ ไอโซเทอร์ม

จลนศาสตร์การดูดซับ

ผลการศึกษาจลนศาสตร์การดูดซับแสดงดังรูปที่ 7 พบว่า ปฏิกิริยาอันดับหนึ่งเสมือน มีค่า $R^2 = 0.7596$ และ ปฏิกิริยาอันดับสองเสมือน มีค่า $R^2 = 1$ ซึ่งแตกต่างกันอย่างมีนัยสำคัญ ดังนั้น จลนศาสตร์การดูดซับจึงสอดคล้องกับปฏิกิริยาอันดับสองเสมือน ซึ่งมีกลไกการดูดซับดังนี้ 1. เกิดการแพร่ของสีย้อมไปยังบริเวณของจีโอโพลิเมอร์ผ่าน subsurface 2. เกิดการแพร่ผ่าน Subsurface ของจีโอโพลิเมอร์ ซึ่งกระบวนการนี้เรียกว่า film diffusion 3. สีย้อมเกิดการแพร่ผ่านไปยังรูพรุนของจีโอโพลิเมอร์ ซึ่งกระบวนการนี้เรียกว่า pore diffusion 4. เกิดอันตรกิริยาระหว่างพื้นผิวของจีโอโพลิเมอร์จากดินขาวระนองกับสีย้อมเมทิลีน บลู (Abechi et al., 2011)

จากการศึกษาจลนศาสตร์การดูดซับสีย้อมด้วยจีโอโพลิเมอร์จากดินขาวมีผลไปในทางเดียวกัน คือ สอดคล้องกับปฏิกิริยาอันดับสองเสมือน โดยขั้นตอนที่ 4 เป็นขั้นกำหนดอัตราในการดูดซับเกิดอันตรกิริยาระหว่างพื้นผิวของจีโอโพลิเมอร์กับสีย้อม แสดงให้เห็นว่าปฏิกิริยาการดูดซับเป็นการดูดซับที่เกิดจากแรงทางเคมี (chemisorptions)

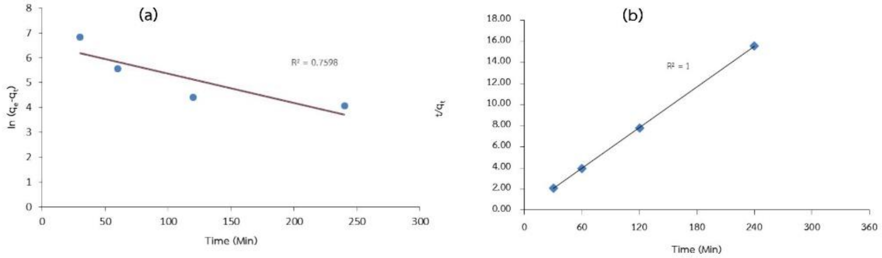

รูปที่ 7 จลนศาสตร์การดูดซับของสีย้อมเมทิลีน บลู บนจีโอโพลิเมอร์จากดินขาวระนอง **:** (a) ปฏิกิริยาอันดับหนึ่งเสมือน และ (b) ปฏิกิริยาอันดับสองเสมือน

อุณหพลศาสตร์การดูดซับ

เมื่อนำผลการทดลองมาพล็อตกราฟระหว่าง 1/T และ lnK_c ดังแสดงในรูปที่ 8 ได้กราฟเส้นตรงที่มีค่าเท่ากับ ∆H°/R และ จุดตัดแกนตั้งเท่ากับ ∆S°/R ซึ่งจากสมการเส้นตรงเมื่อนำมาหาค่า ∆H° (Enthalpy) มีค่าเป็น 39.84 kJ/mol ค่า ∆H° เป็นบวก แสดงว่ากระบวนการดูดซับเป็นปฏิกิริยาดูดความร้อนและเมื่อนำมาหาค่า ∆S° (Entropy) มีค่าเป็น 162.49 J/mol.K ค่า ∆S° เป็นบวก แสดงให้เห็นว่ากระบวนการดูดซับมีผลทำให้โมเลกุลของตัวดูดซับและตัวถูกดูดซับที่บริเวณรอยต่อของพื้นผิวตัวดูดซับกับตัวถูกดูดซับมีความไม่เป็นระเบียบเพิ่มสูงขึ้น ส่วน ∆G° (Gibbs free energy) พบว่า ∆G° แปรผันตามอุณหภูมิ กล่าวคือ เมื่อเพิ่มอุณหภูมิ ค่า ∆G° ก็จะเพิ่มขึ้นด้วย อีกทั้ง ∆G° มีค่าเป็นลบ แสดงว่ากระบวนการดูดซับเกิดขึ้นได้เอง (Al-Rashed et al., 2012)

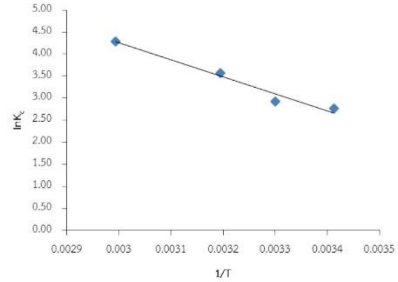

รูปที่ 8 ความสัมพันธ์ระหว่าง 1/T และ lnK_c ของการดูดซับเมทิลีน บลู โดยใช้จีโอโพลิเมอร์จากดินขาวระนอง

อภิปรายและสรุปผลการวิจัย

จีโอพอลิเมอร์สามารถสังเคราะห์จากดินขาวระนองเพื่อเป็นตัวดูดซับที่มีประสิทธิภาพสูง นำมาดูดซับสีย้อมเมทิลีน บลู โดยศึกษาปริมาณที่เหมาะสม เวลาที่เหมาะสม ไอโซเทอร์ม จลนศาสตร์ และอุณหพลศาสตร์ พบว่า ปริมาณที่เหมาะสมคือ 20 กรัมต่อลิตร เวลาที่เหมาะสม 60 นาที โดยความเข้มข้นเริ่มต้นสีย้อมเมทิลีน บลู คือ 300 มิลลิกรัมต่อลิตร ไอโซเทอร์มการดูดซับเป็นแบบชั้นเดียว สอดคล้องกับปฏิกิริยาอันดับสองเสมือน มีค่า ∆H° มีค่าเป็น 39.84 kJ/mol ค่า ∆H° มีค่าเป็นบวก แสดงว่ากระบวนการดูดซับเป็นปฏิกิริยาดูดความร้อน ค่า ∆S° มีค่าเป็น 162.49 J/molK ค่า ∆S° เป็นบวก แสดงว่ากระบวนการดูดซับมีผลทำให้โมเลกุลของตัวดูดซับและตัวถูกดูดซับที่บริเวณรอยต่อของพื้นผิวตัวดูดซับกับตัวถูกดูดซับมีความไม่เป็นระเบียบเพิ่มสูงขึ้น ส่วน ∆G° เมื่อเพิ่มอุณหภูมิ ค่า ∆G° ก็เพิ่มขึ้นด้วย อีกทั้ง ∆G° มีค่าเป็นลบ แสดงว่ากระบวนการดูดซับเกิดขึ้นได้เอง ซึ่ง Marouane El Alouani et al., (2018) ได้สังเคราะห์จีโอพอลิเมอร์จากเถ้าลอยโดยนำมาดูดซับสีย้อมเมทิลีน บลูที่ความเข้มข้น 40 มิลลิกรัมต่อลิตร โดยเวลาที่เหมาะสมในการดูดซับอยู่ที่ 120 นาที ปริมาณตัวดูดซับ 1 กรัมต่อลิตร จึงเข้าสู่สมดุล โดยจลนศาสตร์สอดคล้องกับ

ปฏิกิริยาอันดับสองเสมือน ดังนั้นดินขาวสามารถนำมาใช้ในการสังเคราะห์จีโอพอลิเมอร์ที่มีประสิทธิภาพในการดูดซับสูง อย่างไรก็ตามควรมีการศึกษาเกี่ยวกับการรีไซเคิลจีโอพอลิเมอร์ว่าจีโอพอลิเมอร์ที่เตรียมได้สามารถนำกลับใช้ในการดูดซับกี่ครั้ง รวมทั้งศึกษาสมบัติทางกายภาพของตัวดูดซับ เช่น พื้นที่ผิวจำเพาะ ปริมาตรของรูพรุน เป็นต้น

กิตติกรรมประกาศ

ขอขอบคุณคณะวิทยาศาสตร์ มหาวิทยาลัยอุบลราชธานีสำหรับการสนับสนุนในด้านเครื่องมือและวัสดุอุปกรณ์ต่างๆที่ทำให้งานวิจัยนี้สำเร็จลุล่วงไปด้วยดีผู้วิจัยขอขอบคุณศูนย์ความเป็นเลิศด้านนวัตกรรมทางเคมี (PERCH-CIC) สำนักงานวิจัยแห่งชาติ (วช.) ที่ให้การสนับสนุนทุนในการวิจัยและศูนย์เทคโนโลยีโลหะและวัสดุแห่งชาติ (MTEC) สำนักงานพัฒนาวิทยาศาสตร์และเทคโนโลยีแห่งชาติ (สวทช.) ที่อนุเคราะห์เครื่องมือในการพิสูจน์เอกลักษณ์ และอำนวยความสะดวกในการทำปฏิบัติการ

เอกสารอ้างอิง

Abechi, S., Gimba, C., Uzairu, A., and Kagbu, J. A. (2011). Kinetics of adsorption of methylene blue onto activated carbon prepared from palm kernel shell. *Scholars Research Library Journal, 3,* 154-164.

Al-Rashed, S. M., and Al-Gaid, A. A. (2012). Kinetic and thermodynamic studies on the adsorption behavior of Rhodamine B dye on Duolite C-20 resin. *Journal of Saudi Chemical Society,16,* 209-215.

Cheng, T. W., Lee, M. L., Ko, M. S., Ueng, T. H., and Yang, S. F. (2012). The heavy metal adsorption characteristics on metakaolin-based geopolymer. *Applied Clay Science,* 56, 90-96.

Davidovits, J. (1991). Geopolymers. *Journal of thermal analysis,* 37(8), 1633-1656.

Deng, H., Lu, J., Li, G., Zhang, G., and Wang, X. (2011). Adsorption of methylene blue on adsorbent materials produced from cotton stalk. *Journal of Hazardous Materials,* 172, 326-334.

Derakhshan, Z., Baghapour, M., Ranjbar, M., & Faramarzian, M. (2013). Adsorption of methylene blue dye from aqueous solutions by modified pumice stone: Kinetics and Equilibrium Studies. *Journal* of *Health Scope,* 2(3), 139-44.

El Alouani, M., Alehyen, S., El Achouri, M., and Taibi, M. h. (2018). Adsorption of cationic dye onto fly ash-based geopolymer: Batch and fixed bed column studies. *EDP Sciences Journal,* 149, 6. สืบค้นจากเว็บไซต์ https://www.matec-conferences.org/articles/matecconf/pdf/2018/08/matecconf_cmss2018_02088.pdf (เข้าถึงเว็บไซต์เมื่อวันที่ 13 พฤษภาคม 2562)

H. M. F. Freundlich. Over the adsorption in solution. *The Journal of Physical Chemistry*, 906, 385-471.

Khodaie, M., Ghasemi, N., Moradi, B., and Rahimi, M. (2013). Removal of methylene blue from wastewater by adsorption onto $ZnCl_2$ activated corn husk carbon equilibrium studies. *Journal of Chemistry, 6, 2013.* สืบค้นจากเว็บไซต์ https://www.hindawi.com/journals/jchem/2013/383985/ (เข้าถึงเว็บไซต์เมื่อวันที่ 13 พฤษภาคม 2562)

Langmuir, I. (1918). The adsorption of gases on plane suraces of glass, mica and platinum. *Journal of the American Chemical Society, 40,* 1361-1403.

Li, Y., Du, Q., Liu, T., Peng, X., Wang, J., Sun, J., Xia, L. (2013). Comparative study of methylene blue dye adsorption onto activated carbon, graphene oxide, and carbon nanotubes. *Chemical Engineering Research and Design,* 91, 361-368.

Liu, L., Gao, Z. Y., Su, X. P., Chen, X., Jiang, L., and Yao, J. M. (2015). Adsorption removal of dyes from single and binary solutions using a cellulose-based bioadsorbent. *ACS Sustainable Chemistry & Engineering, 3*(3), 432-442.

Nanavati, S. (2017). A Review on Fly Ash based geopolymer concrete. *IOSR Journal of Mechanical and Civil Engineering,* 14, 12-16.

Chemistry for Catalyzing Sustainability and Prosperity

Utilization of fly ash for industrial dyes removal

Warangkana Kittiwongwisan[1], Pornpan Pungpo[1], Malee Prajuabsuk[1], Somjintana Taweepanich[1], Duangdao Sattayakul[1], Jitlada Deshativong[1], Pharit Kamsri[2], Khemmakorn Gomonsirisuk[3], Pajaree Thavorniti,[3] Saisamorn Lumlong[1]*
[1]*Department of Chemistry, Faculty of Science, Ubon Ratchathani University,*
Ubon Ratchathani 34190, Thailand
[2]*Division of Chemistry, Faculty of Science, Nakhon Phanom University, Nakhon Phanom 48000, Thailand*
[3]*National Metal and Materials Technology Center, NSTDA, 111 Thailand Science Park,*
Pathum Thani 12120, Thailand
E-mail: g3936619@hotmail.com

The aim this work is to investigate potential of fly ash for removal of industrial cationic dye, brilliant green. Fly ash is an abandon waste from power plant. Thailand has expelled fly ash higher than 1.5 million tons each year for almost 2 decades. Fly ash was characterized by X-ray diffraction (XRD), *X-ray fluorescence* (*XRF*) and *Scanning Electron Microscope* (*SEM*). The results showed that silicon dioxide content was 35.6% of fly ash. An attempt to find an alternative way of fly ash utilization as adsorbent for removal of brilliant green, cationic dye from aqueous solutions was performed. With the initial dye concentration of 300 mg/L, the optimal parameters for adsorption such as adsorbent dosage, contact time, and adsorption isotherm were investigated by batch experiments. The results showed that the optimal fly ash dosage was 4 g/L. The optimal adsorption time was 30 minutes. The regression analysis showed a good fit of the Langmuir isotherm model. It can be concluded that the fly ash can be used as an potential adsorbent without modification for the removal of brilliant green, an industrial dye, from aqueous solutions.

1. Introduction

Fly ash is a type of solid waste, which is produced in the process of power plant. It is estimated that the annual production of fly ash waste is about 40,000 tons[1] for power plant of Mae Moh, Lampang province per day, which accounts for a quarter of the power plant waste of Thailand. Fly ash is also used in cement and concrete production[2]. Moreover, new applications of fly ash are used as inexpensive adsorbent for appropriate treatments.

Cationic dyes are important compound commonly used in various industries such as paper[3], leather[4] and plastic manufacture[5]. The textile dyes most used in industry, are methylene blue[6], brilliant green and safranin red[7]. Discharge of colored wastewaters from various industries such as textile and dyeing, pulp and paper, and food process industries is currently a major problem for environmental management. One of the most effective techniques for removal of color from such wastewaters is sorption by activated carbon. However, due to expensive price of it, the use of activated carbon for removal of color from wastewaters is limited. In recent years, many studies have been carried out to find out inexpensive alternatives, i.e. peat, clay, steel plant slag, and bagasse fly ash, etc. This study focused on utilization of fly ash as an alternative adsorbent without modification for removal of brilliant green from aqueous solution using batch adsorption experiment.

2. Materials and Methods

2.1 Materials

Fly ash from, Maemoh, Lampang province was used as an alternative adsorbent for removal of brilliant green from aqueous solution. The composition of materials was characterized by X-ray fluorescence (XRF). The results showed that the fly ash compositions were 44.02, 27.55, 24.18 and 2.98% of SiO_2, CaO, Fe_2O_3 and K_2O, respectively.

2.2 Characterization technique

The phase of fly ash was determined by X-Ray diffraction (XRD, PANalytical X Pert PRO) using Cu Kα radiation (λ = 1.5406 Å) at 40 kV and 30 mA.

2.3 Adsorption experiments

Fly ash was used as adsorbents to remove brilliant green from aqueous solution using batch adsorption method. The effects of adsorbent dosage, initial dye concentration and adsorption time were studied under stirred conditions. A standard technique was used to determine the dye concentration in the solutions using UV–visible spectrophotometry. The maximum absorbance of this dye occurs at 624 nm. The adsorption percentage of dye adsorbed was calculated by the following equation[8]:

$$\%Adsorption=([A_i]-[A_f])[A_i]\times100\% \quad (1)$$

Where $[A_i]$ and $[A_f]$ are the initial and final concentrations of dye solution.

2.3 Optimal conditions

The optimum condition was determined by varying the amounts of adsorbent from 2 - 8 g/L with an initial dye concentration of 300 mg/L. The effect of adsorption times were investigated by varying time from 5- 60 minutes for kinetic study using the optimal adsorbent dosage obtained. The adsorption isotherms were studied with different initial dye concentrations using optimal adsorbent dosage and optimal adsorption time.

3. Results & Discussion

3.1 Characterization of adsorbent material

The XRD patterns of fly ash showed crystalline quartz and mullite at 29˚, 30 ˚, 32 ˚, 39 ˚ and 40 ˚ in Figure 1. The obtained results was corresponded to previously reported by Ting *et al.,* (2008).[9]

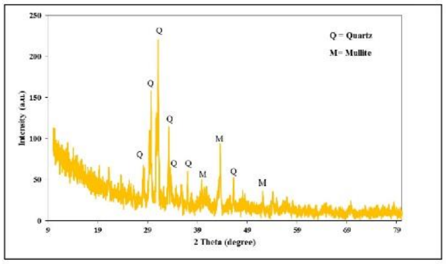

Figure 1. The XRD patterns of fly ash

The morphology of fly ash was analyzed by SEM shown in Figure 2, showing the smooth and pellet particle of surface.

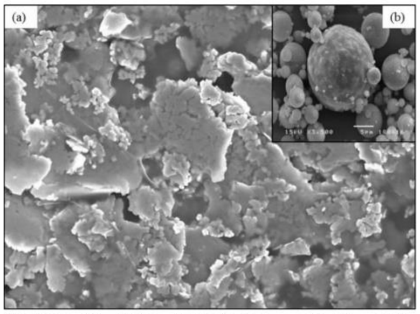

Figure 2. The morphology of fly ash observed by SEM imaging.

3.2 Optimal parameters

The effect of adsorbent dosage on dye adsorption efficiency was studied with initial dye concentration of 300 mg/L and the obtained results are illustrated in Figure 3. At low adsorbent dosage, dye adsorption percentage is low because of low adsorption surface areas for dye adsorption. Increasing the amount of fly ash leads to increase the efficiency of dye adsorption. The adsorption percentage is quite constant when increasing the adsorbent amount higher than 4 g/L and reached the adsorption equilibrium at 4 g/L, with adsorption efficiency higher than 90%. The optimal adsorbent dosage for adsorption dye is 4 g/L.

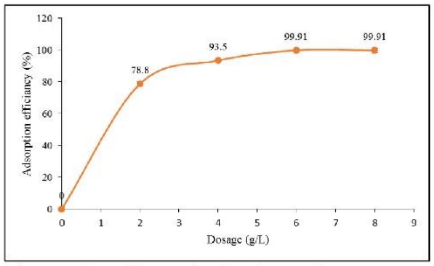

Figure 3. Effect of adsorbent dosage on adsorption efficiency of brilliant green C_0=300 mg/L, 25 mL).

The effect of adsorption time for dye adsorption on fly ash was also investigated. The adsorption efficiency of dye onto adsorbent were shown in Figure 4. At 10 minutes, the adsorption efficiencies were rapidly increased. At 30 minutes, the adsorption efficiency was slowly increased with more than 90% and into the equilibrium at 30 minutes. Figure 5. showed the color of dye on different adsorption time for removal of brilliant green. Therefore, these results clearly indicated that fly ash is an efficient adsorbent to adsorb brilliant green and the optimal time for dye adsorption is 30 minutes.

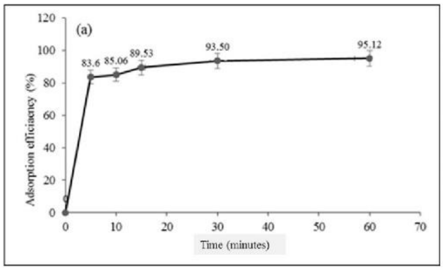

Figure 4. (a) Effect of Time on adsorption efficiency of brilliant green (dosage = 4 g/L, C_0=300 mg/L, 25 mL).

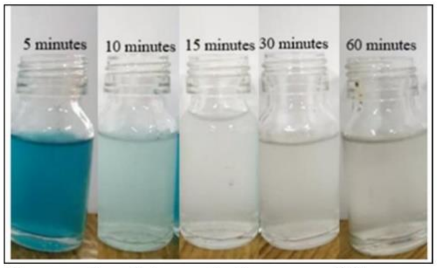

Figure 5. Color of dye on different adsorption time for removal of brilliant green (dosage = 4 g/L, C_0=300 mg/L, 25 mL.

3.3 Isotherm Study

The adsorption equilibrium was established in batch experiments examining brilliant green dye adsorption. Langmuir and Freundlich isotherm models were applied to the experimental data obtained. The Langmuir model was calculated as following equation:[10]

$$C_e/q_e = 1/q_m b + C_e/q_m \quad (2)$$

Where C_e is the equilibrium concentration (mg/L), q_e the amount adsorbed at equilibrium (mg/g), q_m the maximum amount adsorbed (mg/g) and b is the energy of adsorption (Langmuir constant, L/mg). The values of q_m and b were calculated from the slope and intercept of the linear plot C_e/q_e versus C_e. Freundlich isotherm was explained to multilayer surface onto active site. Linear from Freundlich isotherm can write as following: [11]

$$\log (q_e) = \log (K_F) + (1/n)\log (C_e) \quad (3)$$

Where K_F and n are Freundlich constants were calculated from the slope and intercept of the Freundlich plot. The brilliant green removal by fly ash was evaluated by calculating the uptake (q_e) using equation (4):[12]

$$q_e = (C_i - C_e)V/m \qquad (4)$$

where C_i is the initial concentration (mg/L), C_f is final concentration (mg/L), V is the sample volume (L) and m is the weight of the adsorbent (g).

The isotherm parameters obtained from brilliant green adsorption were summarized in Table 1.

Table 1. Langmuir and Freundlich parameters for adsorption of brilliant green onto fly ash.

Langmuir isotherm			Freundlich isotherm		
q_e(mg/g)	N_m	R^2	1/n	K_F	R^2
134.74	96.1538	0.9448	0.1209	1.101	0.8004

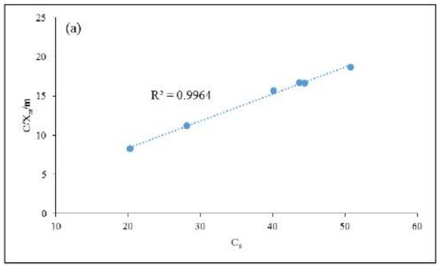

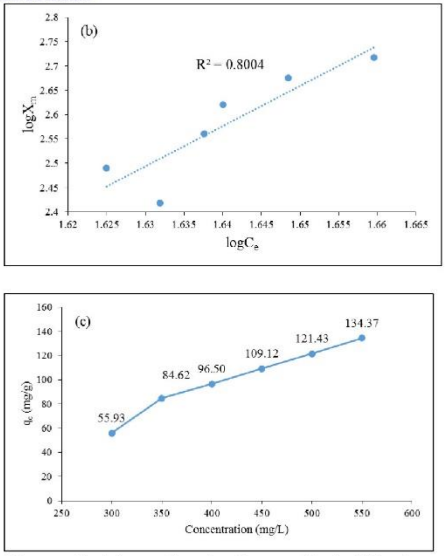

Figure 6. Adsorption isotherms for brilliant green using fly ash: (a) Langmuir isotherm (b) Freundlich isotherm (c) Adsorption efficiency (dosage 4 g/L, contact time: 30 minutes).

In Figure 6a and 6b showed the correlation coefficient (R^2) of Langmuir and Freundlich isotherm with 0.9964 and 0.8004, respectively. The results showed that the adsorption of brilliant green onto the fly ash corresponds well to the Langmuir adsorption isotherm for brilliant green in aqueous solution. So, the information of Langmuir isotherm model indicates the formation of monolayer coverage of brilliant green dye molecules at the surface of the fly ash. Figure 6c presented adsorption efficiency of brilliant green onto fly ash. There is availability of more surface to get adsorbed and basically provides the larger driving force for diffusion to takes place from the solution to the surface as it is totally a mass transfer phenomenon. The maximum adsorption capacity for dye was 134.37 mg/g.

4. Conclusion

The present study investigated the adsorption of brilliant green, a cationic industrial dye from aqueous solution by using fly ash available from Mae Moh power plant in Lampang province, Thailand. The Mae Moh fly ash has been demonstrated as an excellent adsorbent without modification for removal of brilliant green from aqueous solution. At initial concentration at 300 mg/L, the equilibrium time of 30 minutes and the optimal dosage of 4 g/L, the adsorption efficiency was 93 % with high adsorption capacity (q_e uptake at 134.37 mg/g). The best-fit Langmuir isotherm was obtained suggesting monolayer adsorption behaviors of brilliant green onto the fly ash. Accordingly, non-modified Mae Moh fly ash
could be used as a potential and low-cost adsorbent for removal of brilliant green dye from aqueous solutions.

Acknowledgments

Faculty of Science, Ubon Ratchathani University, National Metal and Materials Technology Center (MTEC) and the Center of Excellence for Innovation in Chemistry (PERCH-CIC) are gratefully acknowledged for research support.

References

1. Electricity Generating Authority of Thailand.https://www.egat.co.th/en/business-operation/egat-service-business/byproduct-business (accessed January 20, 2020)

2. Posi, P. *J. of GEOMATE* **2019,** *16*.

3. Kant, R. *Nat Sci*. **2012**, *4*, 22-26.

4.Ting, C.H. *Fuel*. ***2008***, *87,* 3040-3045.

5. Handa, B.K. Treatment and recycle of wastewater in industry. National Environmental Engineering Research Insti-tute, Nagpur. **1991**, *21, 65, 75, 76, 78, 82, 85*, 94.

6. Ehrampoush, M.; Moussavi, G.; Ghaneian, M.; Rahimi, S.; Ahmadian, M. *AJBAS.* **2010,** *4*, 4579-4285.
7. Acisli, O.; Acar, I.; Khataee, A. *J Ind Eng Chem.* **2019**.
8.Chueachot, R.; Wongkhueng, S.; Khankam, K.; Lakrathok, A.; Kaewnon, T.; Naowanon, W. T.; Amnuaypanich, S.; Nakhowong, R. *Mater. Today***. 2018,** *5*, 14079-14085.
9. Ting, C.H. *Water Res*. **2016,** *90*, 277-285.
10. Hsu, T.-C., *Fuel.* **2008,** *87* (13), 3040-3045.
11. H, M. F. Freundlich. *J. Phys. Chem. B.* **1906**, *57,* 385-471.
12. Duc, M.; Hamdi, N.; Nmiri, A.; Yazoghli, O.; Srasra. *J. Adv. Model Earth Sy*. **2017**, *8,* 676-690.

CURRICULUM VITE

NAME	Miss Warangkana Kittiwongwisan
EDUCATION	2014-2017, Bachelor of science (Chemistry), Department of Chemistry, Faculty of Science, Ubon Ratchathani University, Ubon Ratchathani, Thailand.
GRANT	Center of Excellence for Innovation in Chemistry (PERCH-CIC)